UNIVERSITÄT HOHENHEIM
Fakultät Wirtschafts- und Sozialwissenschaften

Four Essays in the Empirical Analysis of Business Cycles and Structural Breaks

Dissertation
zur Erlangung des Grades eines
Doktors der Wirtschaftswissenschaften
(Dr. oec.)

vorgelegt der
Fakultät der Wirtschafts– und Sozialwissenschaften
der Universität Hohenheim

von Dipl. oec.
Martyna Marczak

Stuttgart–Hohenheim
2015

Die vorliegende Arbeit wurde im Januar 2015 von der Fakultät Wirtschafts– und Sozialwissenschaften der Universität Hohenheim als Dissertation zur Erlangung des Grades eines Doktors der Wirtschaftswissenschaften (Dr. oec.) angenommen.

Datum der mündlichen Doktorprüfung: 17. Februar 2015

Dekan: Prof. Dr. Dirk Hachmeister
Prüfungsvorsitz: Prof. Dr. Benjamin Jung
Erstgutachter: Prof. Dr. Thomas Beißinger
Zweitgutachter: Prof. Dr. Robert Jung

Acknowledgements

First and foremost, I would like to thank my supervisor, Thomas Beissinger, for his great support and constant guidance over so many years. His excellent lectures and enthusiasm for macroeconomics I could experience already during my studies aroused my interest in this subject and initiated my long journey the result of which is this work. Without his positive influence I would have probably never decided to go the way I have chosen. I owe him much of my knowledge in macroeconomics and labor economics. I am grateful for his suggestions, continuous inspiration and motivation, as well as the pleasant environment I could work in, without which this thesis would have never been possible. It is a great pleasure and honor to work with him.

I would also like to thank my coauthors, Víctor Gómez and Tommaso Proietti. I have been very fortunate to meet such excellent scientists and, at the same time, very open–minded and helpful people. I have learnt a lot from the work on our joint research projects. I am grateful to Tommaso Proietti for his warm hospitality during my research visit at the University of Rome "Tor Vergata". I enjoyed this time very much and have benefited a lot from our discussions. I feel honored that we could continue with our collaboration after my stay in Rome.

Further, I thank Prof. Robert Jung, who is an expert in time series econometrics, for being referee of this thesis. His valuable comments are always greatly appreciated. I am also indebted to numerous conference and workshop participants for their constructive comments on the articles being part of this thesis.

I thank all my friends and colleagues at the University of Hohenheim, especially Philipp and Sebastian. Great atmosphere in our team, also due to our conversations about work–unrelated subjects made working on this thesis, even with its inevitable downs, an enjoyable time. I am happy that I am surrounded by so many friendly persons.

Finally, the most special thanks are directed to my parents, who are the greatest source of moral support for me. Their constant encouragement and unconditional belief have been accompanying me throughout all stages of my life.

Stuttgart, February 2015 Martyna Marczak

Contents

List of Tables

List of Figures

Chapter 1

Introduction

Business cycle analysis has a long history in the macroeconomics literature and since its origins it poses a challenge for both the empirical and theoretical research. According to the definition of Burns and Mitchell (1946), business cycle can be seen as fluctuations in the aggregate economic activity featuring periodicities between 1.5 and 8 years. This definition makes clear that the concept of business cycles refers to stochastic cycles that may vary in amplitude and length. The fact that the pattern of fluctuations is not directly observable but rather hidden feature makes its detection a challenging task and raises fascination among researchers also after many decades.

One reason for the enduring keen interest in this research area is guided by its high relevance for economic policy. In order to monitor the economic situation and, if necessary, to take appropriate decisions to prevent severe crises or overheating of the economy, it is beneficial to have reliable information on the state of the economy in the present as well as in the (near) future.

From the theoretical perspective, different arguments have been put forward to explain business cycles and cyclical behavior of macroeconomic variables, like prices or wages. Advances in empirical research on business cycles are not only important to produce reliable information on the state of the economy. By providing elaborate statistical methods, they also help to prove the validity of different theoretical approaches. The subsequent discussion will address both these aspects.

As regards the former, the extent of the scientific progress becomes very clear by going back to the beginnings of business cycle research. The analysis was of qualitative nature, merely restricted to graphical inspection of time series, such as industrial production and employment. Transition towards quantitative measurement started with the pioneering work by Burns and Mitchell (1946). The business cycle they were referring to is the so–called "classical cycle" defined in terms of turning points related to the level of the series.

This concept implies that a recession (expansion) is characterized by an absolute decline (increase) in the value of the reference series relative to the respective turning point, i.e. local maximum (minimum) of this series. For the US, the chronology of turning points is officially published by the Business Cycle Dating Committee of the National Bureau of Economic Research (NBER). The respective authority for the euro area is the Dating Committee of the Centre of Economic Policy Research (CEPR). Judgement of committee members about the dates is based on the investigation of several quarterly and monthly indicators. Research concerned with classical business cycles has been trying to develop methods to formalize aspects taken into account in the official procedures. The best known algorithm trying to replicate the official NBER turning points has been set out by Bry and Boschan (1971). Harding and Pagan (2002), Harding and Pagan (2006), Artis et al. (2004) proposed extensions of the Bry and Boschan rule and provided some applications. Another approach based on an autoregressive Markov switching model has been suggested by Hamilton (1989).

A large part of the literature focuses on an alternative business cycle concept, the so–called "growth cycles". Growth cycles are not, as the name may misleadingly suggest, synonymous with the growth rate of the series, but are related to the concept of detrending in a broad sense as they can be described as deviations of a time series from its long–run trend. It is to be noted that this definition implicitly assumes a seasonally adjusted series. An early reference is the work by Mintz (1972). The conceptual difference compared to the classical cycle is that expansions (recessions) associated with the growth cycle are indicated by the acceleration (deceleration) of economic activity. Different approaches have been proposed for the extraction of growth cycles. They can be classified into statistical and theory–based approaches.

As regards statistical approaches, for a long time univariate methods have been dominating, whereby typically real GDP or industrial production series are used as the reference series. The application of filters, like the Hodrick and Prescott (1997) filter and Baxter and King (1999) filter, has become common practice. It has been, however, shown that in the case of nonstationary time series these filters can induce spurious cycles (Cogley and Nason, 1995; Harvey and Jaeger, 1993; Murray, 2003). An alternative to the ad hoc filtering methods are unobserved components models that take the stochastic properties of the data into account. Among these model–oriented approaches, two major modeling strategies are: the structural time series models (Harvey, 1989; Harvey and Trimbur, 2003) and the ARIMA–model–based approach (Box et al., 1978) combined with the canonical

decomposition (Cleveland and Tiao, 1976).

Recent developments show an appreciation of multivariate approaches. The reason is that they can exploit the informational content of both real GDP, the most comprehensive measure of economic activity albeit reported on a quarterly basis, and short–term indicators. This results in more precise business cycle indicators, provided at shorter, typically monthly, time intervals. Moreover, mixed–frequency datasets also allow for real–time nowcasting of quarterly economic activity, i.e. forecasting referring to the current quarter, based on the information set including indicators that become available within the quarter. Forni et al. (2000) and Stock and Watson (2002) are examples of the first works suggesting the possibility of constructing business cycle or growth indicators with a large set of variables. Growth indicators are equal to or based on the growth rate of economic activity. Valle e Azevedo et al. (2006) and Creal et al. (2010) presented business cycle indicators extracted in the framework of multivariate structural time series models. The research on growth indicators seems to be more prominent, only to mention a few publications concerning the euro area: New Eurocoin (Altissimo et al., 2010), the Economic Sentiment Index (compiled by the European Commission), Euro–Sting (Camacho and Pérez-Quirós, 2010) and EuroMInd (Frale et al., 2011).

As far as theory–based approaches for growth cycle estimation are concerned, the business cycle is interpreted as output gap defined as deviations of actual output from its potential level. Potential output measures the productive capacity of the aggregate economy and involves full utilization of production inputs (Okun, 1962). One possible way to derive potential output is to employ the production function approach linking potential output to the labor and capital inputs and to total factor productivity, also called Solow residual; see Giorno et al. (1995), de Masi (1997), Beffy et al. (2006).

Potential output is also referred to as natural output which defines an equilibrium consistent with stable inflation and thus is related to the non–accelerating inflation rate of unemployment (NAIRU) (Phelps, 1967; Friedman, 1968). The output gap reflects then two well–known economic relationships: the expectation–augmented Phillips curve and Okun's law. Whereas the Phillips curve links changes in the inflation rate to deviations of actual unemployment from the NAIRU, Okun's law postulates a negative relation between cyclical components of output and unemployment.Various attempts have been made in the literature to embed these relationships and estimate potential output along with the output gap in the framework of system equations. System estimates can be found in works by, e.g., Kuttner (1994), Apel and Jansson (1999), Gerlach and Smets (1999), Rünstler

(2002) and Doménech and Gómez (2006). Proietti et al. (2007) combine the production function approach with the system approach.

Another category of theory–based approaches represent dynamic stochastic general equilibrium (DSGE) models which impose structure on the whole economy and thus entail tighter theoretical restrictions than the aforementioned methods; see Smets and Wouters (2003), Edge et al. (2008), Vetlov et al. (2011). A discussion of different definitions of the output gap is provided by Kiley (2013).

This review of the literature makes clear that the approaches for business cycle estimation are numerous and can differ fundamentally. In addition to the choice of the method, another aspects have to be taken into account as they may affect the quality of the business cycle (or growth) indicator. One of them is the common practice of using seasonally adjusted series. The data are seasonally adjusted either by an official statistical office or by the analyst prior to cycle estimation. Official procedures comprise X–12 ARIMA, and its enhanced version X–13 ARIMA (U.S. Census Bureau, 2013), TRAMO (Gómez and Maravall, 1996), TSW: TRAMO–SEATS for Windows (Caporello and Maravall, 2004) and Berlin method (Federal Statistical Office of Germany, 2006). Seasonal adjustment can be also performed by means of structural time series models using, e.g., the specialized software STAMP 8 (Koopman et al., 2009). Instead of relying on already preprocessed data, raw series can be alternatively modeled with approaches which allow for a simultaneous treatment of the seasonal component next to the trend and cycle. In this way, all components of the series can be estimated in a coherent manner. All the same, it is to be noted that properties of estimated business cycles can depend on the seasonal adjustment method since different procedures produce, in general, different outcomes.

Another aspect that should be taken into account in the context of business cycles extraction has to do with the fact that the structure of the economy might undergo changes over time. There is, for instance, evidence in the literature that the US economy experienced a decline in output volatility in the mid–1980's (Kim and Nelson, 1999; McConnell and Pérez-Quirós, 2000). Further, the same factors can have different impact across episodes. A prominent example are oil price shocks whose role seems to have become less important; see Blanchard and Galí (2010), Ramey and Vine (2011), Baumeister and Peersman (2013), Blanchard and Riggi (2013). Recessions in different episodes may also exhibit different characteristics as they may be triggered by different factors. This can be illustrated with the example of financial instabilities. In the aftermath of the global economic crisis in 2008–2009, a lot of attention in the literature has been paid to financial crises. It

has been documented that recessions accompanied by financial crises are more severe and prolonged; see the studies by Reinhart and Rogoff (2009), Bordo and Haubrich (2010), Jordá et al. (2010), Jordá et al. (2012) and Schularick and Taylor (2012). As a result of financial crises, not only the business cycle can be affected, but also the long–term trend (or potential output); see Furceri and Mourougane (2012). Time–invariant models or ad hoc methods may not be able to capture changes or breaks in the macroeconomic dynamics. One possible strategy is to include explanatory variables, like financial variables, in the models (Borio et al., 2013; Borio, 2013). Another strategy is to directly model structural breaks by intervention variables of an appropriate type. This approach is more flexible since it is detached from complex interactions of different possible factors responsible for the changing dynamics.

The correction of structural breaks and outliers is related to seasonal adjustment as both contribute to a clear economic signal. Automatic procedures for detection of outliers and structural breaks are implemented in the official seasonal adjustment procedures. In TRAMO, TSW and X13–ARIMA, outlier detection is carried out as described by Tsay (1986), Chang et al. (1988), Chen and Liu (1993) and consists of two stages: forward addition, followed by backward deletion. STAMP, a software developed for structural time series models, provides a rather basic algorithm based on the so–called auxiliary residuals (Harvey and Koopman, 1992). Significant auxiliary residuals indicate outliers corresponding to particular components of the model, like irregular, trend level, trend slope, seasonal etc.

So far, the discussion of this chapter was dealing with methodological advances of the empirical business cycle analysis associated with the concept of the business cycle. As has been mentioned at the beginning, empirical business cycle research might also be useful to validate or discredit theories explaining economic phenomena. This seems particularly important in case of conflicting theories, like those which have been competing in the debate on cyclical behavior of real wages, one of the most lively and long–lasting debates in macroeconomics.

Keynesian economists, for example, postulate anticyclical real wages by arguing that nominal wages are rigid, at least in the short run. According to Barro (1990) and Christiano and Eichenbaum (1992), a similar real wage behavior may be explained with the intertemporal labor–leisure substitution. In this case, anticyclical real wages can arise as an effect of transitory changes in the real interest rate inducing shifts in the labor supply curve. In contrast, as shown by Kydland and Prescott (1982) or Barro and King (1984), real

business cycle models predict procyclical real wages resulting from shifts in labor demand caused by technological shocks. A procyclical or acyclical pattern may also occur in New Keynesian models and is justified by the assumption of the countercylical mark–up of monopolistic firms; see Rotemberg and Woodford (1991). A clearer empirical picture on the cyclical behavior of real wages may be helpful in identifying the main sources of macroeconomic shocks and mechanisms that govern the adjustment of real wages in the course of the business cycle.

This thesis tries to contribute to the literature under the aforementioned viewpoints. It addresses methodological issues associated with the extraction of business cycles and detection of structural breaks. Furthermore, it revisits the topic of real wage cyclicality from the empirical perspective.

In particular, in Chapter 2 (joint work with Víctor Gómez) a new multivariate model is proposed to construct monthly business cycle indicators for the US. First, a model consisting only of trend and irregular is formulated. In this model, the trend is assumed to capture transitory movements and to have a common slope. For this reason, it is more appropriately referred to as a trend–cycle. In the second step, to isolate the cycle, we apply a band–pass filter to the estimated trend–cycle as described in Gómez (2001).

The advantages of this approach are manifold. It provides smooth indicators of economic activity which conform to the idea of the business cycle featuring periodicities between 1.5 and 8 years. Moreover, the obtained indicators embody information inherent in several time series observed at both monthly and quarterly frequency. The two–step strategy avoids the problem of modeling the cycle directly and thus facilitates the estimation of the model in the first step. It is shown that the proposed method is able to replicate historical recessions and can serve as a reliable forecasting framework as well.

Chapter 3 (joint work with Tommaso Proietti) investigates a new perspective to detect outliers and structural breaks in the context of seasonal adjustment. We for the first time combine the indicator saturation (IS) approach for outlier detection with the structural time series model for seasonal adjustment. The IS approach is a relatively new, yet promising concept in the literature. It has been proposed by Hendry (1999) and constitutes a general–to–specific approach. The procedure relies on adding a specific type of an intervention variable at every observation in the sample. Interventions can represent outlying observations, level shifts, slope changes etc. The IS has proven very effective in a regression framework and is implemented in Autometrics (Doornik, 2009), an integral part of PcGive (Doornik and Hendry, 2013).

The reference model for the adjustment purpose is the basic structural model (BSM), proposed by Harvey and Todd (1983) for univariate time series. The BSM is formulated in terms of a trend, a seasonal and an irregular component. Though this model is relatively simple, it is flexible and provides a satisfactory fit to a wide range of seasonal time series. We assess the performance of the IS in an extensive Monte Carlo exercise. We also apply the considered method to the raw industrial production series for five European countries. The primary objective of this empirical application is to test for a potential level shift corresponding to the economic and financial crisis starting in Europe around the end of 2008.

Chapter 4 (joint work with Thomas Beissinger) is the article already published in Empirical Economics under the title "Real Wages and the Business Cycle in Germany" (Marczak and Beissinger, 2013). This works contributes to the literature on real wage cyclicality in several ways. In contrast to the bulk of aggregate–data based research which examines the considered question by applying basic time–domain methods, we propose to additionally refer to the frequency–domain approach while measuring comovements between real wages and the business cycle. The advantage of frequency–domain techniques lies in their ability to differentiate between horizons at which the comovements are measured. In particular, we reintroduce the concept of the phase angle as a suitable tool to identify the pro– or countercyclical behavior as well as the leading or lagging behavior of real wages relative to the business cycle.

In our analysis, we distinguish between consumer and producer real wages, and apply different detrending methods for estimation both real wage cycles and the business cycle. Whereas most of the studies focus on the US, the analysis of this chapter is carried out for Germany. To the best of our knowledge, it is the first study for Germany which combines various methodological aspects, such as comovement and detrending methods, and the role of the price deflator used for the construction of real wages.

Chapter 5 resumes the investigation of real wage cyclicality but this study differs from the one of Chapter 3 in several aspects. First and foremost, I draw on wavelet analysis in exploring cyclical behavior of real wages. The merit of wavelet analysis can be seen in the fact that it can reveal how the relationship between different periodic components of time series evolves over time. In economics, as opposed to physics, meteorology, geology, medicine, oceanography or engineering, wavelet analysis is a rather new field. Early economic applications include works by, e.g., Ramsey et al. (1995), Ramsey and Lampart (1998) and Gençay et al. (2001). This study is the first one which employs wavelet analysis

in the context of the examined research question and has laid the groundwork for the later work with Víctor Gómez.

Another important difference compared to the preceding chapter is that this study does not concentrate on a particular country. Instead, the purpose is to provide a comparison of real wage cyclicality in the USA and Germany, two large economies with strongly differing labor market institutions. Due to a consistent framework with respect to cycle extraction (two model–based methods), comovement measures and price deflators, the analysis may prove useful in establishing whether differences in labor market characteristics carry into country–specific patterns of real wage cyclicality.

In the course of the work on this thesis, I have been often resorting to frequency–domain concepts, especially in the analysis of comovements between variables. This fact has become a motivation for developing a set of computer routines that should facilitate the application of frequency–domain concepts to univariate and multivariate time series. This idea has eventually resulted in the Matlab toolbox Spectran that I have developed under the assistance of Víctor Gómez. This toolbox represents a set of easy–to–use Matlab routines involving a variety of frequency–domain techniques and supporting the statistical inference. In addition, Spectran also allows for a convenient examination of the results by generating output files and graphics. The manual to this toolbox is provided in Appendix A. Next to the description of the routines, it also includes an introduction into the implemented frequency–domain concepts.

References

Altissimo, F., Cristadoro, R., Forni, M., Lippi, M., and Veronese, G. (2010). New Eurocoin: Tracking Economic Growth in Real Time. *Review of Economics and Statistics*, *92*(4), 1024–1034.

Apel, M., and Jansson, P. (1999). System Estimates of Potential Output and the NAIRU. *Empirical Economics*, *24*, 373–388.

Artis, M., Marcellino, M., and Proietti, T. (2004). Dating Business Cycles: A Methodological Contribution with an Application to the Euro Area. *Oxford Bulletin of Economics and Statistics*, *66*(4), 537–565.

Barro, R. J. (1990). *Macroeconomics* (3rd ed.). New York: John Wiley.

Barro, R. J., and King, R. G. (1984). Time-Separable Preferences and Intertemporal-Substitution Models of Business Cycles. *Quarterly Jounal of Economics*, *99*(4), 817–839.

Baumeister, C., and Peersman, G. (2013). Time–Varying Effects of Oil Price Shocks on the US Economy. *American Economic Review*, *5*(4), 1–28.

Baxter, M., and King, R. G. (1999). Measuring Business Cycles. Approximate Band-pass Filters for Economic Time Series. *Review of Economics and Statistics*, *81*, 575–593.

Beffy, P.-O., Ollivaud, P., Richardson, P., and Sédillot, F. (2006). *New OECD Methods for Supply–Side and Medium–Term Assessments: A Capital Services Approach* (Working Paper No. 482). OECD Economics Department.

Blanchard, O., and Galí, J. (2010). The Macroeconomic Effects of Oil Price Shocks: Why Are the 2000s So Different from the 1970s? In J. Galí and M. J. Gertler (Eds.), *International dimensions of monetary policy* (pp. 373–421). University of Chicago Press.

Blanchard, O., and Riggi, M. (2013). Why Are the 2000s So Different from the 1970s? a Structural Interpretation of Changes in the Macroeconomic Effects of Oil Prices. *Journal of the European Economic Association*, *11*(5), 1032–1052.

Bordo, M. D., and Haubrich, J. G. (2010). Credit Crises, Money and Contractions: An Historical View. *Journal of Monetary Economics*, *57*, 1–18.

Borio, C. (2013). The Financial Cycle and Macroeconomics: What Have We Learnt? *Journal of Banking and Finance*, *45*, 182–198.

Borio, C., Disyatat, P., and Juselius, M. (2013). *Rethinking Potential Output: Embedding Information About the Financial Cycle* (Tech. Rep. No. 404). BIS.

Box, G. E. P., Hillmer, S. C., and Tiao, G. C. (1978). Analysis and Modeling of Seasonal Time Series. In A. Zellner (Ed.), *Seasonal Analysis of Economic Time Series* (pp. 309–334). Washington, DC: U.S. Dept. Commerce, Bureau of the Census.

Bry, G., and Boschan, C. (1971). *Cyclical Analysis of Time Series: Selected Procedures and Computer Programs*. New York: NBER.

Burns, A. F., and Mitchell, W. C. (1946). *Measuring Business Cycles*. New York: NBER.

Camacho, M., and Pérez-Quirós, G. (2010). Introducing the Euro–Sting: Short–term Indicator of Euro Area Growth. *Journal of Applied Econometrics*, *25*, 663–694.

Caporello, G., and Maravall, A. (2004). *Program TSW: Revised Reference Manual* (Manual). Banco de España.

Chang, I., Tiao, G. C., and Chen, C. (1988). Estimation of Time Series Parameters in the Presence of Outliers. *Technometrics*, *30*(2), 193–204.

Chen, C., and Liu, L.-M. (1993). Joint Estimation of Model Parameters and Outlier Effects in Time Series. *Journal of the American Statistical Association*, *88*(421), 284–297.

Christiano, L. J., and Eichenbaum, M. (1992). Current Real–Business-Cycle Theories and Aggregate Labor–Market Fluctuations. *American Economic Review*, *82*(3), 430–450.

Cleveland, W. P., and Tiao, G. C. (1976). Decomposition of Seasonal Time Series: A Model for the X-11 Program. *Journal of the American Statistical Association*, *71*, 581–587.

Cogley, T., and Nason, J. T. (1995). Effects of the Hodrick-Prescott Filter on the Trend and Difference Stationary Time Series: Implications for Business Cycle Research. *Journal of Economic Dynamics and Control*, *19*, 253–278.

Creal, D., Koopman, S. J., and Zivot, E. (2010). Extracting a Robust US Business Cycle Using a Time–Varying Multivariate Model–Based Bandpass Filter. *Journal of Applied Econometrics*, *25*, 695–719.

de Masi, P. R. (1997). *IMF Estimates of Potential Output: Theory and Practice* (Working Paper No. 177). IMF.

Doménech, R., and Gómez, V. (2006). Estimating Potential Output, Core Inflation, and the NAIRU as Latent Variables. *Journal of Business and Economic Statistics*, *24*, 354–365.

Doornik, J. A. (2009). *Econometric Model Selection With More Variables Than Observations* (Unpublished paper). Economics Department, University of Oxford.

Doornik, J. A., and Hendry, D. F. (2013). *PcGive 14*. London: Timberlake Consultants. (3 volumes)

Edge, R. M., Kiley, M. T., and Laforte, J.-P. (2008). Natural Rate Measures in an Estimated DSGE Model of the US Economy. *Journal of Economic Dynamics and Control*, *32*, 2512–2535.

Federal Statistical Office of Germany. (2006). *The BV4.1 Procedure for Decomposing and Seasonally Adjusting Economic Time Series* (Methodological Paper).

Forni, M., Hallin, M., Lippi, M., and Reichlin, L. (2000). The Generalized Factor Model: Identification and Estimation. *Review of Economics and Statistics*, *82*, 540–554.

Frale, C., Marcellino, M., Mazzi, G., and Proietti, T. (2011). EUROMIND: A Monthly Indicator of the Euro Area Economic Conditions. *Journal of the Royal Statistical Society: Series A*, *174*, 439–470.

Friedman, M. (1968). The Role of Monetary Policy. *American Economic Review*, *58*(1), 1–17.

Furceri, D., and Mourougane, A. (2012). The Effect of Financial Crises on Potential Output: New Empirical Evidence from OECD Countries. *Journal of Macroeconomics*, *34*, 822–832.

Gençay, R., Selçuk, F., and Whithcher, B. (2001). Scaling Properties of Foreign Exchange Volatility. *Physica A: Statistical Mechanics and its Applications*, *289*, 249–266.

Gerlach, S., and Smets, F. (1999). Output Gaps and Monetary Poicy in the EMU Area. *European Economic Review*, *43*, 801–812.

Giorno, C., Richardson, P., Rooseveare, D., and van den Noord, P. (1995). Potential Output, Output Gaps, and Structural Budget Balances. *OECD Economic Studies*, *24*, 1995/1.

Gómez, V. (2001). The Use of Butterworth Filters for Trend and Cycle Estimation in Economic Time Series. *Journal of Business and Economic Statistics*, *19*(3), 365–373.

Gómez, V., and Maravall, A. (1996). *Programs TRAMO and SEATS; Instructions for the User* (Working Paper No. 9628). Servicio de Estudios, Banco de España.

Hamilton, J. D. (1989). A New Approach to the Economic Analysis of Nonstationary Time Series and the Business Cycle. *Econometrica*, *57*, 357–384.

Harding, D., and Pagan, A. (2002). Dissecting the Cycle: A Methodological Investigation. *Journal of Monetary Economics*, *49*, 365–381.

Harding, D., and Pagan, A. (2006). Synchronization of Cycles. *Journal of Econometrics*,

132, 59–79.

Harvey, A. C. (1989). *Forecasting, Structural Time Series Models and the Kalman Filter*. Cambridge: Cambridge University Press.

Harvey, A. C., and Jaeger, A. (1993). Detrending, Stylized Facts and the Business Cycle. *Journal of Applied Econometrics*, *8*, 231–247.

Harvey, A. C., and Koopman, J. S. (1992). Diagnostic Checking of Unobserved-Component Time Series Models. *Journal of Business and Economic Statistics*, *10*(4), 377–389.

Harvey, A. C., and Todd, P. H. J. (1983). Forecasting Econometric Time Series with Structural and Box-Jenkins Models (with discussion). *Journal of Business and Economic Statistics*, *1*(4), 299–315.

Harvey, A. C., and Trimbur, T. M. (2003). General Model-Based Filters for Extracting Cycles and Trends in Economic Time Series. *Review of Economics and Statistics*, *85*, 244–255.

Hendry, D. F. (1999). An Econometric Analysis of US Food Expenditure, 1931–1989. In J. R. Magnus and M. S. Morgan (Eds.), *Methodology and Tacit Knowledge: Two Experiments in Econometrics* (pp. 341–361). Chichester: John Wiley and Sons.

Hodrick, R. J., and Prescott, E. C. (1997). Postwar U.S. Business Cycles: An Empirical Investigation. *Journal of Money, Credit and Banking*, *29*, 1–16.

Jordá, Ó., Schularick, M., and Taylor, A. M. (2010). *Financial Crises, Credit Booms, and External Imbalances: 140 Years of Lessons* (Working Paper No. 16567). NBER.

Jordá, Ó., Schularick, M., and Taylor, A. M. (2012). *When Credit Bites Back: Leverage, Business Cycles, and Crises* (Working Paper No. 27). Federal Reserve Bank of San Francisco.

Kiley, M. T. (2013). Output Gaps. *Journal of Macroeconomics*, *37*, 1–18.

Kim, C.-J., and Nelson, C. R. (1999). Has the U.S. Economy Become More Stable? A Bayesian Approach Based on a Markov–Switching Model of the Business Cycle. *The Review of Economic and Statistics*, *81*, 608–616.

Koopman, S. J., Harvey, A. C., Doornik, J. A., and Shephard, N. (2009). *STAMP 8.2: Structural Time Series Analyser, Modeller and Predictor*. London: Timberlake Consultants.

Kuttner, K. N. (1994). Estimating Potential Output as a Latent Variable. *Journal of Business and Economic Statistics*, *12*(3), 361–368.

Kydland, F. E., and Prescott, E. C. (1982). Time to Build and Aggregate Fluctuations.

Econometrica, *50*, 1345–1370.

Marczak, M., and Beissinger, T. (2013). Real Wages and the Business Cycle in Germany. *Empirical Economics*, *44*, 469–490.

McConnell, M. M., and Pérez-Quirós, G. (2000). Output Fluctuations in the United States: What Has Changed Since the Early 1980's? *American Economic Review*, *90*, 1464–1476.

Mintz, I. (1972). Dating American Growth Cycles. In V. Zarnowitz (Ed.), *Economic Research: Retrospect and Prospect: The Business Cycle Today* (Vol. 1). UMI.

Murray, C. J. (2003). Cyclical Properties of Baxter-King Filtered Time Series. *Review of Economics and Statistics*, *85*(2), 472–476.

Okun, A. M. (1962). *Potential GNP: Its Measurement and Significance* (Research Paper). Cowles Foundation: Yale University.

Phelps, E. (1967). Phillips Curves, Expectations of Inflation and Optimal Unemployment over Time. *Economica*, *34*, 254–281.

Proietti, T., Musso, A., and Westermann, T. (2007). Estimating Potential Output and the Output Gap for the Euro Area: A Model–Based Production Function Approach. *Empirical Economics*, *33*, 85–113.

Ramey, V. A., and Vine, D. J. (2011). Oil, Automobiles, and the US Economy: How Much Have Things Really Changed? In D. Acemoglu and M. Woodford (Eds.), *NBER Macroeconomics Annual 2010* (Vol. 25, pp. 333–367). University of Chicago Press.

Ramsey, J. B., and Lampart, C. (1998). Decomposition of Economic Relationships by Time Scale Using Wavelets: Money and Income. *Macroeconomic Dynamics*, *2*, 49–71.

Ramsey, J. B., Usikov, D., and Zaslavsky, G. M. (1995). An Analysis of US Stock Price Behavior Using Wavelets. *Fractals*, *3*(2), 377–389.

Reinhart, C. M., and Rogoff, K. S. (2009). The Aftermath of Financial Crises. *American Economic Review*, *99*(2), 466–472.

Rotemberg, J. J., and Woodford, M. (1991). Markups and the Business Cycle. In O. Blanchard and S. Fisher (Eds.), *NBER Macroeconomics Annual:1991* (pp. 63–129). Cambridge and London: MIT Press.

Rünstler, G. (2002). *The Information Content of Real–Time Output Gap Estimates: An Application to the Euro Area* (Working Paper No. 182). ECB.

Schularick, M., and Taylor, A. M. (2012). Credit Booms Gone Bust: Monetary Policy,

Leverage Cycles, and Financial Crises, 1870–2008. *American Economic Review*, *102*(2), 1029–1061.

Smets, F., and Wouters, R. (2003). An Estimated Dynamic Stochastic General Equilibrium Model of the Euro Area. *Journal of the European Economic Association*, *1*(5), 1123–1175.

Stock, J. H., and Watson, M. W. (2002). Macroeconomic Forecasting Using Diffusion Indexes. *Journal of Business and Economic Statistics*, *20*, 147–162.

Tsay, R. S. (1986). Time Series Model Specification in the Presence of Outliers. *Journal of the American Statistical Association*, *81*, 132–141.

U.S. Census Bureau. (2013). X–13 ARIMA–SEATS Reference Manual [Computer software manual].

Valle e Azevedo, J., Koopman, S. J., and Rua, A. (2006). Tracking the Business Cycle of the Euro Area: A Multivariate Model–Based Bandpass Filter. *Journal of Business and Economic Statistics*, *24*, 278–290.

Vetlov, I., Hlédik, T., Jonsson, M., Kucsera, H., and Pisani, M. (2011). *Potential Output in DSGE Models* (Working Paper No. 1351). ECB.

Chapter 2

Monthly US Business Cycle Indicators: A New Multivariate Approach Based on a Band–Pass Filter*

2.1 Introduction

Economic policy is a subject which often sparks off an active public debate. For example, policy makers pursuing stabilization policy are expected to take appropriate actions to stimulate the economy if it is on the brink of a crisis, or to prevent the overheating of the economy if an expansion is likely to take place. However, such measures are risky since wrong decisions entail high costs for the society. It is therefore all the more important to have reliable information in the decision making process. Moreover, the decisions must be often made early enough and thus under uncertainty about the future state of the economy. Information available at high frequencies can thus prove helpful in revealing the stage of the business cycle. The aim of this article is to develop a methodology that can both provide reliable information on the course of the economy and reduce the lag in the recognition of its future state.

To identify the course of the economy on the basis of macroeconomic data, a clear signal supposed to represent the business cycle has to be extracted. For that purpose, it is necessary to separate out long–term movements and noisy elements from the data. The question as to how to accomplish this constitutes the central question of business cycle analysis and has been investigated since the seminal work by Burns and Mitchell (1946). They for the first time gave a more narrow definition of business cycles as fluctuations in the economic activity that last between 1.5 and 8 years. The following research attempted

*This chapter is the result of the joint work with Víctor Gómez and has appeared as Marczak and Gómez (2013).

to construct business cycle indicators characterized by these periodicities. Some studies focus on univariate approaches, like the filters proposed by Hodrick and Prescott (1997) and Baxter and King (1999) that have become very popular mostly because of their relatively simple implementation.

Among the univariate approaches, an alternative to these ad hoc filtering methods are the unobserved components models that take the stochastic properties of the data into account. As regards this signal extraction approach, two tendencies have emerged in the literature. One direction corresponds to the structural time series models proposed by, e.g., Harvey (1989) or their generalized version allowing for smoother cycles (see Harvey and Trimbur, 2003). The other direction is determined by the ARIMA–model–based approach (see, e.g., Box et al., 1978) combined with the canonical decomposition (see Cleveland and Tiao, 1976).

Since in the univariate approach only one series, typically real GDP or industrial production, can serve as a basis for the construction of a business cycle indicator, the informational content of other macroeconomic time series cannot be exploited. In contrast, the multivariate framework takes the contribution of different time series into account. This advantage of a multivariate setting has been recognized by, e.g., Forni et al. (2000) who develop a euro area business cycle indicator in a generalized dynamic–factor model using a large panel of macroeconomic indicators. The indicator of Valle e Azevedo et al. (2006) for the euro area is designed with a structural model including a common cycle, and extracted using a moderate set of series. Creal et al. (2010) extend their approach by taking time–varying volatility into account and adopt this method for the US.

In this article, we propose another multivariate method which is also based on a structural time series model. However, because of the well–known difficulties in modeling cycles directly, a model consisting only of trend plus irregular is initially specified. In this model, the trend is assumed to capture transitory movements and to have a common slope. For this reason, it is more appropriately referred to as a trend–cycle. After estimating the trend–cycle, we apply to it a multivariate band–pass filter to estimate the cycle following the methodology proposed by Gómez (2001). In fact, the filter is designed for univariate series, but then it is extended to multivariate series using diagonal matrices. The whole procedure is fully model–based and is applied to the same set of 11 monthly and quarterly US time series as in Creal et al. (2010). The extracted cycles of real GDP and the industrial production index can act as two alternative monthly business cycle indicators.

The proposed approach exhibits very appealing properties. From the modeling point of

view, it provides indicators of the economic activity which conform to the idea of the business cycle featuring periodicities between 1.5 and 8 years. Hence, one can be sure that these indicators are not contaminated with higher– or lower–frequency movements. In addition, the model is flexible since only a few restrictions are imposed, and yet quite simple in that it does not involve special constructs, like time–variant parameters, to capture specific behavior of the series components. The complexity of the proposed method is kept at a rather low level also due to the fact that a dataset with small or moderate number of series is sufficient in the implementation of the procedure. Moreover, the algorithms used for this method are able to deal with data recorded at different frequencies, and can handle missing values straightforwardly.

As regards the policy relevance of the methodology, it is shown that not only previous recessions can be spotted by the resulting business cycle indicators, but also future recessions can be very well predicted. As a reliable forecasting framework, this model can perform better than univariate methods and some elaborate multivariate models. Further, the indicator represented by the real GDP cycle and its predictions are given on a monthly basis even though real GDP itself is recorded quarterly. This leads to a more precise picture on the economic situation and makes it possible to detect changes in the economic course early. To summarize, with its quite simple setup, good forecasting performance and the ability to generate realtime forecasts not distorted by, e.g., highly volatile movements, this method proves to be a well–suited tool for policy makers.

As the information stemming from different time series helps to build the business cycle indicators, it may be of interest to know how these series are related to the business cycle. In contrast to the idea by Stock and Watson (1989), they are not constrained to be coincident indicators only. The behavior of the included series is examined by drawing on the concepts of the phase angle and the mean phase angle. These spectral measures allow for classifying the series as leading, lagging or coincident indicators as well as identifying procyclical or countercyclical patterns.

The remainder of the article is organized as follows. In Section 2.2, we present the multivariate monthly model. The model is then applied to the US data described in Section 2.3.1. The resulting business cycle indicators and the behavior of other indicators with respect to the business cycle are analyzed in Section 2.3.2. Section 2.3.3 focusses on the forecasting performance of the proposed approach. Section 2.4 concludes.

2.2 Multivariate monthly model

Given a multivariate monthly time series $\{y_t\}$, $t = 1, \ldots, n$ with $y_t = (y_{1t}, \ldots, y_{kt})'$, the decomposition of y_t is based on a trend plus noise model, i.e.

$$y_t = \mu_t + \epsilon_t, \tag{2.1}$$

where $\mathrm{Var}(\epsilon_t) = D_\epsilon$ is a diagonal matrix. In the presence of a cycle, μ_t is not seen as a smooth trend but rather as a component containing cyclical movements too. Therefore, it will hereafter be referred to as the trend–cycle.
Alternatively, it would be possible to add a cycle component to model (2.1) to explicitly take cyclical movements into account. However, it is well known that cycles are not easy to model and that most of the time one ends up fixing some parameters in the cycle model to obtain sensible results (see, e.g., Valle e Azevedo et al., 2006). The difficulty of modeling cycles is also apparent in the univariate case when one starts with an ARIMA model fitted to the series and the models for the components are specified according to the canonical decomposition (see, e.g., Cleveland and Tiao, 1976). In this case, a model for the cycle cannot usually be found using traditional tools of ARIMA modeling, such as graphs or correlograms.
The approach proposed in this paper avoids these problems. It consists of applying a fixed band–pass filter to the trend–cycle component, μ_t in model (2.1), following the methodology proposed by Gómez (2001). The filter is designed to extract the business cycle fluctuations that correspond to the periods between 1.5 and 8 years. One might wonder why a two–step approach is utilized here instead of simply applying the filter to the original series. The advantage of the two–step framework is that it allows for a complete decomposition of the series into trend, cycle and irregular. The procedure is fully model–based and will be described in the following subsections.

2.2.1 Model for the trend–cycle component

The trend–cycle component μ_t follows the model

$$\begin{aligned} \mu_{t+1} &= \mu_t + K\beta_t + \zeta_t \\ \beta_{t+1} &= \beta_t + \eta_t, \end{aligned} \tag{2.2}$$

where $K\beta_t$ denotes the slope of μ_t. By assuming $K = [1, b_{21}, ..., b_{K1}]'$, $\Delta\mu_{t+1} = \mu_{t+1} - \mu_t$ is allowed to be driven by one common slope, β_t. Moreover, η_t and ζ_t are white noise processes with $\text{Var}(\eta_t) = \sigma_\eta^2$ and $\text{Var}(\zeta_t) = D_\zeta$, respectively, where D_ζ is a diagonal matrix. The so–called multivariate local linear trend model (2.2) has been proposed by Harvey (1989, p. 452).

The rationale for imposing a common slope in model (2.2) is motivated by the assumption that the different elements of the series $\{y_t\}$ have the same or a similar cyclical behavior. The intuition behind the assumption of a common slope is, however, not as straightforward as that of a common cycle. The common slope, β_t, should not be mistakenly seen here as a substitute for a common cycle. Since the cycle is not explicitly modeled in eq. (2.1), an assumption of a common slope helps to account for a similar short–term evolution of the different elements of the series $\{y_t\}$. This can be illustrated by considering the first difference of the series

$$\nabla y_t = K\beta_{t-1} + \zeta_{t-1} + \nabla\epsilon_t$$

As in most macroeconomic applications the time series are expressed in logs, ∇y_t corresponds in such cases to the growth rate of y_t. The growth rate of a series is thereby related to the notion of the business cycle inasmuch as negative growth rates accompany economic downturns whereas positive growth rates occur during boom phases. Since $\zeta_{t-1} + \nabla\epsilon_t$ is stationary, it becomes apparent that the growth rate of y_t is strongly affected by the common slope, β_t.

To estimate the trend–cycle μ_t, model (2.1) along with the trend–cycle specification (2.2) can be first put into the state space form as described in Appendix 2.A. Then, the Kalman filter is applied to this state space form to estimate the the unknown parameters of the state space model. Finally, the Kalman smoother yields the estimate of μ_t. Details on these filtering and smoothing methodologies are given in Appendix 2.B.

The estimated trend–cycle is used in the second step for cycle estimation. The whole procedure is model–based, meaning that, first, the model for the trend–cycle serves as a basis to derive the models for the trend and the cycle. Second, the parameters of the trend–cycle model estimated in the first step are used in the estimation of the cycle. As will be seen in the next subsection, we draw on the reduced–form model of the trend–cycle in the derivation of the models for the trend and cycle components. A starting point to arrive at the reduced–form is the following equation derived from model (2.2):

$$\nabla^2\mu_{t+1} = K\eta_{t-1} + \nabla\zeta_t$$

Taking into account that for any square matrix M, its square root is defined as any matrix $M^{1/2}$ satisfying $M^{1/2}M^{1/2'} = M$, we let $\eta_t = D_\eta^{1/2}u_t^\eta$ and $\zeta_t = D_\zeta^{1/2}u_t^\zeta$. Then, the previous equation can be rewritten as

$$\begin{aligned}\nabla^2\mu_t &= K\eta_{t-2} + (\zeta_{t-1} - \zeta_{t-2}) \\ &= KD_\eta^{1/2}u_{t-1}^\eta + D_\zeta^{1/2}u_t^\zeta - D_\zeta^{1/2}u_{t-1}^\zeta,\end{aligned}$$

where $\mathrm{Var}([u_t^{\zeta'}, u_t^{\eta'}]') = I$. Thus, by defining $v_t = [u_t^{\zeta'}, u_t^{\eta'}]'$, the following reduced–form model for μ_t can be obtained:

$$\begin{aligned}\nabla^2\mu_t &= C_0v_t + C_1v_{t-1} \\ &= C(B)v_t,\end{aligned} \tag{2.3}$$

where B is the backshift operator such that $Bv_t = v_{t-1}$, and $C(B) = C_0 + C_1B$ is a matrix polynomial in B with

$$C_0 = \begin{bmatrix} D_\zeta^{1/2} & 0 \end{bmatrix}, \qquad C_1 = \begin{bmatrix} -D_\zeta^{1/2} & KD_\eta^{1/2} \end{bmatrix} \tag{2.4}$$

2.2.2 Cycle estimation

In order to extract the cycle, a fixed band–pass filter is applied to the estimated trend–cycle component, μ_t. The filter is in this article referred to as the multivariate filter but its use amounts to the application of the same univariate filter to each individual trend–cycle component, μ_{lt}, $l = 1, ...k$. We design a two–sided version of a univariate band–pass Butterworth filter based on the tangent function using the specification parameters δ_1, δ_2, x_{p1}, x_{p2}, x_{s1} and x_{s2} (see Gómez, 2001). The values of these parameters determine the shape of the gain function of the filter, $G(x)$, where x denotes the angular frequency. To be more specific, it holds that $1 - \delta_1 < G(x) \leq 1$ for $x \in [x_{p1}, x_{p2}]$ and $0 \leq G(x) < \delta_2$ for $x \in [0, x_{s1}]$ and $x \in [x_{s2}, \pi]$.

It is possible and convenient to first design a low–pass filter and then, by means of a transformation, to derive from it its band–pass version (see Oppenheim and Schafer, 1989, pp. 430–434). While designing the low–pass filter, we let $x_p = x_{p2} - x_{p1}$ and $x_s = x_{s2} - x_{p1}$ so that the gain function of the low–pass filter, $G_{lp}(x)$, satisfies $1 - \delta_1 < G_{lp}(x) \leq 1$ for $x \in [0, x_p]$ and $0 \leq G_{lp}(x) < \delta_2$ for $x \in [x_s, \pi]$. For such a choice of the parameters x_p and x_s, the appropriate transformation from a low–pass to a band–pass filter is $z =$

$-s(s-\alpha)/(1-\alpha s)$, where $\alpha = \cos((x_{p2}+x_{p1})/2)/\cos((x_{p2}-x_{p1})/2)$ and $-1 < \alpha < 1$. It is shown in Gómez (2001) that the band–pass filters obtained from Butterworth filters based on the tangent function admit a model–based interpretation. According to this interpretation, the considered band–pass filter is the Wiener–Kolmogorov filter that estimates the signal in the signal plus noise model

$$z_t = s_t + n_t, \tag{2.5}$$

where the signal, s_t, follows the model

$$(1 - 2\alpha B + B^2)^d s_t = (1 - B^2)^d b_t \tag{2.6}$$

The parameters d, α and the quotient of the standard deviations of n_t and b_t, $\lambda = \sigma_n/\sigma_b$, depend on the specification parameters δ_1, δ_2, x_p, and x_s.[1] The reduced–form model for z_t in (2.5) is

$$(1 - 2\alpha B + B^2)^d z_t = \theta_z(B) a_t,$$

where $\theta_z(B)$ is of degree $2d$. Letting $\delta_z(B) = (1 - 2\alpha B + B^2)^d$, the Wiener–Kolmogorov filters to estimate s_t and n_t in (2.5) are

$$h_s = \frac{\sigma_b^2}{\sigma_a^2} \frac{(1-B^2)^d (1-F^2)^d}{\theta_z(B)\theta_z(F)}, \qquad h_n = \frac{\sigma_n^2}{\sigma_a^2} \frac{\delta_z(B)\delta_z(F)}{\theta_z(B)\theta_z(F)},$$

respectively, where F is the forward operator such that $Fz_t = z_{t+1}$, $\sigma_b^2 = \mathrm{Var}(b_t)$, $\sigma_n^2 = \mathrm{Var}(n_t)$ and $\sigma_a^2 = \mathrm{Var}(a_t)$.[2]

The previous considerations allow for the integration of the fixed band–pass filter described earlier into a multivariate model–based approach. To show this, we first consider the pseudo covariance generating function (CGF) of μ_t. Denoted by f_μ, the CGF of μ_t can

[1] The parameters d and λ can be computed using the low–pass version of the filter as explained in Gómez (2001, p. 372). It should be thereby taken into account that $\lambda = 1/\tan^d(x_c/2)$, where x_c is a frequency such that $G_{lp}(x_c) = 1/2$. For the filter used in this article, the values for the parameters in (2.6) are $d = 3$, $\alpha = 0.9921$ and $\lambda = 437.19$.

[2] The derivation of the polynomial $\theta_z(B)$ and the variance σ_a^2 is provided by Gómez (2001, p. 371). Without loss of generality, we set for the filter used in this article $\sigma_b^2 = 1$. Then, for this filter $\sigma_n = 437.19$ and $\sigma_a = 568.58$.

be decomposed as follows:

$$\begin{aligned} f_\mu &= h_s f_\mu + (1-h_s) f_\mu \\ &= f_c + f_p, \end{aligned}$$

where $f_c = h_s f_\mu$ and $f_p = (1-h_s) f_\mu$. This decomposition defines the decomposition of μ_t into two orthogonal unobserved components, c_t and p_t, with CGFs f_c and f_p, respectively. Since the Wiener–Kolmogorov filter to estimate c_t in the model $\mu_t = c_t + p_t$ is the band–pass filter $h_s = f_c/f_\mu$, the subcomponent c_t is considered as the cycle, whereas the other subcomponent, p_t, represents the trend.

The models for c_t and p_t are obtained from their CGFs. Using the reduced–form model for μ_t in eq. (2.3), the CGF of c_t can be written as

$$\begin{aligned} f_c &= h_s f_\mu \\ &= \frac{1}{(1-B)^2}(C_0 + C_1 B)(C_0' + C_1' F)\frac{1}{(1-F)^2}\frac{\sigma_b^2}{\sigma_a^2}\frac{(1-B^2)^d(1-F^2)^d}{\theta_z(B)\theta_z(F)} \\ &= \frac{(1-B)^{d-2}(1+B)^d}{\theta_z(B)}(C_0 + C_1 B)\frac{\sigma_b^2}{\sigma_a^2}(C_0' + C_1' F)\frac{(1-F)^{d-2}(1+F)^d}{\theta_z(F)}, \end{aligned}$$

where C_0 and C_1 are as in (2.4). From this, it follows that the model for c_t is

$$\theta_z(B) c_t = (1-B)^{d-2}(1+B)^d \overline{C}(B)\overline{v}_t, \tag{2.7}$$

where $\overline{C}(B) = (\sigma_b/\sigma_a)C(B)$ and $\mathrm{Var}(\overline{v}_t) = I$. In a similar way, it can be shown that the model for p_t is

$$(1-B)^2 \theta_z(B) p_t = \delta_z(B)\widetilde{C}(B)\widetilde{v}_t, \tag{2.8}$$

where $\widetilde{C}(B) = (\sigma_n/\sigma_a)C(B)$ and $\mathrm{Var}(\widetilde{v}_t) = I$.

Knowing the models for c_t and p_t, the cycle can be estimated using the state space framework. The state space model is set up by taking into account decomposition (2.1) and the decomposition of μ_t into c_t and p_t. Details on this state space representation are provided in Appendix 2.A. The matrices of this state space form contain the parameters of the trend–cycle mode as well as the parameters of the band–pass filter. The former have been estimated as described in the previous subsection whereas the values of the filter parameters have been selected so as to extract the waves corresponding to business cycle frequencies. Therefore, the matrices of the state state representation of the total

model do not have to be estimated. The covariance square root Kalman smoother applied to this state space model yields the estimated cycle.

2.3 Empirical results

2.3.1 Data with mixed frequencies and missing values

In this section, the proposed methodology is used to construct US business cycle indicators on the basis of a set of US macroeconomic time series. To assess the performance of this method, the results in Creal et al. (2010) are considered as a benchmark. For notational convenience, we will use the acronym CKZ when referring to this study. To make the comparison as reliable as possible, the same dataset consisting of 11 seasonally adjusted time series from 1953.M4 to 2007.M9 is used (for details see Creal et al., 2010, p. 702). The monthly series are: the industrial production index (IPI), the unemployment rate, average weekly working hours in manufacturing, and two series from the retail sales category. One of them, retail sales, is discontinued in 2001.M4 whereas the other one, retail sales and food services, is observed between 1991.M1 and 2007.M9. The remaining series, i.e. real GDP, consumer price index inflation, consumption, investment, productivity of the non–farm business sector and hours of the non–farm business sector are available on a quarterly basis. All series except for the unemployment rate and inflation are in logs and multiplied by 100.

An important property of the dataset is the presence of missing values. This, however, poses no problem because the Kalman filter can easily handle missing observations. Another feature of the data is the different observation frequency. Even though the models presented in the previous section as well as their corresponding state space forms are formulated for monthly data, quarterly data can be accommodated in this framework in a straightforward manner.

It is to be noted that different time aggregation patterns apply depending on whether the variables are stocks, time–averaged stocks or flows. It would be possible to account for these different types of variables by incorporating the so–called cumulator variables (see Harvey, 1989, pp. 306–239). They are defined in terms of variables not being transformed so that the correct use of the cumulator variables in the case of series in logs would imply non–linear state space models. Proietti and Moauro (2006) offered an estimation and signal extraction approach for these models. If, instead, the definitions of the cumulator

variables are assumed to hold also for series in logs as in Mariano and Murasawa (2003), this can lead to inaccuracies in the components estimates.
In this study, we proceed as Valle e Azevedo et al. (2006) and Creal et al. (2010). For simplicity, we disregard the different time aggregation schemes and treat quarterly data as monthly data with two missing observations added between two consecutive quarterly observations. In this way, non–linearities and larger model dimensions caused by the cumulator variables can be avoided. Since we are primarily interested in capturing the cycle dynamics, this simplification should not have a great impact on the objective of this study.

2.3.2 Business cycle indicators

Figure 5.1 depicts the business cycle indicators, the IPI and real GDP cycles, estimated in the multivariate framework.[3] It is apparent that the recessions implied by both cycles are in line with the recessions dated by NBER. The IPI cycle is undoubtedly much more volatile than the GDP cycle. Whereas the standard deviation of the GDP cycle is equal to 1.59, the corresponding value for the IPI case is 3.31, more than twice as high. However, both cycles show a very similar pattern. This observation can be also confirmed by their contemporary correlation of 0.945. The high degree of synchronization let them act as alternative recession indicators. The most remarkable deviation in values of each cycle within a single recession can be observed between 1973 and 1975. The strong fall from high positive to high negative values suggests the most severe downturn in the analyzed time span. A further, very sharp decline in the economic activity occurs in the early 1980s and is a result of two recessions separated by a peak in 1981, as is evident from Figure 5.1. Beside the dips classified by NBER as recessions, both cycles exhibit three smaller dips: the first one in the late 1960s, the second one between 1984 and 1987 and the third one in the mid–1990s. The IPI and GDP cycles are not only able to reproduce the previous US history of downturns, as is made clear by Figure 5.1, but they also nearly coincide with the respective cycles extracted by Creal et al. (2010).
Given the business cycle indicator, the remaining series can be classified as leading, lagging or coincident indices depending on how they are shifted relative to the business cycle. If the cycle is explicitly modeled in a multivariate structural model, a possible way to identify the lead–lag pattern is to directly incorporate phase shifts into the model with a common

[3] All computations have been performed with Matlab R2012b (64–bit) using the SSMMatlab toolbox by Gómez (2012) and procedures written by Víctor Gómez.

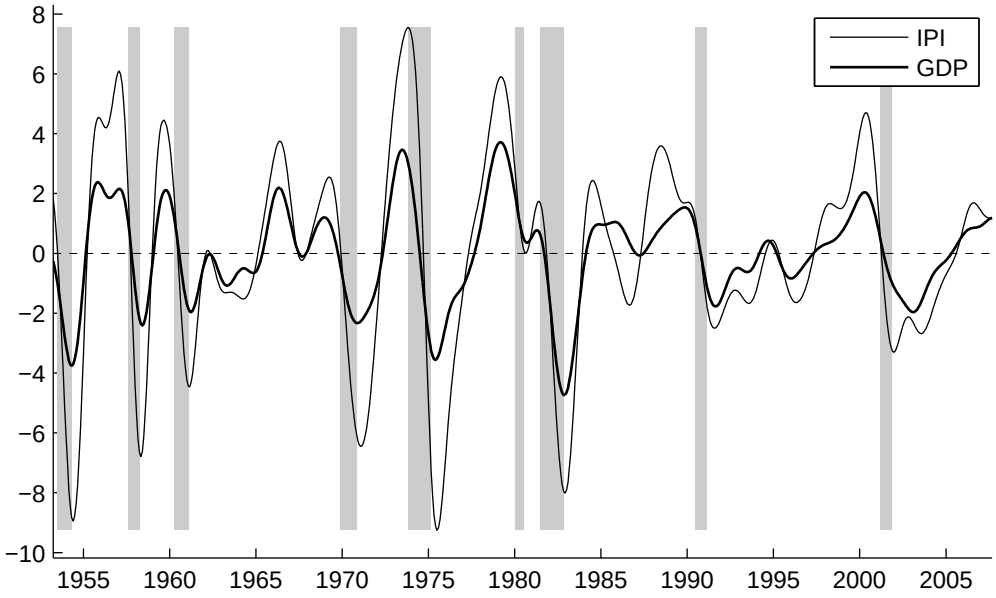

Figure 2.1: Cycles of the industrial production index (IPI) and real GDP as the business cycle indicators

Note: NBER recession dates are represented by the vertical bands.

cycle according to the approach of Rünstler (2004) that has been applied in Creal et al. (2010) and Valle e Azevedo et al. (2006). This has an advantage that the inherent feature of business cycle dynamics is accounted for in the generalized structural model in a consistent way. On the other hand, this procedure also increases the number of parameters to be estimated. In order to keep the model tractable, Valle e Azevedo et al. (2006) fixed the frequency of the common cycle to a specific value so that the inclusion of the shift parameter necessitates additional restrictions. The Bayesian approach for parameter estimation adopted by Creal et al. (2010) per se involves choosing prior distributions for the parameters. The classification procedure we follow in this article has the advantage that it does not increase the model complexity nor does it require certain assumptions. It relies on the concept of phase angle. This measure is well suited to establish the lead–lag relation of two time series as well as the direction (positive or negative) of their relationship. By means of the phase angle, the behavior of the particular cycle with respect to the business cycle can be examined.

If the value of the phase angle at the angular frequency ω, $\theta(\omega)$, lies between 0 and π, the particular series is said to lag the business cycle at ω. The opposite case is implied

by $-\pi < \theta(\omega) < 0$. The particular series is defined as coincident at ω, if $\theta(\omega)$ equals zero. Moreover, values of the phase angle ranging between $(-\pi/2, \pi/2)$ point to a positive relation between the particular cycle and the business cycle (procyclical behavior/in–phase movement), whereas the values of $\theta(\omega)$ in the interval $[-\pi, -\pi/2)$ or $(\pi/2, \pi]$ indicate a negative relationship (countercyclical behavior/anti–phase movement) between them.[4]
Judgement of the overall behavior can be made based on the phase angle value with respect to a reference frequency. In the case of the CKZ model, it is the frequency of the common cycle. It corresponds to the largest mass of the spectrum of the common cycle and is thus the same for all series under consideration. In contrast, we allow the cycles to have different spectral densities. The natural counterpart of the reference frequency in the CKZ model therefore seems to be the frequency associated with the strongest relationship between the business cycle and the particular cycle. The strength of their frequency–by–frequency relationship is here measured using the concept of coherence. Though the lead–lag classification approach resting on the strongest coherence creates a link to the CKZ phase shift modeling, it can disregard possible countervailing patterns in the business cycle frequency interval. This problem becomes severe, especially if the spectrum or, in this case, the coherence displays more than one peak and contrasting patterns can be identified among some of them. To avoid this potential problem, it may be useful to analyze the overall behavior of the particular series by evaluating the mean phase angle in the whole business cycle frequency interval $[2\pi/96, 2\pi/18]$. For that purpose, we employ the concept of a mean appropriate for data measured on the angular scale (see Fisher and Lewis, 1983).
The results of the lead–lag analysis pertaining to the IPI cycle as a business cycle indicator can be found in Table 2.1. In addition to the single estimates of the phase angle based on the reference frequency, $\theta(\omega_h)$, and the mean phase angles $\bar{\theta}$, the respective confidence intervals are reported.[5] It is evident that manufacturing working hours, productivity and investment are leading the business cycle at the 5% significance level. According to the statistically significant negative value of the mean phase angle, consumption can be also

[4]Note that the range of the phase angle is constrained to the interval $[-\pi, -\pi]$. The rationale for this common practice and a comprehensive discussion on the values of the phase angle are provided by Marczak and Beissinger (2013).

[5]The confidence bounds for the estimates of the phase angle and the mean phase angles have been constructed as described in Koopmans (1974, pp. 285–287) and Fisher and Lewis (1983), respectively. All computations for the lead–lag analysis have been performed with Matlab R2012b (64–bit) using the Spectran toolbox by Marczak and Gómez (2012). Manual to this toolbox is also provided in Appendix A of this thesis.

classified as a leading indicator. Similar observation can be made for both series from the retail sales category. All these results confirm the CKZ findings. One of the few divergences relative to the CKZ results pertains to the unemployment rate. From the significance of the negative values of $\theta(\omega_h)$ and $\bar{\theta}$, it can be inferred that this series is leading the business cycle. However, the values of $\theta(\omega_h)$ and $\bar{\theta}$ are both very close to π, a value for which the unemployment rate could be characterized as leading or as lagging the business cycle. In fact, it can be observed that the unemployment rate increases before the business cycle reaches its peak, but it also rises after a trough in the economic activity. In the real GDP case, a coincident behavior cannot be ruled out whereas the CKZ findings suggest a leading behavior of real GDP instead. The remaining series, inflation and, as opposed to the CKZ results, hours in the non–farm business are lagging the business cycle at the 5% significance level.

Table 2.1: Leading, lagging and coincident indicators relative to the IPI cycle[a)]

IPI and	Period τ_h in years [b)]	$\theta(\omega_h)$	95% Conf. interval for $\theta(\omega_h)$		$\bar{\theta}$ [c)]	95% Conf. interval for $\bar{\theta}$	
Unemployment	3.41	−0.920	−0.975	−0.865	−0.929	−0.942	−0.916
Manufacturing	3.63	−0.170	−0.237	−0.103	−0.157	−0.173	−0.140
Inflation	5.45	0.329	0.243	0.415	0.166	0.108	0.224
Retail	4.54	−0.070	−0.180	0.040	−0.086	−0.131	−0.041
Retail/food	3.41	−0.050	−0.242	0.142	−0.061	−0.089	−0.033
Productivity	4.19	−0.388	−0.508	−0.267	−0.241	−0.287	−0.195
Real GDP	7.79	−0.030	−0.076	0.016	0.007	−0.014	0.028
Hours	3.03	0.096	0.050	0.141	0.111	0.096	0.126
Consumption	4.54	0.006	−0.109	0.121	−0.146	−0.213	−0.079
Investment	7.79	−0.151	−0.210	−0.092	−0.002	−0.028	0.025

[a)] Angular measures are expressed in terms of shares of π.
[b)] τ_h corresponds to the frequency ω_h at which the coherence between the business cycle indicator and the respective series attains the highest value.
[c)] $\bar{\theta}$ denotes the mean phase angle computed in the frequency interval $[2\pi/96, 2\pi/18]$.

As regards the movements with or against the business cycle, almost all indicators exhibit a statistically significant procyclical pattern. Only the unemployment rate is statistically significant countercyclical. It is worth noting that the similar cyclical behavior for both series, retail sales and retail sales with food services, is not a consequence of any restrictions.

Analogously to Table 2.1 related to the IPI cycle, Table 2.2 summarizes the results related to the GDP cycle as a business cycle indicator. It can be noticed that they do not

qualitatively differ from the ones corresponding to the IPI cycle. Hence, both business cycle indicators can in this case serve as equivalent reference measures.

Table 2.2: Leading, lagging and coincident indicators relative to the GDP cycle[a)]

Real GDP and	Period τ_h in years [b)]	$\theta(\omega_h)$	95% Conf. interval for $\theta(\omega_h)$		$\bar{\theta}$ [c)]	95% Conf. interval for $\bar{\theta}$	
Unemployment	4.54	−0.930	−0.986	−0.874	−0.931	−0.947	−0.915
Manufacturing	6.81	−0.180	−0.255	−0.105	−0.151	−0.167	−0.135
Inflation	6.06	0.308	0.191	0.425	0.241	0.197	0.286
Retail	2.27	−0.121	−0.205	−0.036	−0.080	−0.108	−0.052
Retail/food	1.56	−0.222	−0.438	−0.006	−0.054	−0.084	−0.025
Productivity	3.63	−0.293	−0.384	−0.201	−0.217	−0.249	−0.186
IPI	7.79	0.030	−0.016	0.076	−0.007	−0.028	0.014
Hours	3.41	0.131	0.083	0.178	0.110	0.098	0.123
Consumption	4.54	−0.009	−0.095	0.077	−0.066	−0.105	−0.028
Investment	5.45	−0.101	−0.128	−0.075	−0.010	−0.030	0.011

[a)] Angular measures are expressed in terms of shares of π.
[b)] τ_h corresponds to the frequency ω_h at which the coherence between the business cycle indicator and the respective series attains the highest value.
[c)] $\bar{\theta}$ denotes the mean phase angle computed in the frequency interval $[2\pi/96, 2\pi/18]$.

2.3.3 Forecasting

Forecasts of the recessions

Apart from providing stylized facts about the past and the current state of the economy, a method for extracting a business cycle indicator should perform well with respect to forecasting. Accurate forecasts of the economic activity in the near future are of a vital importance for economic policy. What is more, the timeliness of the forecasts also plays an essential role in the decision making process, as the information at a higher frequency, e.g. on a monthly basis, gives a more detailed picture on the future economic situation. This aspect has become a motivation for the recently growing literature on the so–called nowcasting dealing with real–time data (see, e.g., Giannone et al., 2008, and Bańbura et al., 2012). From the computational point of view, a simple model is advantageous over an elaborate one since it is easier to understand, implement and adjust, and it possibly requires less restrictions. In this section, we show that the multivariate method proposed in this article embodies all these features of a good forecasting model as it is able to yield good realtime predictions in a relatively simple modeling framework.

To examine the performance of the presented approach, we first compute one–year forecasts of the IPI and GDP cycle based on the whole sample to check whether the forecasts can reproduce the last recession starting in 2007.M12. Further, the model is estimated with two shorter samples, until 2000.M12 and 1990.M4, respectively. In both cases we also calculate one–year forecasts for both business cycle indicators. In this way, the robustness of this methodology shall be investigated. Figure 2.2 depicts the smoothed IPI and GDP cycle estimates along with the respective forecasts in three intervals. The results make clear that the proposed method can predict the last three recessions very well.

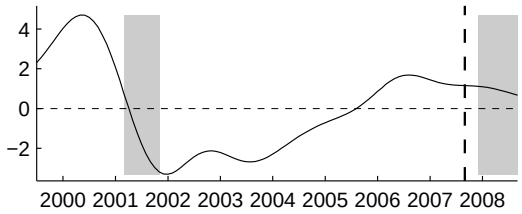

(a) IPI: Forecast interval 2007.M10–2008.M9

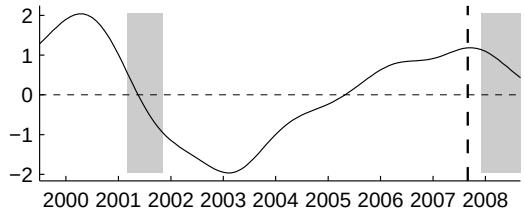

(d) GDP: Forecast interval 2007.M10–2008.M9

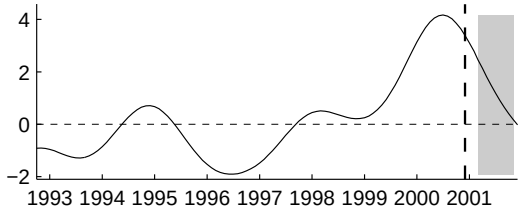

(b) IPI: Forecast interval 2001.M1–2001.M12

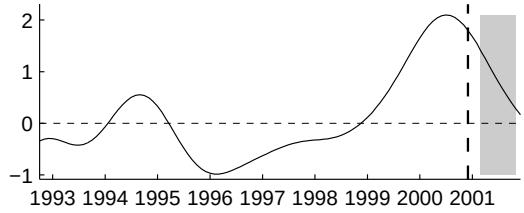

(e) GDP: Forecast interval 2001.M1–2001.M12

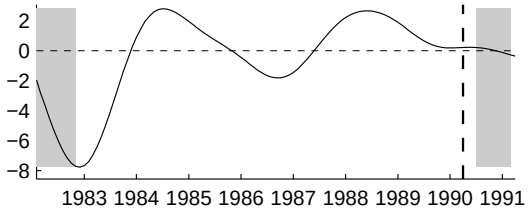

(c) IPI: Forecast interval 1990.M5–1991.M4

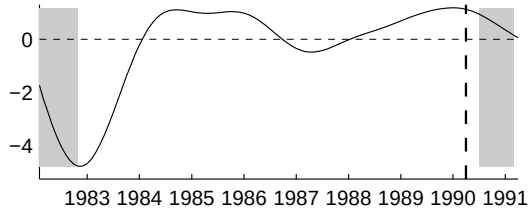

(f) GDP: Forecast interval 1990.M5–1991.M4

Figure 2.2: Smoothed cycle estimates and one–year forecasts for three time intervals
Notes: NBER recession dates are represented by the vertical bands.

2.3.3.1 Comparison with the model with a structural volatility break

Since the focus of this article lies on developing a reliable, albeit simple, model for the cycle extraction and forecasting, the model presented in Section 2.2 cannot explicitly take into account any possible structural changes present in the data. Indeed, initiated by the studies of Kim and Nelson (1999) and McConnell and Pérez-Quirós (2000), the recent literature provides an evidence of a substantial reduction in the volatility of many macroeconomic time series in the US. There is no consensus whether the moderation has occurred in form of a break, as suggested by Stock and Watson (2002) (or maybe multiple breaks discussed by Sensier and van Dijk, 2004), or rather a gradual change in the volatility, as advocated by Blanchard and Simon (2001). Even though in this part of the study we try to address the issue of the volatility decline, we do not aim to contribute to the literature on the Great Moderation. We rather intend to find out whether accounting for this effect influences the forecast performance. For this reason, a single (one–time) volatility break is considered. we rely on the break time point in 1984.M1 initially detected for output growth by Kim and Nelson (1999) and McConnell and Pérez-Quirós (2000). This single volatility break is incorporated in the common slope and in the multivariate irregular component. We thereby follow the approach proposed by Tsay (1988). For the sake of comparison, Figure 2.3 presents the IPI and GDP cycles and their forecasts from the model with the volatility break and the base model. The differences between these results refer to the IPI case but are rather small, so that the specification without the volatility break seems to be even better in terms of forecasting than the more complex alternative. In contrast, the stochastic volatility specification in the CKZ model helps correctly predict the last recession.

2.3.3.2 Comparison with the univariate model based on a band–pass filter

The obvious advantage of a multivariate model over an univariate approach is that it is capable of yielding monthly information on the GDP cycle. Forecasts of the economic situation based on real GDP are in this case more precise in terms of timing than quarterly forecasts resulting from an univariate model. Hence, they represent an alternative to forecasts based on the monthly IPI. The question arises whether, apart from realtime forecasts, the multivariate model presented in Section 2.2 can as well warrant an improvement in the forecasts quality over univariate methods. To examine this aspect, it seems natural to consider the univariate version of the proposed multivariate model. In so do-

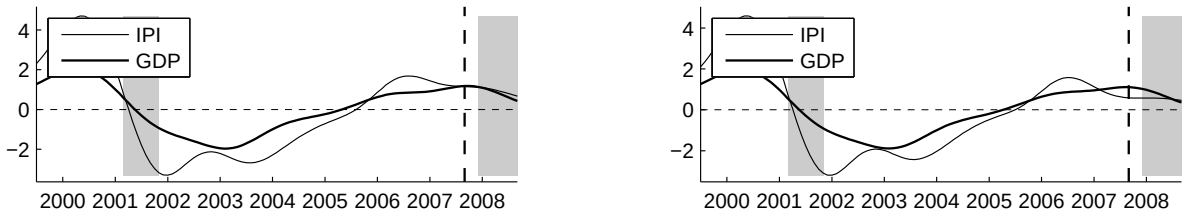

(a) Base model **(b)** Model with the volatility break

Figure 2.3: Smoothed cycle estimates and one–year forecasts from 2007.M10 onwards based on the base model and the model with the volatility break in 1984.M1, respectively

Notes: NBER recession dates are represented by the vertical bands.

ing, it can be ensured that potential differences in the outcomes are not a consequence of fundamental differences in the modeling principles and thus in the resulting stochastic features. In particular, the univariate structural model with trend–cycle and irregular is estimated for the IPI and real GDP. In the second step, the univariate band–pass filter described in Section 2.2.2 is applied to the estimated trend–cycle. Similarly to the multivariate counterpart, the procedure is fully model–based. To facilitate the comparison of both approaches, the forecasts are investigated in the same time intervals as in the multivariate case: 2007.M10–2008.M9, 2001.M1–2001.M12 and 1990.M5–1991.M4. For real GDP, these forecasts intervals are translated to the corresponding quarters. The smoothed IPI and GDP cycles along with their forecasts obtained with the univariate model are depicted in Figure 2.4.

As regards the IPI cycle (Figures 2.4a, 2.4b and 2.4c), the forecasts are almost identical with those resulting from the multivariate model (see Figures 2.2a, 2.2b and 2.2c). In the GDP case, on the other hand, the forecasts misleadingly suggest an expansion in the intervals 2007.Q4–2008.Q3 and 1990.Q2–1991.Q1 as can be seen in Figures 2.4d and 2.4f, respectively. This observation is consistent with the finding of Creal et al. (2010). They show that the univariate version of their model (without stochastic volatility) applied to real GDP is not capable of predicting the last recession. The preceding analysis leads to the conclusion that the multivariate model not only can produce forecasts at a frequency higher than the frequency of the data itself, but also offers a better framework for forecasting purposes than the univariate counterpart, at least for real GDP.

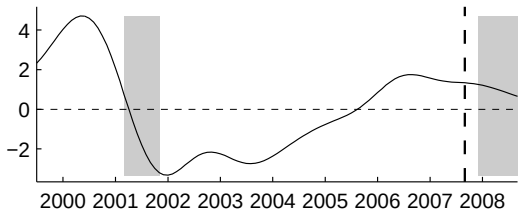

(a) IPI: Forecast interval 2007.M10–2008.M9

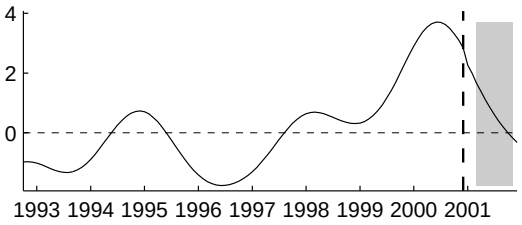

(b) IPI: Forecast interval 2001.M1–2001.M12

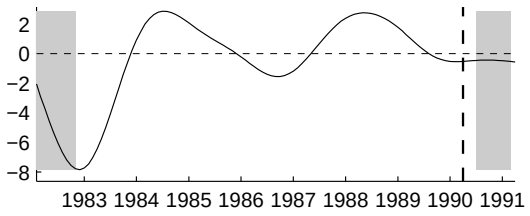

(c) IPI: Forecast interval 1990.M5–1991.M4

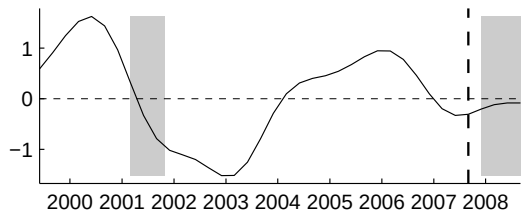

(d) GDP: Forecast interval 2007.Q4–2008.Q3

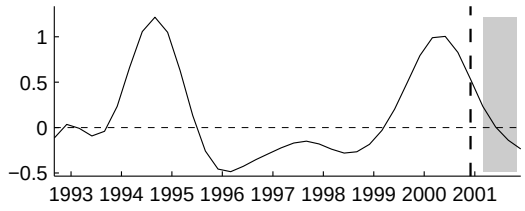

(e) GDP: Forecast interval 2001.Q1–2001.Q4

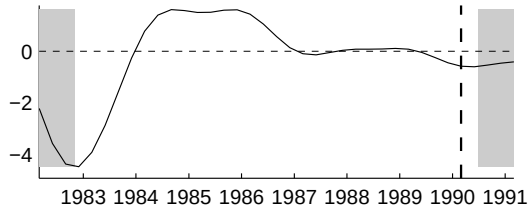

(f) GDP: Forecast interval 1990.Q2–1991.Q1

Figure 2.4: Smoothed cycle estimates based on the univariate model and one–year forecasts for three time intervals

Notes: NBER recession dates are represented by the vertical bands.

2.4 Conclusions

This article presents a new multivariate model used to construct monthly business cycle indicators for the US. This approach is based on a multivariate structural model and a univariate band–pass filter. It contributes to the literature on the business cycle analysis in several ways. The model allows for considering series observed at different frequencies. Therefore, advantage can be taken of the information contained in several monthly and quarterly macroeconomic indicators which are considered in this article. The two obtained business cycle indicators are, however, given on a monthly basis. They are represented by the cycles of the industrial production index (IPI) and real GDP, respectively. The indicators are smooth and thus consistent with the definition of a business cycle. Moreover,

they can reproduce previous recessions very well. Another feature of the approach is its two–step framework as opposed to the single–step framework of the conventional multivariate structural time series models with explicitly modeled cycle. The proposed strategy avoids the problem of modeling the cycle directly so that it reduces the complexity of the structural model in the first step and facilitates its estimation.

The different series used in the proposed procedure are not restricted to be coincident. Their behavior in relation to the business cycle is, however, not explicitly modeled by extra parameters which would increase the complexity of the model. The relationship of other indicators with the real GDP or IPI cycle can still be analyzed after cycle estimation has been performed. For that purpose, the frequency–domain concepts of the phase angle and the mean phase angle are employed. The analysis reveals that the results are virtually the same for both reference cycles. Manufacturing working hours, productivity and retail sales are leading the business cycle at the 5% significance level. Inflation and hours in the non–farm business are statistically significant lagging indicators. For the unemployment rate, the results are somewhat ambiguous. Almost all of the indicators are statistically significant procyclical indicators, whereas the unemployment rate is statistically significant countercyclical.

The greatest strength of the presented approach lies in its forecasting performance. The ability to produce high quality forecasts provided at high frequency can represent a valuable feature for policy making. It is demonstrated that the model is capable of predicting not only the most recent recession but also the two previous ones. No additional assumptions, like changes in the volatility, are needed to achieve such good results. For the sake of completeness, the forecasts obtained with the base model are compared with the forecasts from the model with a volatility break. This comparison cannot uncover any differences. The comparison with the forecasts from the univariate counterpart of the proposed model, on the other hand, shows that the multivariate version performs far better, at least in the real GDP case.

Appendix

2.A State space representations

Monthly model with the trend–cycle

A state space form for the trend–cycle in eq. (2.2) is

$$\begin{aligned} \alpha_{t+1} &= T_\mu \alpha_t + H_\mu v_t \\ \mu_t &= Z_\mu \alpha_t, \end{aligned} \tag{2.A.1}$$

where $\alpha_t = (\mu_t', \beta_t')'$, v_t is as in eq. (2.3), and

$$\begin{aligned} T_\mu &= \begin{bmatrix} I_k & K \\ 0 & I_r \end{bmatrix}, \qquad H_\mu = \begin{bmatrix} D_\zeta^{1/2} & 0 \\ 0 & D_\eta^{1/2} \end{bmatrix}, \\ Z_\mu &= \begin{bmatrix} I_k & 0 \end{bmatrix}, \qquad r = 1 \end{aligned} \tag{2.A.2}$$

Then, a state space form for the monthly model is

$$\begin{aligned} \alpha_{t+1} &= T\alpha_t + Hu_t \\ y_t &= Z\alpha_t + Gu_t, \qquad t = 1, \ldots, n, \end{aligned}$$

where $u_t = (v_t', \varepsilon_t')'$ with $\mathrm{Var}(u_t) = I$, $T = T_\mu$, $Z = Z_\mu$ and

$$H = \begin{bmatrix} D_\zeta^{1/2} & 0 & 0 \\ 0 & D_\eta^{1/2} & 0 \end{bmatrix}, \qquad G = \begin{bmatrix} 0 & 0 & D_\epsilon^{1/2} \end{bmatrix}$$

The initial state vector $\alpha_1 = (\mu_1', \beta_1')'$ is

$$\alpha_1 = A\delta + p,$$

where δ has dimension $k + r$ and is diffuse, A is a suitable nonstochastic matrix, and p has zero mean and a well defined covariance matrix.

Monthly model including the cycle

For numerical reasons, the model for p_t in eq. (2.8) is implemented in cascade form as

$$p_t = \left[\theta_z^{-1}(B)\delta_z(B)\right] w_t, \tag{2.A.3}$$

where w_t follows the model

$$w_t = \left[(1-B)^{-2}\widetilde{C}(B)\right] \widetilde{v}_t$$

A state space model for w_t can be easily derived from (2.A.1), namely

$$\begin{aligned} \gamma_{t+1} &= T_w\gamma_t + H_w\widetilde{v}_t, \\ w_t &= Z_w\gamma_t, \end{aligned}$$

where $T_w = T_\mu$, $Z_w = Z_\mu$ and $H_w = (\sigma_n/\sigma_a)H_\mu$, and the matrices T_μ, Z_μ and H_μ are given in (2.A.2). As for p_t in eq. (2.A.3), we select the multivariate version of the state space representation used by Gómez and Maravall (1994), which is an extension to the nonstationary case of the approach proposed by Akaike (1974). Thus, the state space representation of (2.A.3) is

$$\begin{aligned} \xi_t &= T_v\xi_{t-1} + H_v w_t \\ p_t &= Z_v\xi_t, \end{aligned} \tag{2.A.4}$$

where $\xi_t = (p_t', p_{t+1|t}', ..., p_{t+q|t}')'$, $\theta_z(B) = 1 + \sum_{i=1}^{q}\theta_{z,i}B^i$, $q = 2d$ is the degree of both polynomials, $\theta_z(B)$ and $\delta_z(B)$,

$$\begin{aligned} T_v &= \begin{bmatrix} 0 & I & 0 & \cdots & 0 \\ 0 & 0 & I & \cdots & 0 \\ \vdots & \vdots & \vdots & \ddots & \vdots \\ 0 & -\theta_{z,q}I & -\theta_{z,q-1}I & \cdots & -\theta_{z,1}I \end{bmatrix}, \qquad H_v = \begin{bmatrix} I \\ V_1 I \\ \vdots \\ V_q I \end{bmatrix}, \\ Z_v &= \begin{bmatrix} I & 0 & \cdots & 0 \end{bmatrix}, \end{aligned} \tag{2.A.5}$$

and V_i, $i = 0, ..., q$, are the coefficients obtained from $V(B) = \delta_z(B)/\theta_z(B)$. Thus, the state space model for the cascade form of the model for p_t described earlier is

$$\begin{aligned} \varphi_{t+1} &= T_p\varphi_t + H_p\widetilde{v}_{t+1} \\ p_t &= Z_p\varphi_t, \end{aligned} \tag{2.A.6}$$

where $\varphi_t = (\xi_t', \gamma_{t+1}')'$ and

$$T_p = \begin{bmatrix} T_v & H_v Z_w \\ 0 & T_w \end{bmatrix}, \qquad H_p = \begin{bmatrix} 0 \\ H_w \end{bmatrix}, \qquad Z_p = \begin{bmatrix} Z_v & 0 \end{bmatrix}$$

Similarly to (2.A.4), the state space form considered for c_t in eq. (2.7) is

$$\begin{aligned} \chi_{t+1} &= T_c\chi_t + H_c\overline{v}_{t+1} \\ c_t &= Z_c\chi_t, \end{aligned} \tag{2.A.7}$$

where $\chi_t = (c_t', c_{t+1|t}', ..., c_{t+q-1|t}')'$,

$$T_c = \begin{bmatrix} 0 & I & 0 & \cdots & 0 \\ 0 & 0 & I & \cdots & 0 \\ \vdots & \vdots & \vdots & \ddots & \vdots \\ -\theta_{z,q}I & -\theta_{z,q-1}I & -\theta_{z,q-2I} & \cdots & -\theta_{z,1}I \end{bmatrix}, \qquad H_c = \begin{bmatrix} I \\ Z_1 I \\ \vdots \\ Z_{q-1}I \end{bmatrix},$$
$$Z_c = \begin{bmatrix} I & 0 & \cdots & 0 \end{bmatrix}$$

and Z_i, $i = 0, ..., q-1$, are the coefficients of the following polynomial

$$Z(B) = (1-B)^{d-2}(1+B)^d \frac{\overline{C}(B)}{\theta_z(B)}$$

Taking models (2.A.6) and (2.A.7) into account, the state space form for $\mu_t = p_t + c_t$ is

$$\begin{aligned} \alpha_{t+1} &= \begin{bmatrix} T_p & 0 \\ 0 & T_c \end{bmatrix} \alpha_t + \begin{bmatrix} H_p & 0 \\ 0 & H_c \end{bmatrix} \begin{bmatrix} \widetilde{v}_{t+1} \\ \overline{v}_{t+1} \end{bmatrix} \\ \mu_t &= \begin{bmatrix} Z_p & Z_c \end{bmatrix} \alpha_t, \end{aligned}$$

where $\alpha_t = (\varphi_t', \chi_t')'$. Thus, the state space form for y_t is

$$\begin{aligned} \alpha_{t+1} &= T\alpha_t + Hu_t \\ y_t &= Z\alpha_t + Gu_t, \qquad t = 1, \ldots, n, \end{aligned}$$

where $u_t = (\widetilde{v}_{t+1}', \overline{v}_{t+1}', \varepsilon_t')'$, $\mathrm{Var}(u_t) = I$, and

$$\begin{aligned} T &= \begin{bmatrix} T_p & 0 \\ 0 & T_c \end{bmatrix}, \qquad H = \begin{bmatrix} H_p & 0 & 0 \\ 0 & H_c & 0 \end{bmatrix}, \\ Z &= \begin{bmatrix} Z_p & Z_c \end{bmatrix}, \qquad G = \begin{bmatrix} 0 & 0 & D_\epsilon^{1/2} \end{bmatrix} \end{aligned}$$

The initial state vector $\alpha_1 = (\varphi_1', \chi_1')'$, where φ_1 and χ_1 are uncorrelated, is

$$\alpha_1 = \begin{bmatrix} A \\ 0 \end{bmatrix} \delta + \begin{bmatrix} p \\ \chi_1 \end{bmatrix}$$

2.B Kalman filter and covariance square root Kalman smoother

Consider a state space model

$$\begin{aligned} x_{t+1} &= T_t x_t + H_t \epsilon_t \\ Y_t &= Z_t x_t + G_t \epsilon_t, \qquad t = 1, ..., n \end{aligned}$$

where $\mathrm{Var}(\epsilon_t) = I$. The initial state vector x_1 is specified as

$$x_1 = c + a + A\delta,$$

where c has zero mean and covariance matrix Ω, a is a constant vector, δ is diffuse and A is a constant matrix. In the following, it is assumed that $\delta = 0$. Even though the model proposed in this article implies $\delta \neq 0$ (see Appendices 2.A and 2.A), this simplifying assumption allows to convey the idea of the applied filtering and smoothing algorithms

in a comprehensive way. The Kalman filter is given by the recursions

$$E_t = Y_t - Z_t\hat{x}_{t|t-1}, \qquad \Sigma_t = Z_tP_tZ_t' + G_tG_t',$$
$$K_t = (T_tP_tZ_t' + H_tG_t')\Sigma_t^{-1}, \qquad \hat{x}_{t+1|t} = T_t\hat{x}_{t|t-1} + K_tE_t,$$
$$P_{t+1} = (T_t - K_tZ_t)P_tT_t' + (H_t - K_tG_t)H_t',$$

initialized with $\hat{x}_{1|0} = a$ and $P_1 = \Omega$. In the general case with $\delta \neq 0$, the so–called diffuse Kalman filter and smoother are applied (see de Jong, 1991).
The formulae for the fixed–interval Kalman smoother are as follows. For $t = n, n-1, \ldots, 1$, define the so–called adjoint variable, λ_t, and its covariance matrix, Λ_t, by the recursions

$$\lambda_t = T_{p,t}'\lambda_{t+1} + Z_t'\Sigma_t^{-1}E_t, \quad \Lambda_t = T_{p,t}'\Lambda_{t+1}T_{p,t} + Z_t'\Sigma_t^{-1}Z_t,$$

initialized with $\lambda_{n+1} = 0$ and $\Lambda_{n+1} = 0$, where $T_{p,t} = T_t - K_tZ_t$. Then, for $t = n, n-1, \ldots, 1$, the projection, $\hat{x}_{t|n}$, of x_t onto the whole sample $\{Y_t : 1 \leq t \leq n\}$ and its MSE, $P_{t|n}$, satisfy the recursions

$$\hat{x}_{t|n} = \hat{x}_{t|t-1} + P_t\lambda_t, \quad P_{t|n} = P_t - P_t\Lambda_tP_t$$

In this article the covariance square root smoother is applied since it proves to be a stable algorithm if the state vector has a large dimension. For square root smoothing, let $\widehat{Z}_t = \Sigma_t^{-1/2}Z_t$ and $T_{p,t} = T_t - \widehat{K}_t\widehat{Z}_t$, where $\widehat{K}_t = T_tP_tZ_t' + H_tG_t')\Sigma_t^{-1/2'}$. Let the QR algorithm produce an orthogonal matrix U_t such that

$$U_t'\begin{bmatrix} \widehat{Z}_t \\ \Lambda_{t+1}^{1/2'}T_{p,t} \end{bmatrix} = \begin{bmatrix} \Lambda' \\ 0 \end{bmatrix},$$

where Λ' is an upper triangular matrix. Then, $\Lambda = \Lambda_t^{1/2}$ and $\lambda_t = T_{p,t}'\lambda_{t+1} + \widehat{Z}_t'\widehat{E}_t$, where $\widehat{E}_t = \Sigma_t^{-1/2}E_t$. The square root form of the fixed interval smoother used in this article is as follows.

Step 1 In the forward pass, compute and store the quantities $\widehat{E}_t$, $\widehat{K}_t$, $\widehat{Z}_t$, $\hat{x}_{t+1|t}$ and $P_{t+1}^{1/2}$.

Step 2 In the backward pass, compute λ_t recursively by means of the formula $\lambda_t = T_{p,t}'\lambda_{t+1} + \widehat{Z}_t'\widehat{E}_t$. In addition, compute $\Lambda_t^{1/2}$ as explained earlier.

Step 3 Finally, using the output given by steps 1 and 2, compute recursively in the backward pass the fixed interval smoothing quantities

$$\begin{aligned} \hat{x}_{t|n} &= \hat{x}_{t|t-1} + P_t^{1/2}\left(P_t^{1/2\prime}\lambda_t\right) \\ P_{t|n} &= P_t^{1/2}\left[I - \left(P_t^{1/2\prime}\Lambda_t^{1/2}\right)\left(\Lambda_t^{1/2\prime}P_t^{1/2}\right)\right]P_t^{1/2\prime} \end{aligned}$$

References

Akaike, H. (1974). Markovian Representation of Stochastic Processes and Its Application to the Analysis of Autoregressive Moving Average Processes. *Annals of the Institute of Statistical Mathematics*, *26*, 363–387.

Bańbura, M., Giannone, D., Modugno, M., and Reichlin, L. (2012). *Now–Casting and the Real–Time Data Flow* (Discussion Paper No. 9112). CEPR.

Baxter, M., and King, R. G. (1999). Measuring Business Cycles. Approximate Band-pass Filters for Economic Time Series. *Review of Economics and Statistics*, *81*, 575–593.

Blanchard, O., and Simon, J. (2001). The Long and Large Decline in U.S. Output Volatility. *Brookings Papers on Economic Activity*, *1*, 135–164.

Box, G. E. P., Hillmer, S. C., and Tiao, G. C. (1978). Analysis and Modeling of Seasonal Time Series. In A. Zellner (Ed.), *Seasonal Analysis of Economic Time Series* (pp. 309–334). Washington, DC: U.S. Dept. Commerce, Bureau of the Census.

Burns, A. F., and Mitchell, W. C. (1946). *Measuring Business Cycles*. New York: NBER.

Cleveland, W. P., and Tiao, G. C. (1976). Decomposition of Seasonal Time Series: A Model for the X-11 Program. *Journal of the American Statistical Association*, *71*, 581–587.

Creal, D., Koopman, S. J., and Zivot, E. (2010). Extracting a Robust US Business Cycle Using a Time–Varying Multivariate Model–Based Bandpass Filter. *Journal of Applied Econometrics*, *25*, 695–719.

de Jong, P. (1991). The Diffuse Kalman Filter. *The Annals of Statistics*, *19*, 1073–1083.

Fisher, N. I., and Lewis, T. (1983). Estimating the Common Mean Direction of Several Circular or Spherical Distributions with Differing Dispersions. *Biometrika*, *70*, 333–341.

Forni, M., Hallin, M., Lippi, M., and Reichlin, L. (2000). The Generalized Factor Model: Identification and Estimation. *Review of Economics and Statistics*, *82*, 540–554.

Giannone, D., Reichlin, L., and Small, D. (2008). Nowcasting: The Real–Time Informational Content of Macroeconomic Data. *Journal of Monetary Economics*, *55*, 665–676.

Gómez, V. (2001). The Use of Butterworth Filters for Trend and Cycle Estimation in Economic Time Series. *Journal of Business and Economic Statistics*, *19*(3), 365–373.

Gómez, V. (2012). *SSMMATLAB, a Set of MATLAB Programs for the Statistical Analysis*

of State–Space Models. Downloadable at `http://www.sepg.pap.minhap.gob.es/sitios/sepg/en-GB/Presupuestos/Documentacion/Paginas/SSMMATLAB.aspx`

Gómez, V., and Maravall, A. (1994). Estimation, Prediction, and Interpolation for Nonstationary Series With the Kalman Filter. *Journal of the American Statistical Association*, *89*, 611–624.

Harvey, A. C. (1989). *Forecasting, Structural Time Series Models and the Kalman Filter.* Cambridge: Cambridge University Press.

Harvey, A. C., and Trimbur, T. M. (2003). General Model-Based Filters for Extracting Cycles and Trends in Economic Time Series. *Review of Economics and Statistics*, *85*, 244–255.

Hodrick, R. J., and Prescott, E. C. (1997). Postwar U.S. Business Cycles: An Empirical Investigation. *Journal of Money, Credit and Banking*, *29*, 1–16.

Kim, C.-J., and Nelson, C. R. (1999). Has the U.S. Economy Become More Stable? A Bayesian Approach Based on a Markov–Switching Model of the Business Cycle. *The Review of Economic and Statistics*, *81*, 608–616.

Koopmans, L. H. (1974). *The Spectral Analysis of Time Series.* London: Academic Press.

Marczak, M., and Beissinger, T. (2013). Real Wages and the Business Cycle in Germany. *Empirical Economics*, *44*, 469–490.

Marczak, M., and Gómez, V. (2012). *SPECTRAN, A Set of Matlab Programs for Spectral Analysis* (Discussion Paper No. 60). FZID. Downloadable at `https://labour.uni-hohenheim.de/81521`

Marczak, M., and Gómez, V. (2013). *Monthly US Business Cycle Indicators: A New Multivariate Approach Based on a Band–Pass Filter* (Discussion Paper No. 64). FZID.

Mariano, R. S., and Murasawa, Y. (2003). A New Coincident Index of Business Cycles Based on Monthly and Quarterly Series. *Journal of Applied Econometrics*, *18*, 427–443.

McConnell, M. M., and Pérez-Quirós, G. (2000). Output Fluctuations in the United States: What Has Changed Since the Early 1980's? *American Economic Review*, *90*, 1464–1476.

Oppenheim, A. V., and Schafer, R. W. (1989). *Discrete–Time Signal Processing.* New Jersey: Prentice Hall.

Proietti, T., and Moauro, F. (2006). Dynamic Factor Analysis with Non–Linear Temporal

Aggregation Constraints. *Journal of the Royal Statistical Society, Series C*, *55*, 281–300.

Rünstler, G. (2004). Modelling Phase Shifts Among Stochastic Cycles. *Econometrics Journal*, *7*, 232–248.

Sensier, M., and van Dijk, D. (2004). Testing for Volatilty Changes in U.S. Macroeconomic Time Series. *The Review of Economics and Statistics*, *86*, 833–839.

Stock, J. H., and Watson, M. W. (1989). New Indexes of Coincident and Leading Economic Indicators. In O. J. Blanchard and S. Fisher (Eds.), *NBER Macroeconomics Annual* (Vol. 4, pp. 351–409). MIT Press.

Stock, J. H., and Watson, M. W. (2002). Has the Business Cycle Changed and Why? In M. Gertler and K. Rogoff (Eds.), *NBER Macroeconomics Annual* (Vol. 17, pp. 159–230). MIT Press.

Tsay, R. S. (1988). Outliers, Level Shifts, and Variance Changes in Time Series. *Journal of Forecasting*, *7*, 1–20.

Valle e Azevedo, J., Koopman, S. J., and Rua, A. (2006). Tracking the Business Cycle of the Euro Area: A Multivariate Model–Based Bandpass Filter. *Journal of Business and Economic Statistics*, *24*, 278–290.

Chapter 3

Outlier Detection in Structural Time Series Models: The Indicator Saturation Approach*

3.1 Introduction

Structural change affects the estimation of economic signals, like the underlying growth rate or the seasonally adjusted series. An important issue is its detection by an expert procedure. Automatic outlier detection is already implemented in official seasonal adjustment procedures, like TRAMO–SEATS (Gómez and Maravall, 1996) and X–12 ARIMA (and its enhanced version X–13 ARIMA–SEATS). Both procedures consist of two main stages. First, the observed time series is modeled by means of a seasonal ARIMA (SARIMA) model with possible regression effects, which may include outlier effects. In the subsequent step, based on the identified model, the series is decomposed into different components, e.g.trend or seasonal component, according to the so–called canonical decomposition (TRAMO–SEATS) or by using a cascade filter (X–12 ARIMA). Outlier detection is carried out in the first stage and follows a specific–to–general approach based on sequential addition (potential outliers are identified one after the other), followed by backward deletion.

In this paper, we take a new look at the detection of structural change in seasonal economic time series. In particular, we consider the structural time series approach proposed by Harvey (1989) and West and Harrison (1997), according to which a parametric model for the series is directly formulated in terms of unobserved components. The reference model for the adjustment purpose is the basic structural model (BSM), proposed by Harvey and

*This chapter is the result of the joint work with Tommaso Proietti and has appeared as Marczak and Proietti (2014).

Todd (1983) for univariate time series, and extended by Harvey (1989) to the multivariate case. The BSM postulates an additive decomposition of the series into a trend, a seasonal and an irregular component. Though this model is relatively simple, it is flexible and provides a satisfactory fit to a wide range of seasonal time series. The model can be represented in state space form, which enables the use of efficient algorithms, such as the Kalman filter and smoother, for likelihood evaluation, prediction and the estimation of the unobserved components. We refer to Durbin and Koopman (2012) for a comprehensive and up–to–date treatment of state space methods.

Seasonal adjustment using structural time series models is well established and can be performed by the specialized software STAMP 8 (Koopman et al., 2009). However, in contrast to the officially used software packages for seasonal adjustment, the latter offers only a basic facility for automatic treatment of outliers. This aspect justifies the necessity for investigation of different approaches to outlier detection in this particular framework. We follow here the indicator saturation (IS) approach which is a new, yet very promising strand of research on outlier detection. It has been proposed by Hendry (1999) and constitutes a general–to–specific approach. In his seminal work, Hendry (1999) introduced the impulse–indicator saturation (IIS) as a test for an unknown number of breaks, occurring at unknown times, with unknown duration and magnitude. The procedure relies on adding a pulse dummy as an intervention at every observation in the sample. Significant dummies at individual points in time indicate additive outliers. Properties of this method have been studied by Johansen and Nielsen (2009), Hendry et al. (2008) and Castle et al. (2012). Economic applications of IIS have been provided by, e.g., Hendry and Mizon (2011), Hendry and Pretis (2011) and Ericsson and Reisman (2012).

Recently, also other types of indicator saturation have been discussed in the literature. They are related to different types of intervention functions representing level shifts, slope changes etc. Considering different indicator functions should aid finding the most appropriate types of a structural change; see, for example, Doornik et al. (2013). From the computational point of view, IIS and its extensions pose a problem of having more regressors than observations, which can be solved by dividing all dummies into blocks and selecting over blocks; see, e.g., Hendry and Krolzig (2004). A more elaborate search algorithm, also accounting for collinearity between indicators, is provided by Autometrics (Doornik, 2009c) which is an integral part of PcGive (Doornik and Hendry, 2013). Even though indicator saturation has proven to be both practical and effective in the context of the stationary dynamic regression model, its performance in the structural time series

models framework has not been examined yet.

This paper contributes to the literature in that it for the first time combines seasonal adjustment using BSM with the general–to–specific approach to outlier detection. The method presented here substantially differs from the procedures in TRAMO–SEATS and X–12 ARIMA in both the modeling and the outlier detection strategy. In the first step, we assess the performance of indicator saturation via Monte Carlo simulations. After that, we provide an empirical application of the considered method to raw industrial production series in France, Germany, Italy, Spain and UK in the time span 1991.M1 – 2014.M1. In our analysis, we apply impulse–indicator saturation (IIS) and step–indicator saturation (SIS). The reason for this specific choice is twofold. Pulse and step dummies are the most simple and at the same time the most flexible way of modeling structural changes. Moreover, in the empirical exercise our greatest interest lies in the question whether the procedure is capable of identifying a potential level shift corresponding to the economic and financial crisis starting in Europe around the end of 2008.

The remainder of the article is organized as follows. In Section 3.2, we describe the framework for modeling seasonal time series with outlying observations and location shifts. In particular, in Section 3.2.1 we set out the basic structural model with calendar effects, whereas in Section 3.2.2 we present the concept of indicator saturation and explain how it is integrated in the current framework. Section 3.3 summarizes findings on the detection power of IIS and SIS, obtained by Monte Carlo simulations using differing settings for the model and outlier detection. In Section 3.4, IIS and SIS are applied to real data to detect outliers and level shifts. Section 3.5 concludes.

3.2 Modeling framework

3.2.1 The basic structural time series model

The BSM postulates an additive and orthogonal decomposition of a time series into unobserved components representing the trend, seasonality and the irregular component. If y_t denotes a time series observed at $t = 1, 2, \ldots, T$, the decomposition can be written as follows:

$$y_t = \mu_t + \gamma_t + \sum_{k=1}^{K} \delta_{xk} x_{kt} + \epsilon_t, \quad t = 1, \ldots, T, \tag{3.1}$$

where μ_t is the trend component, γ_t is the seasonal component, the x_{kt}'s are appropriate regressors that account for any known interventions as well as calendar effects, namely trading days, moving festivals (Easter) and the length of the month, and $\epsilon_t \sim$ IID $\mathrm{N}(0, \sigma_\epsilon^2)$ is the irregular component.

The trend component has a local linear representation:

$$\begin{array}{rcll} \mu_{t+1} & = & \mu_t + & \beta_t + \eta_t \\ \beta_{t+1} & = & & \beta_t + \zeta_t \end{array} \tag{3.2}$$

where η_t and ζ_t are mutually and serially uncorrelated normally distributed random shocks with zero mean and variance σ_η^2 and σ_ζ^2, respectively.

The seasonal component can be modeled as a combination of six stochastic cycles whose common variance is σ_ω^2. The single stochastic cycles have a trigonometric representation and are defined at the seasonal frequencies $\lambda_j = 2\pi j/12$, $j = 1, \ldots, 6$. The parameter λ_1 denotes the fundamental frequency (corresponding to a period of 12 monthly observations) and the remaining ones represent the five harmonics (corresponding to periods of 6 months, i.e. two cycles in a year, 4 months, i.e. three cycles in a year, 3 months, i.e. four cycles in a year, 2.4, i.e. five cycles in a year, and 2 months):

$$\gamma_t = \sum_{j=1}^{6} \gamma_{jt}, \qquad \begin{bmatrix} \gamma_{j,t+1} \\ \gamma_{j,t+1}^* \end{bmatrix} = \begin{bmatrix} \cos\lambda_j & \sin\lambda_j \\ -\sin\lambda_j & \cos\lambda_j \end{bmatrix} \begin{bmatrix} \gamma_{j,t} \\ \gamma_{j,t}^* \end{bmatrix} + \begin{bmatrix} \omega_{j,t} \\ \omega_{j,t}^* \end{bmatrix}, j = 1, \ldots, 5, \tag{3.3}$$

and $\gamma_{6,t+1} = -\gamma_{6t} + \omega_{6t}$. The disturbances ω_{jt} and ω_{jt}^* are normally and independently distributed with common variance σ_ω^2 for $j = 1, \ldots, 5$, whereas $\mathrm{Var}(\omega_{6t}) = 0.5\sigma_\omega^2$.

Calendar effects are treated by adding regression effects in the model equation for y_t. Trading day (working day) effects occur when the level of activity varies with the day of the week, e.g. it is lower on Saturdays and Sundays. Letting D_{jt} denote the number of days of type j, $j = 1, \ldots, 7$, occurring in month t and assuming that the effect of a particular day is constant, the differential trading day effect for series i is given by:

$$TD_{it} = \sum_{j=1}^{6} \delta_{ij} \left(D_{jt} - D_{7t} \right) \tag{3.4}$$

The regressors are the differential number of days of type j, $j = 1 \ldots, 6$, compared to the number of Sundays, to which type 7 is conventionally assigned. The Sunday effect on the i-th series is then obtained as $\left(-\sum_{j=1}^{6} \delta_{ij} \right)$. This expedient ensures that the trading day

effect is zero over a period corresponding to multiples of the weekly cycle.
As far as moving festivals are concerned, the Easter effect is modeled as $E_t = \delta h_t$ where h_t is the proportion of 7 days before Easter that fall in month t. Subtracting the long run average, computed over the first 400 years of the Gregorian calendar (1583-1982), from h_t yields the regressor $h_t^* = h_t - \bar{h}_t$, where $\bar{h}_t$ takes the values 0.354 and 0.646 in March and April, respectively, and zero otherwise. Finally, the length–of–month regressor results from subtracting from the number of days in each month, $\sum_j D_{jt}$, its long run average, which is 365.25/12.

3.2.2 Indicator saturation

Indicator saturation is a general–to–specific approach according to which for every observation an indicator of a specific type is included in the set of candidate regressors. This means that, if T is the number of observations, T indicator variables are added. In this article, we consider two types of indicator saturation: IIS and SIS.
IIS has been the first approach extensively discussed in the indicator saturation literature. If $I_t(\tau)$ denotes an indicator variable, then $I_t(\tau)$ is in the IIS case a pulse dummy taking value 1 for $t = \tau$, and 0 otherwise. Hendry et al. (2008) analyze the distributional properties of IIS when the observations are generated according to the model $y_t = \mu + \varepsilon_t, t = 1, \ldots, T$, where ε_t is normally and independently distributed with mean zero and variance σ_ε^2. For that purpose, they integrate IIS into the model for y_t using the so–called split–half approach. More specifically, in the first step $[T/2]$ indicators for the first half of the sample are added to the model, where $[\cdot]$ denotes integer division, i.e.:

$$y_t = \mu + \sum_{k=1}^{[T/2]} \delta_{Ik} I_t(k) + \varepsilon_t, \quad t = 1, \ldots, T$$

Once the indicators have been selected at the significance level α, the second $T - [T/2]$ indicators replace the first ones, and the selection procedure is repeated. Finally, both sets of significant dummies are combined to determine the terminal model. On average, in the absence of any outlier, αT indicators are expected to be retained by chance in the final stage, so that setting $\alpha = 1/T$ leads to the misclassification of only one observation on average. Hendry et al. (2008) also show that the different number of splits or unequal splits do not affect the retention rate. Johansen and Nielsen (2009) generalize the analysis to stationary and nonstationary autoregressions.

SIS can be seen as an extension of IIS to the case when $I_t(\tau)$ represents a step variable taking value 0 for $t < \tau$, and 1 for $t \geq \tau$. SIS has been evaluated by Doornik et al. (2013) in view of its ability to deal with level shifts. Their study is based on a comprehensive set of Monte Carlo simulations within a simple static framework. While selecting significant indicators, they apply the standard split–half approach as well as split–half with sequential selection. The latter relies on the iterative elimination of the least significant indicators in each split, until only the significant ones are retained. The finding is that sequential selection considerably improves the power of SIS in detecting location shifts.

In situations when a single set of indicators constitutes the only set of regressors in the model, like in the references previously mentioned, split–half is always a feasible approach. It is, however, possible that the total number of regressors exceeds the number of the available observations, for example if additional regressor variables are included in the model, or different types of indicator saturation are considered at the same time. A simple method to deal with this problem is the cross–block algorithm proposed by Hendry and Krolzig (2004). After partitioning all the indicators into m blocks and performing the initial selection, cross–pairings are formed for which the selection algorithm is run again. This leads in total to $m(m-1)/2$ runs of the selection algorithm. A disadvantage of the cross–block algorithm is that it does not make use of learning and can be thus very slow. A more elaborate method offering a more progressive search is the Autometrics block–search algorithm consisting of expansion and reduction steps (see Doornik, 2009a). Moreover, in cases when different indicator saturation types are used, block–search with an appropriate partitioning of indicators can solve the problem of perfect collinearity. Doornik (2009b) demonstrates that Autometrics block–search is not only faster, but also more successful in finding breaks than the cross–block algorithm.

The indicator saturation approach is integrated in the BSM in the following way. If m denotes the number of blocks into which indicators are split, assuming that the blocks are of equal size and that T is a multiple of m, then in the first stage eq. (3.1) is extended to:

$$y_t = \mu_t + \gamma_t + \sum_{k=1}^{K} \delta_{xk} x_{kt} + \sum_{k=(T/m)(i-1)+1}^{(T/m)i} \delta_{Ik} I_t(k) + \epsilon_t, \quad t = 1, \ldots, T, \;\; i = 1, \ldots, m \tag{3.5}$$

where $I_t(k)$ represents an impulse or a step indicator, depending on whether IIS or SIS is considered. Eq. (3.5) along with models (3.2) and (3.3) is put into state space form.

Estimation is carried out by maximum likelihood; the initial states and the regression

effects are considered as diffuse and the likelihood is evaluated by the augmented Kalman filter (see de Jong, 1991), which also yields estimates of the intervention effects, $\tilde{\delta}_{xk}, k = 1, \ldots, K$, and $\tilde{\delta}_{Ik}, k = 1, \ldots, T$.[1] Once significant indicators are found for every block i, cross–block search is applied to find the terminal model.[2]

3.3 A Monte Carlo experiment

3.3.1 Design of the experiment

We investigate the performance of the indicator saturation approach to outlier detection by means of an extensive Monte Carlo experiment.[3] For that purpose, we generate time series from a BSM given in eq. (3.1) and include an additive outlier (outliers) or a level shift (shifts), thereafter abbreviated by AO and LS, respectively. For simplicity, calendar effects are omitted in the simulations. First, we design a benchmark specification for the data generating process (DGP) and the outlier detection procedure. We subsequently check the robustness of the procedure by considering alternative settings. They are obtained by modifying a single attribute of the DGP and/or the outlier detection procedure, keeping the remaining ones fixed. Every single experiment is based on $M = 1000$ replications.
As regards the simulation settings, we consider a reference DGP with the following specifications:

- The variance parameters are set equal to $\sigma^2_\epsilon = 1, \sigma^2_\eta = 0.08, \sigma^2_\zeta = 0.0001, \sigma^2_\omega = 0.05$. There is no loss of generality in setting the irregular variance equal to 1; the remaining parameters are thus interpreted as signal to noise ratios. The benchmark DGP is chosen on the basis of our experience in fitting the BSM to industrial production and turnover time series.

- $T = 144$ observations (12 years of monthly data).

- A single additive (AO) or level shift (LS) outlier is located at 0.5 of the sample (observation number 72).

[1] In the SIS case, $I_t(1)$ is left out as it is perfectly collinear with the initial level effect.
[2] Since there does not exist any evidence on indicator saturation within structural time series models at all so far, we want to concentrate on a search algorithm which is easier to implement. Applying Autometrics block–search in context of structural time series models might be, however, an attractive line of future research.
[3] All computations are performed with Ox 6.2 (64-bit version), see Doornik (2008).

- The magnitude of the AO/LS is 7 times the prediction error standard deviation (PESD). The prediction error standard deviation is thereby obtained from the innovations form of the model in the steady state.

Examples of benchmark–based simulated series with an AO and LS are given in Figure 3.1a and Figure 3.1b, respectively.

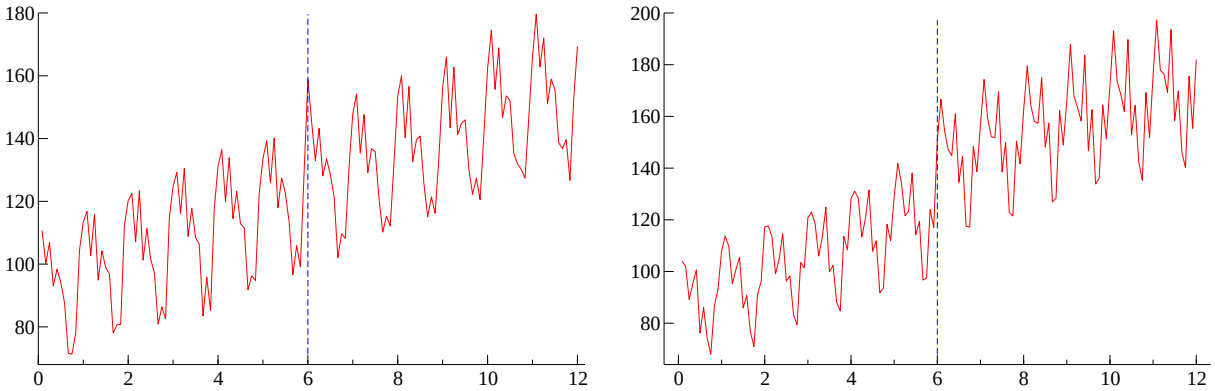

(a) Series with an additive outlier **(b)** Series with a level shift

Figure 3.1: Examples of series simulated using the benchmark specification

As regards outlier detection with the IIS and SIS, we also specify a benchmark setting:

- the indicator variables are split into 2 blocks,
- the variance parameters are not re-estimated when the split–half indicators are added to the model.

Computation of the vector of regressor effects is thus based on the parameter values estimated with the model excluding indicators. Holding the parameter values fixed can introduce bias in the estimated parameter values, but in our framework it seems to be of crucial importance for the feasibility of indicator saturation from the computational standpoint. Each iteration step often requires several passes of the Kalman filter. This involves several computations of a large vector of regressor effects which introduces instability problems when applying a maximization algorithm. In an alternative setting, we allow for one re-estimation using a single iteration to keep the computational burden at a minimum level and still be able to reduce the bias in the variance estimates. The same argument has been put forward by Atkinson et al. (1997) who propose, albeit in a different framework, score–based one–step estimates of intervention effects.

We move away from the benchmark scenario in several directions. As regards the variance parameters regulating the DGP, we consider four alternative DGPs: a stable trend – stable seasonal setup (labelled sT – sS), such that the level and seasonal variances are small compared to the irregular variance; an unstable trend–stable seasonal DGP (uT–sS) where the level evolution variance is 0.8; a stable trend–unstable seasonal DGP (sT–uS), such that $\sigma_\omega^2 = 0.5$; and finally we formulate a DGP with unstable trend and seasonality (uT–uS). As for the sample size, we consider shorter time series ($T = 72$, corresponding to 6 years of monthly observations) and longer time series ($T = 288$, i.e. 24 years of monthly data). We also consider different locations for a single outlier and different magnitudes. Concerning the outlier detection settings, we use two alternative numbers of blocks, 3 and 4, respectively, so as to assess the role of further splits in the performance of the outlier detection procedure. Finally, we also examine the role of re-estimation of the parameters within the blocks. A summary of all different settings is provided in Table 3.A.1.
The ability of indicator saturation to detect multiple outliers is also evaluated. Table 3.A.2 provides details on the number of additive outliers and temporary level shifts and their location as a fraction of the total sample size. A temporary level shift occurs when two level shifts have the same magnitude but opposite sign.
For illustrative purposes, examples of series simulated with different settings are presented in Appendix 3.B in Figures 3.B.1 – 3.B.3 for the AO case, and in Figures 3.B.4 – 3.B.7 for the LS case. Independently of the setup, the significance level for retention of respective indicators is always equal to $\alpha = 1/T$.

3.3.2 Assessing the performance of indicator saturation

In the next subsection, the performance of IIS is evaluated in the presence of additive outliers (in the benchmark as well as alternative setups). Section 3.3.4 reports the corresponding results of applying SIS to the series with level shifts. The last subsection shows how the performance of IIS compares to SIS in presence of additive outliers or level shifts. The effectiveness of the procedure is throughout the current section assessed using the concepts of *potency* and *gauge*. The former is the fraction of relevant indicator variables that are retained in the final model, whereas the latter is the fraction of irrelevant variables in the final model. More formally, let M denote the number of Monte Carlo replications and let n be the number of relevant indicators, i.e. true outliers in any particular time series of length T (e.g.in the benchmark case $n = 1$). Moreover, let $\mathcal{I}_n$ and $\mathcal{I}_{T-n}$ be sets

of time indices corresponding to relevant and irrelevant indicators, respectively. Then, potency and gauge are calculated based on the *retention rate*, denoted by $\tilde{p}_k, k = 1, ..., T$, as follows:

$$\tilde{p}_k = \frac{1}{M}\sum_{i=1}^{M} 1[\tilde{\delta}_{Ik} \neq 0], \quad k = 1, \ldots, T$$
$$\text{potency} = \frac{1}{n}\sum_{k} \tilde{p}_k, \quad k \in \mathcal{I}_n$$
$$\text{gauge} = \frac{1}{T-n}\sum_{k} \tilde{p}_k, \quad k \in \mathcal{I}_{T-n}$$

where $\tilde{\delta}_{Ik}$ denotes the estimated coefficient on the impulse or step indicator, $I_t(k)$, in replication i, if $I_t(k)$ is selected (0 otherwise); $1[\tilde{\delta}_{Ik} \neq 0]$ is variable taking value 1, if the argument in brackets is true, and 0 otherwise.

Potency and gauge as well as their links with concepts commonly used in the multiple testing literature can be illustrated by means of the following confusion matrix summarizing the outcome of a single Monte Carlo experiment:

	Decision		
Actual	No outlier	Outlier	Total
No outlier	A	B	$M(T-n)$
Outlier	C	D	Mn
Total	A+B	B+D	MT

A and D denote numbers of correct decisions in the cases of no outlier and in the cases of an outlier (at a particular observation), respectively. B and C, on the other hand, summarize all false decisions when no outlier is present, and in situations when there is an outlier (at a particular observation), respectively. Potency is then defined as the ratio $D/(Mn)$, which is the true positive rate (also called hit rate, recall or sensitivity) in the classification literature. Gauge is given by the ratio $B/[M(T-n)]$, the so–called false positive rate (or false alarm rate). The misclassification rate is $(B+C)/(Mn)$, $B/(B+D)$ is the false discovery proportion, and $P(B > 0)$ denoting probability of at least one false retention is the family–wise error rate.

Using the benchmark specification for simulations and outlier detection, we also examine an effectiveness measure which we call *probability of first detection*. More specifically, this probability is defined as the rate at which the true outlier is for the first time spotted. Since it is crucial to detect potential structural breaks as quickly as possible, this property

is particularly important to assess the application of indicator saturation for forecasting purposes if the break is close to the forecast origin. For that reason, we consider a situation in which the AO/LS is placed at the end of the benchmark sample (observation number 144). Using simulated series of length 155 observations, the model is estimated recursively along with the outlier detection. Probability of first detection is then computed for the 12 observations starting with the occurrence of the change.

3.3.3 Additive outliers and impulse–indicator saturation

The simulation results for the benchmark specification featuring a single AO are reported in the first column of Table 3.1. It can be seen that IIS is capable of identifying the outlier in nearly 100% of cases with a small error rate only. As the other columns show, different variance combinations do not change the potency of the procedure. Gauge remains at a low level, except for the case of a stable trend and unstable seasonal component (fourth column).

Table 3.1: IIS and AO in the benchmark setup and in alternative setups with different parameter values

	Benchmark	(sT–sS)	(uT–sS)	(sT–uS)	(uT–uS)
Potency in %	99.9	99.3	99.9	99.5	99.5
Gauge in %	0.03	0.04	0.00	0.15	0.06

Comparison of results related to different simulation and outlier detection settings for a single AO are summarized in Tables 3.A.3 – 3.A.6. Similarly as with different parameter values, potency does not change much if different numbers of observations are considered (see Table 3.A.3). Gauge, however, seems to decrease with series length. Potency of the procedure is considerably affected by the location of the outlier – it decreases towards the ends of the sample (see Table 3.A.4). The lowest gauge values can also be observed against the ends of the series. Moreover, the pattern displays symmetry as the potency and gauge values for outliers located in the same distance from the middle are very similar. As regards the magnitude of the outlier, the effectiveness of IIS increases with outlier size up to some point and then deteriorates (see Table 3.A.5). Using 3 or 4 blocks instead of 2, while keeping parameter values fixed, does not have any impact on potency. In contrast, re-estimation of the variance parameters, when the respective blocks of indicator variables are included, leads to a slightly lower potency of 96.3% (see Table 3.A.6).

As regards the probability of first detection (see Table 3.A.7), it is conspicuous that the performance of IIS strongly depends on the outlier magnitude. For the benchmark outlier size, the probability of first detection of 35% at the time point of the AO is very low. Moreover, small positive probabilities are still observed at the remaining 11 observations. When the size of the AO is doubled, the chance of immediate detection of the AO increases to almost 73%.

Table 3.A.8 summarizes the results for multiple outliers. The findings suggest that it is easier to detect outliers if they are placed in the same sample half, irrespective of whether 2 outliers (first column) or 4 outliers (fourth column) are considered. This finding can be explained by the fact that using the indicators set covering the same half in which all the outliers are present allows for immediate outlier detection.

3.3.4 Level shifts and step–indicator saturation

An important factor in the detection of LS using SIS is the sequential or non-sequential nature of the outlier detection procedure in each block. As has been mentioned in Section 3.2.2, sequential selection is supposed to have beneficial effects on the efficiency of SIS.

The results for the benchmark case are presented in the first column of Table 3.2. Even though potency is smaller than in the benchmark case of detecting AO with IIS, a value of about 90% for both non-sequential and sequential selection is still satisfactory, especially when coupled with the low rates of false retentions. Examination of different combinations of parameter values leads to three observations:

1. Potency is smaller when both components are stable. It increases as the variance of the trend or the seasonal component increases, and it eventually attains the highest value when both components variances are high.

2. Gauge is at its lowest level when trend and seasonal variances are high.

3. Sequential selection improves the detection performance of SIS. This, however, comes at a computational cost. For example, in the benchmark setting, the total simulations time for the non-sequential selection amounts to about 43 minutes whereas for the sequential selection it extends to 3 hours 9 minutes.

The results corresponding to a single LS and alternative settings are given in the Tables 3.A.9 – 3.A.12 of the Appendix. The length of the series seems to matter more for

Table 3.2: SIS and LS in the benchmark setup and in alternative setups with different parameter values

		Benchmark	(sT–sS)	(uT–sS)	(sT–uS)	(uT–uS)
Potency	non-seq.	89.3	72.3	74.3	95.2	98.4
in %	seq.	90.7	79.4	82.0	96.8	98.8
Gauge	non-seq.	0.04	0.09	0.02	0.02	0.01
in %	seq.	0.01	0.02	0.03	0.01	0.00

the effectiveness of the outlier detection procedure than in the case of a single AO (see Table 3.A.9). After doubling the number of observations, potency increases to 99% with a concurrent decrease in gauge to 0%, for both non-sequential and sequential selection.
The location of the shift has similar implications as for a single AO (see Table 3.A.10). However, even though the general pattern of decreasing potency for shift locations more distant from the middle of the sample is maintained, the location symmetry is not existent anymore. A shift location in the second half of the sample allows for higher detectability compared to its mirror location in the first half. Moreover, it becomes apparent that sequential selection plays a crucial role if SIS is applied to identify level shifts, as it raises the chance of spotting the true shift once its location is moved away from the middle.
Sequential selection can also help detect shifts of smaller magnitude whereas there is no gain of applying this procedure when the size is bigger than in the benchmark case (see Table 3.A.11). As can be seen in Table 3.A.12, using more blocks improves the accuracy of the detection for both considered selection procedures. In contrast, this precision becomes very poor if re-estimation of the model with each block of indicators is performed.
Next, we evaluate probability of first detection (see Table 3.A.13). Similar observations emerge to those made for IIS, as far as SIS is performed with non-sequential selection. In this case, SIS is not reliable enough to detect the shift immediately if the shift is of the benchmark size. Sequential selection, however, has again a beneficial effect for the SIS performance. It is to be noted that in 98.5% of the cases, the shift can be spotted after one observation at the latest. When the size of the shift is doubled, these discrepancies between non-sequential and sequential selection vanish, and they both serve the purpose of timely identification of level shifts.
In addition to a single LS, we also analyze multiple LS. In particular, we focus on temporary LS, by which we mean level shifts that are reversed after some time, so that the initial level is restored. Hence, modeling a temporary LS requires two step indicators

having countervailing effects on a series. Table 3.A.14 reports results of the simulation exercise dealing with 1 and 2 temporary shifts. As for 1 shift, it is more demanding to identify it using non-sequential selection when the shift occurs close to the beginning of the series (first column). Interestingly, a temporary LS spanning both halves of the sample can be detected with high probability. Potency corresponding to non-sequential selection generally decreases when 2 temporary shifts are present, especially when they are distributed over both sample halves. The same observation has been made in the context of multiple AO spread across both sample halves. Sequential selection essentially improves performance of SIS, irrespective of the number or position of temporary LS.

3.3.5 Comparison of impulse– and step–indicator saturation

So far we have investigated the effectiveness of indicator saturation when the intervention (pulse or step dummy) coincides with the indicator type used by the procedure (IIS and SIS, respectively). In practice, however, it is usually not known which type of structural change occurs. It is therefore relevant to assess the performance of SIS when an AO is present, as well as that of IIS in the case of a temporary LS. This entails the necessity to redefine the concepts of potency and gauge. A single AO can in fact be modeled by two adjacent step indicators, whose effects have the same magnitude but opposite signs. As a result, for a single AO to be identified by SIS, both relevant step indicators have to be retained, which implies that, instead of a single relevant impulse indicator, two relevant step indicators are the reference in the computation of potency and gauge. As for a temporary LS, it can be represented by impulse indicators covering the whole span of the shift and having effects of the same magnitude.[4] Therefore, retaining all indicators in this time span would be required to detect a temporary LS. However, as this condition is very restrictive, we follow Doornik et al. (2013) and measure the effectiveness of IIS in the case of a LS using the so–called *proportional potency*, defined as the average percentage of the level shift captured by the impulse indicators.

The Monte Carlo results for a single AO with two different magnitudes and located at three different fractions of the sample are summarized in Table 3.3. The results for IIS are also provided for comparison. When the AO is located at 0.25 and 0.4 of the

[4]Castle et al. (2012) examines the ability of IIS to detect multiple level shifts and outliers. Hendry and Santos (2010) show in context of a single level shift that the detection power of IIS depends on the magnitude of the shift, sample size, the duration of the shift, the error variance and the significance level.

sample, SIS applied with non-sequential selection performs manifestly worse than IIS, but a substantial improvement can be gained by applying sequential selection. Gauge is low for both implementations of SIS. The overall conclusion is that SIS can successfully identify the true outlier. When the AO is located in the middle of the sample, results are less satisfactory, as a consequence of the application of the split–half approach. In the best of the considered scenarios, potency reaches up to only 6.5% at the cost of 0.57% gauge. This implies that, in contrast to IIS, SIS fails at finding the correct AO at the border between two blocks with indicators.

Table 3.3: Comparison of IIS and SIS in presence of AO at different locations and with different magnitudes

Location[a)]			0.25		0.4		0.5	
Magnitude[b)]			7	14	7	14	7	14
Potency in %	IIS		86.40	98.20	98.70	98.90	99.30	98.70
	SIS	non-seq.	33.60	51.00	40.30	53.75	0.25	0.05
		seq.	68.95	66.20	70.45	64.90	4.40	6.50
Gauge in %	IIS		0.03	0.09	0.01	0.08	0.02	0.10
	SIS	non-seq.	0.01	0.01	0.00	0.00	0.33	0.25
		seq.	0.02	0.02	0.01	0.02	0.50	0.57

[a)] Location is given as a share of the sample length T.
[b)] Magnitude is given as a factor to be multiplied with the prediction error standard deviation (PESD).

The performance of SIS and IIS in the presence of a temporary LS at different locations and with different magnitudes is presented in Table 3.4. It is apparent that, compared to SIS, the proportional potency of IIS is very low and gauge is relatively large, except for the first considered shift location. However, some care has to be taken when interpreting these results. As a matter of fact, to get a better insight into the results it is necessary to examine which indicators are retained in the individual simulations.[5] Detailed examination reveals that there are essentially two scenarios that account for the overall poor potency values of IIS. In the first, corresponding to the time span between 0.25 and 0.35 of the sample, only a small fraction of impulse indicators from the relevant range is retained, and the gauge is zero, so that no false positive outlier is found. In the second scenario, which corresponds to the remaining locations, IIS predominantly identifies clusters of few adjacent indicators bordering the time span of the LS on both sides. As the

[5]Due to large simulation output, additional results are not presented in the article. They can, however, be made available upon request.

estimated effects of these dummies are negative, the periods before and after the actual LS are treated as periods of negative LS. Although this can be considered as an equivalent way of modeling series with a temporary positive LS, the concepts of potency and gauge are not tailored to deal with this possibility, since they classify the retained indicators as false positives.[6] As a result, the performance of IIS is underestimated. It is worth noting that for a LS occurring in the middle of the sample, i.e. on the boundary of the indicator blocks, few dummies from the first block are retained only so that it is nearly impossible to detect such a shift by IIS. A similar conclusions was drawn for SIS in the context of detection of a single AO at the middle of the series.

Table 3.4: SIS and IIS in presence of temporary LS at different locations and with different magnitudes

Location[a)]			[0.25, 0.35]		[0.45, 0.55]		[0.5, 0.6]	
Magnitude[b)]			7	14	7	14	7	14
Potency in %[c)]	IIS		0.67	9.81	0.03	0.00	0.11	0.00
	SIS	non-seq.	74.10	89.45	89.00	97.55	92.85	98.40
		seq.	91.15	87.20	95.80	97.20	97.30	98.20
Gauge in %	IIS		0.00	0.00	1.68	3.49	1.15	2.03
	SIS	non-seq.	0.03	0.04	0.01	0.01	0.02	0.00
		seq.	0.00	0.01	0.00	0.01	0.00	0.00

[a)] Location is given as a share of the sample length T.
[b)] Magnitude is given as a factor to be multiplied with the prediction error standard deviation (PESD).
[c)] For IIS, the numbers refer to proportional potency.

3.4 Applications

In the statistical analysis of economic time series, the detection of structural change has important consequences for the purposes of signal extraction and forecasting. In this section, we illustrate the application of indicator saturation to the monthly industrial production time series referring to the manufacturing sector of five European countries: Spain, France, Germany, Italy and the United Kingdom. More specifically, the series concern the monthly seasonally unadjusted volume index of production in manufacturing (according

[6] At first sight, it seems difficult to distinguish between a single positive temporary LS and 2 negative temporary LS when only few indicators are kept on both sides of the true shift. All the same, the largest t–values relate to indicators in the direct neighborhood of the borders and thus help recognize a positive LS.

to the NACE Rev.2 classification). The data covers the time span 1991.M1 – 2014.M1 (277 observations) and is provided by Eurostat (download at: `http://epp.eurostat.ec.europa.eu/portal/page/portal/short_term_business_statistics/data/main_tables`). The objective is to assess how the recent recessionary episode, triggered by the global financial crisis, is characterized by the application of IIS and SIS – whether it can be accommodated by the regular evolution of the stochastic components, or it represents a major structural change.

3.4.1 Outlier detection with indicator saturation

The reference modeling framework for application of IIS and SIS is the BSM with calendar effects, see Section 3.2.1. Selection of significant impulse or step indicators is governed by the significance level $1/T = 0.0036$. As far as the implementation of SIS is concerned, we consider both non-sequential and sequential selection. In the sequential procedure, we follow the strategy of splitting the indicators in two blocks. For IIS and non-sequential selection in the SIS case, the number of blocks is an important factor affecting the outcome in terms of detected AO or LS. Therefore, we have decided to take the results generated with different numbers of blocks into consideration, and combine them suitably to obtain the final results. To that end, we separately identify significant indicators choosing a block number from the range between two and ten. Subsequently, we take the union of all the significant indicators and select the significant ones from this set. The choice of the maximum of ten blocks can be justified by the fact that this is a reasonably high number to reduce the risk of missing any important structural changes.[7]

The results for IIS are reported in Table 3.5. We can observe a similar pattern for all countries – the procedure retains a couple of dummies with negative effects on the series, starting from 2009.M1 for Spain, Germany and the UK, from 2008.M11 for France and from 2008.M12 for Italy. This finding points to a LS corresponding to the economic and financial crises and enables dating the inception of the recession. For France, Germany and Italy, the AO pattern is very articulate, whereas for Spain and the UK only three impulse indicators show a significant impact. Interestingly, for Spain, Germany and Italy, a positive AO is detected in 2008.M4. Moreover, after a positive AO in 2011.M5, a negative AO is identified in France and Germany in the next month.

The results for SIS are presented in Table 3.6, separately for the non-sequential and

[7] In fact, increasing the number of blocks over ten did not lead to the detection of any additional AO or LS in the examined series.

Table 3.5: Outliers detected in five European countries using IIS[a),b)]

ES		FR		GER		IT		UK	
2008.M4	(4.77)	2008.M11	(−3.09)	2008.M4	(3.45)	2008.M4	(3.36)	2002.M6	(−6.20)
2008.M7	(3.08)	2008.M12	(−3.68)	2008.M6	(3.63)	2008.M12	(−3.98)	2005.M3	(−4.50)
2009.M1	(−3.55)	2009.M1	(−5.03)	2008.M9	(3.18)	2009.M1	(−3.85)	2009.M1	(−3.72)
2009.M3	(−3.87)	2009.M2	(−4.92)	2009.M1	(−4.83)	2009.M2	(−5.05)	2009.M2	(−3.17)
2009.M5	(−2.92)	2009.M3	(−5.90)	2009.M2	(−4.75)	2009.M3	(−6.48)	2009.M3	(−3.41)
		2009.M4	(−4.33)	2009.M3	(−4.48)	2009.M4	(−4.39)		
		2009.M5	(−4.19)	2009.M4	(−4.79)	2009.M5	(−6.03)		
		2009.M6	(−3.64)	2009.M5	(−3.40)	2009.M6	(−5.29)		
		2009.M7	(−3.15)	2009.M6	(−3.77)	2009.M7	(−4.77)		
		2011.M5	(6.28)	2009.M7	(−2.92)				
		2011.M6	(−3.00)	2011.M5	(5.03)				
				2011.M6	(−3.25)				

[a)] ES: Spain, FR: France, GER: Germany, IT: Italy, UK: United Kingdom
[b)] t–values of the indicator effects are reported in parentheses.

sequential implementations. For all countries except Spain, the non-sequential procedure detects a LS in 2008.M11 (France, UK) or 2008.M12 (Germany, Italy), associated with the beginning of the global recession. In the case of Spain, a LS is, however, detected by the sequential selection already in 2008.M10. It is worth noting that SIS is capable of detecting most of the AOs identified by IIS, such as those in 2011.M5 in France and Germany, or in 2002.M6 and 2005.M3 in the UK. The comparison of the results obtained with non-sequential and sequential procedure shows particularly striking differences for Spain and Italy. In the case of Spain, non-sequential selection leads to a more generous specification, whereas for Italy a richer specification is chosen by sequential selection. An interesting common pattern emerges from these two cases: every year starting from 2009, a positive LS detected in August is followed by a negative level shift in September. This systematic pattern may mimic a break in the seasonal component, associated with the month August, which possibly occurred in Spain and Italy in 2009.

The estimated trends resulting from the BSM model with the AO and LS identified by IIS and SIS are jointly displayed in Figure 3.2 for each country[8]. In particular, the plot represents the evolution of the underlying component μ_t, estimated by the Kalman filter and smoother based on the entire sample. The vertical displacement reflects the location and magnitude of the identified level shifts. In general, SIS interprets the recession as a permanent level shift, whereas according to IIS the recession is a temporary shift taking place around the end of 2008 and affecting part of 2009. For France, the two SIS methods provide exactly the same results and the results are similar for Italy and the UK. For

[8]For the sake of clarity, the pictures are restricted to the periods 2005.M1 – 2014.M1 since no outlier was detected before 2005, except in the UK case.

Table 3.6: Outliers detected in five European countries using SIS[a),b)]

	ES		FR		GER		IT		UK	
non-seq.	2008.M3	(−3.18)	2008.M11	(−6.78)	2008.M12	(−8.48)	2008.M8	(−2.95)	1993.M6	(−3.62)
	2008.M4	(3.30)	2011.M5	(5.22)	2010.M3	(3.74)	2008.M12	(−6.94)	1998.M1	(4.10)
	2008.M5	(−3.48)	2011.M6	(−7.08)	2011.M5	(4.56)	2009.M8	(3.03)	2002.M6	(−5.93)
	2009.M8	(5.20)			2011.M6	(−5.91)			2002.M7	(5.13)
	2009.M9	(−4.46)			2011.M7	(3.13)			2005.M3	(−4.10)
	2010.M8	(4.94)							2005.M4	(4.05)
	2010.M9	(−5.03)							2008.M11	(−6.22)
	2011.M8	(4.32)								
	2011.M9	(−4.52)								
	2012.M8	(5.24)								
	2012.M9	(−5.89)								
	2013.M8	(5.97)								
	2013.M9	(−5.13)								
seq.	2008.M10	(−4.36)	2008.M11	(−6.78)	2008.M11	(−5.78)	2008.M12	(−7.50)	2002.M6	(−5.94)
			2011.M5	(5.22)	2009.M1	(−4.72)	2009.M8	(6.90)	2002.M7	(4.76)
			2011.M6	(−7.08)	2010.M3	(3.77)	2009.M9	(−5.37)	2005.M3	(−3.79)
					2011.M5	(4.88)	2010.M8	(4.99)	2005.M4	(3.94)
					2011.M6	(−5.57)	2010.M9	(−4.84)	2008.M11	(−6.41)
							2011.M8	(4.60)		
							2011.M9	(−6.16)		
							2012.M8	(5.48)		
							2012.M9	(−6.35)		
							2013.M8	(6.55)		
							2013.M9	(−6.54)		

[a)] ES: Spain, FR: France, GER: Germany, IT: Italy, UK: United Kingdom
[b)] t–values of the indicator effects are reported in parentheses.

Germany, there is a sizable difference between the trends estimated by the two versions of SIS.

Figure 3.3 plots the sum of the estimated trend component and the outlier effects resulting from IIS and SIS. It is evident that the combined trends and outliers effects obtained with the IIS approach are more flexible and they adjust more closely to the observed data. IIS possibly leads to overfitting the data. A more parsimonious model could be obtained by SIS, which yields more steady trends, in particular when applied with the sequential procedure. The combined components are very similar across different indicator saturation versions, except for Spain and Italy. As it was mentioned before, SIS with non-sequential selection for Spain and with sequential selection for Italy leads to the identification of a seasonal cluster of additive outliers occurring every August after 2008, which may reflect the consequences of the global recession on the seasonal pattern.

To facilitate the comparison across models for different countries, we employ goodness–of–fit measures for the BSM model without any interventions as well as for different specifications following from indicator saturation. The goodness–of–fit measures include the log-likelihood, the coefficient of determination, R_S^2, suitable for series exhibiting trend

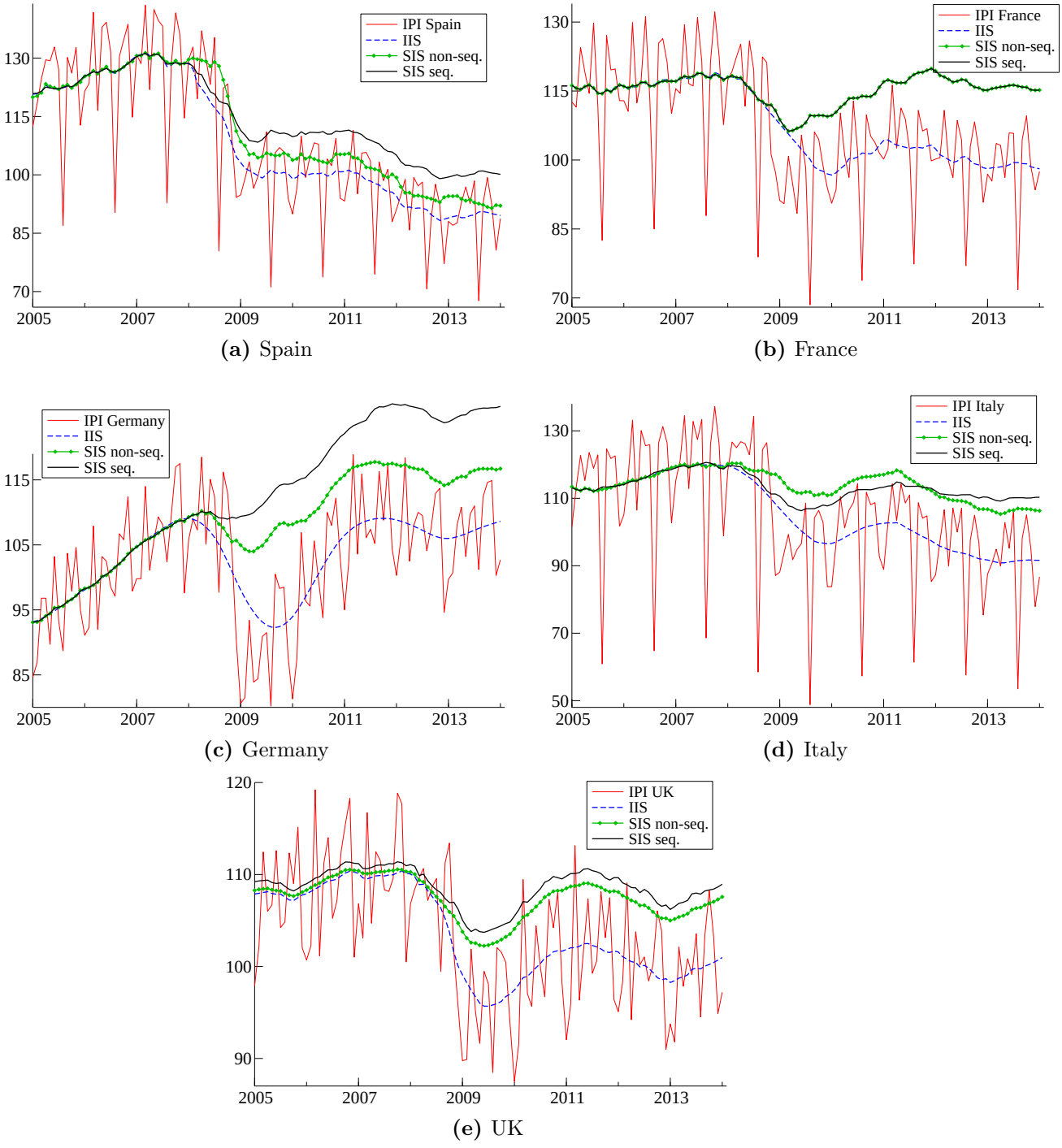

Figure 3.2: Trend components estimated using the BSM with IIS and SIS for five European countries

and seasonal movements (constructed as the ratio of the innovations variance and the variance of the first differences around a seasonal drift), and the AIC and BIC informa-

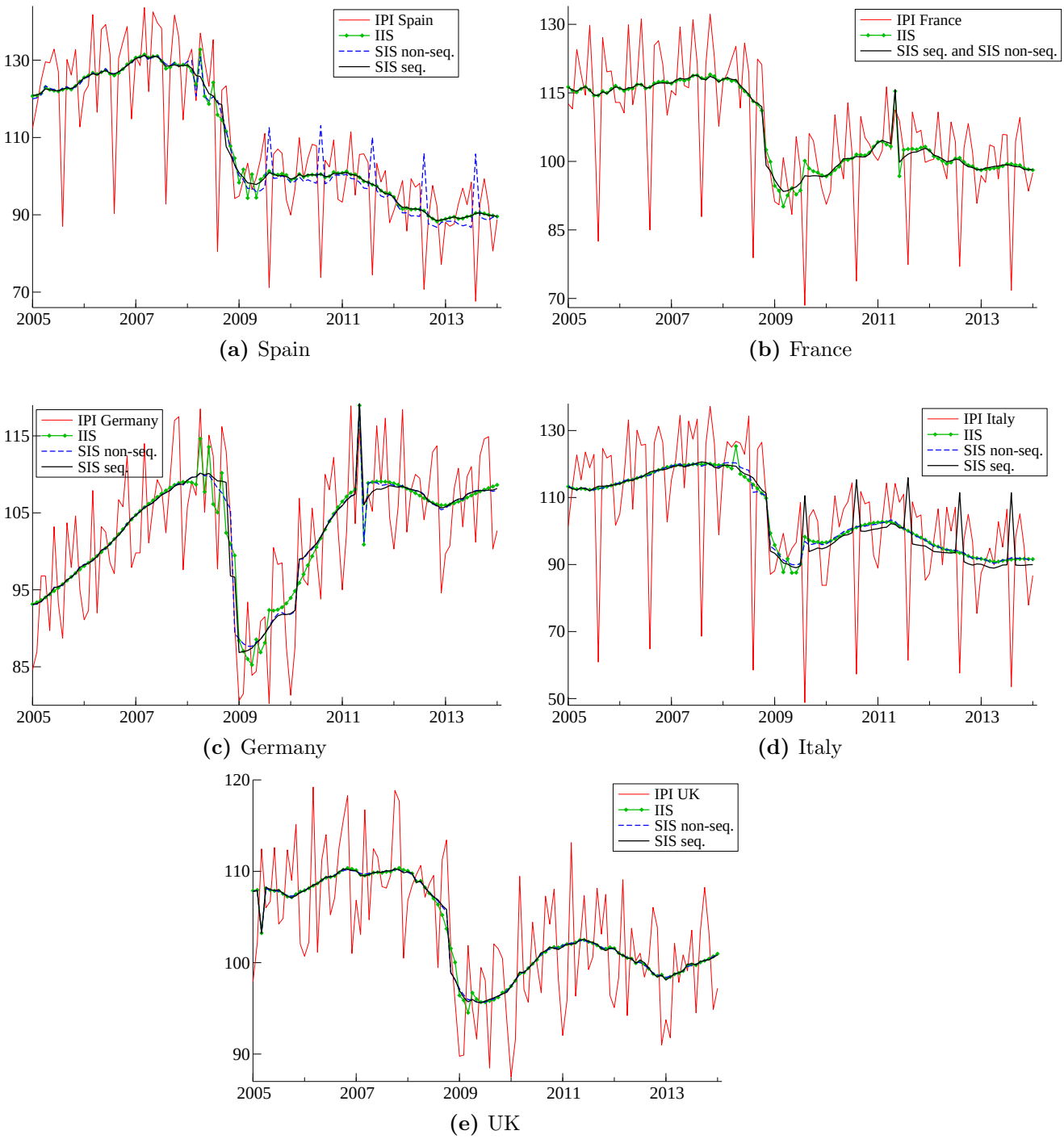

(a) Spain **(b)** France

(c) Germany **(d)** Italy

(e) UK

Figure 3.3: Trend components with outlier effects estimated using IIS and SIS for five European countries

tion criteria. Additionally, we provide the results of the following diagnostic tests: the Ljung–Box autocorrelation test, the Durbin–Watson autocorrelation test, the Goldfeld–

Quandt heteroscedasticity test, and the Bowman–Shenton normality test. The results are reported in Table 3.A.15. The goodness–of–fit assessment is strongly in favor of the SIS specifications: SIS with non-sequential selection performs best for Spain and the UK, whereas SIS with sequential selection seems to be superior for Germany and Italy. SIS imparts the best fit also in the case of France. For Spain, Germany and the UK, the specifications associated with the best fit ensure that at least some of the model assumptions (no autocorrelation, homoscedasticity, normality) cannot be rejected, or provide the smallest departures from them compared to other specifications. In contrast, in the case of Italy and France no clear improvement in the diagnostic test statistics relative to inferior models can be ascertained.

We can conjecture that the change in the behavior of European IPI series after the end of 2008 cannot be fully attributed to the natural evolution of the stochastic trend. The conjecture is based on the fact that the best specifications suggest either a shift in the level of the trend (France, Germany, UK) or/and a change in the seasonal pattern (Italy, Spain). Though the model allows for stochastic evolution in the trend, this cannot fully explain the observed decline in the IPI series during the economic crisis.

3.4.2 Comparison with alternative outlier detection methods

In the following, we compare the results of the indicator saturation approach with those obtained with alternative methods of automatic outlier detection for seasonal time series. The considered methods are implemented in publicly available statistical software packages, namely TRAMO (see Gómez and Maravall, 1996), TSW: TRAMO–SEATS version for Windows (see Caporello and Maravall, 2004), X13–ARIMA (see U.S. Census Bureau, 2013), STAMP (see Koopman et al., 2009).

In TRAMO, TSW and X13–ARIMA, outlier detection is performed in the framework of seasonal ARIMA models for the underlying series, with models chosen automatically after a few user–predefined settings. Outlier detection is implemented as described by Tsay (1986), Chang et al. (1988), Chen and Liu (1993). In brief, this procedure searches for different types of outliers: additive outliers, level shifts, transitory changes, and innovation outliers (not considered in X13–ARIMA) and consists of two stages. The first one, forward addition, amounts to computing t–statistics for interventions referring to every outlier type at each observation and adding the most significant ones to the model. In the second one, backward deletion, the least significant interventions are eliminated.

In STAMP, the series are modeled in terms of unobserved components. For our analysis, we apply the BSM without any variance restrictions. Outlier detection in STAMP is based on the so–called auxiliary residuals which are the smoothed estimates of the disturbances driving the evolution of the components of the BSM (see Harvey and Koopman, 1992). Significant auxiliary residuals indicate outliers corresponding to particular components, like irregular, trend level, trend slope or seasonal in the case of the BSM.
The outliers identified by the aforementioned procedures are listed in Table 3.A.16. For Spain, TRAMO, TSW and X13–ARIMA identify only one outlier, a LS in 2008.M12, while STAMP detects a number of AOs in addition to a LS in 2008.M12. Generally speaking, these findings contrast with the indicator saturation outcomes. A LS related to the economic crisis could be detected only with the SIS sequential procedure, albeit already in 2008.M10. Further, none of these algorithms identifies a break in the seasonal pattern, as suggested by SIS with non-sequential selection. For France, all software packages find a LS in 2008.M11 and an AO in 2011.M5, also detected by IIS and SIS. However, TRAMO, TSW and X13–ARIMA additionally identify a LS in 2009.M1 and an AO in 2000.M5 (TRAMO, X13–ARIMA) or a transitory change in 2000.M6, not captured by the indicator saturation. As for Germany, a LS in 2008.M12 detected by TRAMO, TSW and X13–ARIMA, as well as an AO in 2011.M5, detected by TSW, X13–ARIMA and STAMP, are consistent with the outcome of the preferred SIS with sequential selection. In the case of Italy, all the above procedures identify a LS in 2008.M12, which accords with the corresponding findings for indicator saturation. It is worth noting that, except for STAMP, all softwares also find a LS in 2009.M8, which corresponds to one of the LS associated with possible seasonality change uncovered by SIS with sequential selection. As regards the UK, TRAMO, TSW and X13–ARIMA date the LS referring to the economic crisis, just as both SIS versions, at 2008.M11. Both AOs, in 2002.M6 and 2005.M3, detected by IIS and SIS, emerge also from the alternative methods considered. More specifically, the AO in 2002.M6 is also found by TRAMO, X13–ARIMA and STAMP, and the AO in 2005.M3 is also detected by TRAMO and TSW. To sum up, the comparison with different outlier detection procedures reveals that, whereas for some countries, like Germany or the UK, the discrepancies are small and mostly related to AO, in other cases, with Spain as the most distinct example, the mismatch is larger.

3.4.3 Forecasting

We have seen in Section 3.4.1 that for the IPI series under investigation the BSM without any interventions may not sufficiently explain potential structural changes, and that a much improved fit can be achieved by applying the indicator saturation approach to the BSM. In this situation, the major structural break identified by the procedures was relatively distant from the end of the sample. It should be recalled that in such a case outlier detection by both IIS and SIS is effective (i.e. has high potency), as was shown by Monte Carlo simulation.

However, for forecasting purposes, an essential property is the timely recognition of abrupt changes in the data occurring towards the end of the sample. Clements and Hendry (2011) show that an unanticipated location shift at the forecast origin can heavily impair forecast precision. The question also arises as to whether specifications resulting from indicator saturation can still prove to be superior to those without any interventions.

To address this question, we perform a recursive forecasting exercise aiming at testing the forecast ability of the BSM without interventions and the BSM with SIS. In other words, we investigate whether the detection of structural change is timely and whether it contributes positively to the accuracy of the predictions. We focus only on SIS as it proved superior in terms of goodness–of–fit, with particular reference to the information criteria computed on the full series. The series under consideration are the five IPI series; the training sample period is the pre-recessionary period ending in 2008.M9, and we use the subsequent observations as a test period.

For every specification (BSM with no interventions, BSM with SIS non-sequential selection, BSM with SIS sequential selection), starting with 2008.M9 as the first forecast origin, we compute 1– to 12–period–ahead recursive forecasts. Then the sample is extended by one month and again 1– to 12–period–ahead forecasts are calculated. These steps are repeated until 2009.M8, which is the last forecast origin.

This pseudo real–time forecasting exercise yields 12 forecasts at horizons from 1 to 12. We choose the 12–month interval between 2008.M9 and 2009.M8 for computing forecasts since the resulting predictions cover the periods shortly before, during and after the occurrence of the LS at the end of 2008. The forecasting performance is evaluated by the the root mean square errors (RMSE) for every specification and every forecast horizon between 1 and 12.

Several observations emerge from the comparison of RMSE values reported in Table 3.7.

Table 3.7: Root mean square error (RMSE) of recursive forecasts of the industrial production index for five European countries[a),b)]

Forecast horizon			1	2	3	4	5	6	7	8	9	10	11	12
ES	no SIS		7.88	10.02	11.86	13.82	16.09	17.94	19.35	21.37	22.37	23.53	24.65	26.99
	SIS	non-seq.	8.47	10.42	12.08	14.03	16.29	18.29	19.69	21.64	22.67	23.78	24.71	27.61
		seq.	8.32	10.36	11.93	13.54	15.74	17.53	18.86	20.75	21.63	22.82	23.77	26.24
FR	no SIS		6.54	8.90	10.86	13.50	15.41	16.72	17.86	19.19	20.56	21.98	23.73	26.00
	SIS	non-seq.	6.81	9.02	10.89	13.50	15.40	16.70	17.86	19.18	20.63	22.00	23.79	26.24
		seq.	6.29	8.12	9.70	11.41	12.43	12.80	12.51	12.88	13.56	13.77	14.52	16.45
GER	no SIS		7.03	10.22	13.56	15.93	18.17	20.05	22.66	24.19	26.89	28.58	31.32	33.91
	SIS	non-seq.	6.55	9.77	12.32	14.65	16.17	17.75	19.47	20.31	21.70	23.47	25.54	27.78
		seq.	5.06	8.03	10.43	11.81	11.89	12.19	12.75	12.33	12.54	12.09	12.02	12.22
IT	no SIS		9.43	11.98	14.95	17.83	20.84	22.56	24.05	25.91	27.01	29.21	31.38	34.28
	SIS	non-seq.	9.51	11.17	12.91	15.30	16.60	16.38	16.06	16.56	14.94	15.39	15.72	17.37
		seq.	9.33	11.06	12.65	14.61	16.32	15.92	15.30	15.94	13.94	14.02	14.07	15.70
UK	no SIS		2.94	4.32	5.20	6.11	6.82	7.48	8.49	9.33	10.31	11.31	12.42	13.62
	SIS	non-seq.	2.69	4.08	5.14	6.15	6.97	7.68	8.80	9.68	10.75	11.79	13.01	14.22
		seq.	2.37	3.56	4.32	4.97	5.15	5.11	5.36	5.51	5.74	5.84	6.26	6.76

[a)] ES: Spain, FR: France, GER: Germany, IT: Italy, UK: United Kingdom

[b)] The reported RMSE values are computed for every forecast horizon with reference to the 12 1–step and multi–step forecast errors for the forecast lead times from 2008.M9 to 2009.M8.

For Germany and Italy, SIS, both with non-sequential and sequential selection, by and large outperforms the specification without interventions (with the only exception represented by the 1–step–ahead forecast for Italy related to SIS with non-sequential selection). Interestingly, the gap between the RMSE values corresponding to the approach without SIS and with SIS increases with the forecast horizon. For France and the UK, SIS with non-sequential selection does not impart any improvement in the predictive accuracy. The accuracy improves considerably, however, when sequential selection is used. Similarly to the case of Germany and Italy, the RMSE progressively declines as the forecast horizon increases. As far as Spain is concerned, SIS with non-sequential selection performs worse than the approach without SIS. Sequential selection in general helps to improve the predictive accuracy, even though the RMSE values referring to the 1– to 3–step–ahead forecast are higher than in the case without any intervention. The remaining RMSE values are lower, but, unlike in the case of the other series, they do not differ much from those obtained with the BSM without interventions.

Summing up, SIS, particularly applied with sequential selection, proves to be suitable for forecasting purposes even when a structural break is close to the end of the sample. This conclusion is consistent with the simulation results discussed in Section 3.3.4, according to which, for large shifts, both non-sequential and sequential selection guarantee high probability of first detection right after the shift. For a smaller LS size, sequential selection

is, though, of vital importance for timely outlier detection. An explanation for the different findings across countries is provided in Table 3.A.17. The disappointing results obtained for Spain can be explained with the difficulty of identifying the LS associated with the economic crisis. If, on the other hand, the relevant LS is detected timely, like for Germany and Italy, SIS leads to models yielding substantially better results than the basic model.

3.5 Conclusions

This article has investigated the performance of the indicator saturation approach as a methodology for detecting additive outliers and location shifts when dealing with non-stationary seasonal series in a model based framework. While the currently available automatic outlier detection procedures follow a specific–to–general approach to uncover structural change, indicator saturation, as a general–to–specific approach, constitutes a relatively new concept in the literature.

Indicator saturation has proven very effective in a regression framework and is currently implemented in Autometrics. Its use for the class of structural time series models has not yet been investigated and this article aimed at filling the gap. The considered model–based framework is interesting as the time series model is directly formulated in terms of unobserved components that are evolving over time. Hence, stochastic change occurs with every new observation, as the components are driven by random disturbances. The issue is then to locate and quantify large economic shocks that configure a structural break differing from the regular endogenous variation of the dynamic system.

We have implemented both impulse–indicator and step–indicator saturation (IIS and SIS) in the framework of the basic structural time series model (BSM). IIS is customized to detect additive outliers (AO), whereas SIS, both with non-sequential as well as with sequential selection, is tailored to detect level shifts (LS). First, we have evaluated the effectiveness of IIS and SIS, by measuring their potency and gauge, in a comprehensive Monte Carlo simulation exercise. It has been shown that, for a reference data generating process and a baseline specification of the procedures, IIS and SIS are very effective methods for outlier detection, especially when SIS is combined with sequential selection. We then explored several factors that can affect the performance of indicator saturation, and we concluded the following:

- The relative variability of the disturbances driving the evolution of the level and the seasonality does do not matter for the performance of the IIS procedure in detecting

AOs. In the SIS case, on the other hand, the detection of LS is easier the higher the evolution error variance of the trend and seasonal.

- The time location of an AO strongly affects the performance of IIS, with potency and gauge deteriorating when the AO occurs towards the beginning or the end of the sample. In the SIS case, similar considerations hold, but potency and gauge do not vary symmetrically with respect to the location of the LS (LS are easier to detect in the second half of the sample).

- The number of blocks considered in the implementation of the procedure are important drivers of its performance. For instance, if several AOs/LS are present, it is beneficial for both IIS and SIS if they are located in the same sample split.

- SIS with sequential selection provides systematically better results than SIS with non-sequential selection in all the alternative settings considered in the simulations.

- When SIS is used for AO detection, the success rate is satisfactory provided that the AO is not placed at the border between sample splits. IIS, in contrast, does not show acceptable properties when applied to identify LS.

In the last part of the article, we have applied indicator saturation to the monthly industrial production time series for five European countries, with the intent of investigating how the different methodologies characterized the global recessionary movements affecting the euro area economies towards the end of 2008. In general, SIS provided the best specification in terms of goodness–of–fit, capturing a LS in November or December 2008, depending on the series. The comparison with the currently available automatic outlier detection procedures showed a good degree of similarity of the results for Germany and the UK and some important differences for Spain.
Finally, we conducted a pseudo real–time recursive forecasting exercise comparing the out–of–sample performance of the BSM with and without indicator saturation, so as to investigate whether the timely detection of structural change leads to an improvement in the quality of the predictions. As a test sample, we considered the inception and the continuation of the global recession. SIS proved effective in detecting potential location shift close to the forecast origin. The overall conclusion is that the detection of structural change is necessary to obtain accurate forecasts. The sooner the relevant level shift is detected, like for Germany and Italy, the bigger is the improvement in the forecast precision. Sequential selection substantially helps to accomplish this goal.

Appendix

3.A Tables

Table 3.A.1: Simulation and outlier detection specifications for series with a single additive outlier (AO) / single level shift (LS)

Attributes	Benchmark	Alternative settings
	Data generating process	
Parameter values	$\sigma_\epsilon^2 = 1$	1) (sT–sS) $\sigma_\eta^2 = 8 \cdot 10^{-5}$, $\sigma_\omega^2 = 5 \cdot 10^{-5}$
	$\sigma_\zeta^2 = 0.0001$	2) (uT–sS) $\sigma_\eta^2 = 0.8$, $\sigma_\omega^2 = 5 \cdot 10^{-5}$
	$\sigma_\eta^2 = 0.08$	3) (sT–uS) $\sigma_\eta^2 = 8 \cdot 10^{-5}$, $\sigma_\omega^2 = 0.5$
	$\sigma_\omega^2 = 0.05$	4) (uT–uS) $\sigma_\eta^2 = 0.8$, $\sigma_\omega^2 = 0.5$
Number of observations	144	1) 72, 2) 288
Outlier location[a)]	0.5	1) 0.05, 2) 0.1 3) 0.15 4) 0.25, 5) 0.4, 6) 60, 7) 0.75, 8) 0.85, 9) 0.9, 10) 0.95
Outlier magnitude	$7 \cdot PESD$,	$[2, 14] \cdot PESD$
	Outlier detection settings	
Blocks number	2	1) 3, 2) 4
Re-estimation in blocks	no	yes

[a)] Location is given as a share of the sample length T.

Table 3.A.2: Outlier location for series with multiple additive outliers (AO) / multiple level shifts (LS)

Number of outliers	Location[a), b)]
	Additive outliers
2 outliers	1) 0.25, 0.35; 2) 0.3, 0.6
4 outliers	2) 0.2, 0.4, 0.6, 0.8; 2) 0.6, 0.7, 0.75, 0.9
	Temporary level shift[c)]
1 shift	1) [0.25, 0.35], 2) [0.45, 0.55], 3) [0.5, 0.6]
2 shifts	1) [0.2, 0.3], [0.35, 0.45]; 2) [0.25, 0.35], [0.65, 0.75]

[a)] Location is given as a share of the sample length T.

[b)] All other attributes used in simulations of series and outlier detection are as in the benchmark setup described in Table 3.A.1.

[c)] Temporary level shift requires two level shifts of the same magnitude but opposite signs.

Table 3.A.3: IIS and AO in the benchmark setup and in alternative setups with different numbers of observations

	Benchmark: 144	72	288
Potency in %	99.9	99.0	99.9
Gauge in %	0.03	0.06	0.01

Table 3.A.4: IIS and AO in the benchmark setup and in alternative setups with different locations of the outlier[a)]

	Benchmark: 0.5	0.05	0.10	0.15	0.25	0.40	0.60	0.75	0.85	0.90	0.95
Potency in %	99.9	42.8	68.7	68.8	83.4	98.2	98.8	90.5	71.8	67.4	42.2
Gauge in %	0.03	0.01	0.02	0.03	0.04	0.01	0.01	0.02	0.04	0.02	0.01

[a)] Location is given as a share of the sample length T.

Table 3.A.5: IIS and AO in the benchmark setup and in alternative setups with different magnitudes of the outlier[a)]

	Benchmark: 7	2	4	6	8	10	12	14
Potency in %	99.9	14.2	85.0	99.4	99.9	99.6	98.5	98.4
Gauge in %	0.03	0.01	0.03	0.02	0.01	0.02	0.02	0.08

[a)] Magnitude is given as a factor to be multiplied with the prediction error standard deviation (PESD).

Table 3.A.6: IIS and AO in the benchmark setup and in alternative detection settings

	Benchmark: 2 blocks, no re-estimation	3 blocks, no re-estimation	4 blocks, no re-estimation	2 blocks, re-estimation[a)]
Potency in %	99.9	100	99.7	96.3
Gauge in %	0.03	0.01	0.02	0.01

[a)] Results are obtained after 1 iteration.

Table 3.A.7: Probability of first detection of AO using IIS in the benchmark setup and an alternative setup[a)]

Obs. no.	144	145	146	147	148	149	150	151	152	153	154	155
Benchmark: $7 \cdot PESD$	35.2	4.6	4.2	2.7	2.6	1.6	1.1	1.3	0.7	1.0	0.5	0.6
$14 \cdot PESD$	72.8	11.8	7.6	1.4	1.7	1.3	1.0	0.7	0.2	0.1	0.1	0.0

[a)] Probability is expressed in %.

Table 3.A.8: IIS in presence of multiple AO at different locations[a)]

	2 outliers		4 outliers	
	0.25, 0.35	0.3, 0.6	0.2, 0.4, 0.6, 0.8	0.6, 0.7, 0.75, 0.9
Potency in %	91.70	84.45	70.07	94.07
Gauge in %	0.05	0.00	0.03	0.27

[a)] Location is given as a share of the sample length T.

Table 3.A.9: SIS and LS in the benchmark setup and in alternative setups with different numbers of observations

		Benchmark: 144	72	288
Potency in %	non-seq.	89.3	67.4	98.9
	seq.	90.7	77.6	98.9
Gauge in %	non-seq.	0.04	0.06	0.00
	seq.	0.01	0.10	0.00

Table 3.A.10: SIS and LS in the benchmark setup and in alternative setups with different locations of the shift[a)]

		Benchmark: 0.5	0.05	0.1	0.15	0.25	0.40	0.60	0.75	0.85	0.90	0.95
Potency in %	non-seq.	89.3	34.0	53.7	53.9	64.5	77.1	92.4	83.3	62.0	63.8	44.4
	seq	90.7	61.8	92.6	93.1	90.4	90.8	97.8	96.6	97.8	96.9	96.5
Gauge in %	non-seq.	0.04	0.01	0.04	0.05	0.02	0.01	0.01	0.02	0.04	0.05	0.01
	seq.	0.01	0.36	0.00	0.01	0.01	0.01	0.02	0.01	0.02	0.01	0.02

[a)] Location is given as a share of the sample length T.

Table 3.A.11: SIS and LS in the benchmark setup and in alternative setups with different magnitudes of the shift[a)]

		Benchmark: 7	2	4	6	8	10	12	14
Potency in %	non-seq.	89.3	13.5	60.9	85.4	92.1	92.4	94.3	94.4
	seq.	90.7	70.5	87.4	90.8	92.8	92.1	93.8	94.4
Gauge in %	non-seq.	0.04	0.06	0.10	0.05	0.03	0.02	0.01	0.01
	seq.	0.01	0.02	0.01	0.01	0.01	0.01	0.01	0.00

[a)] Magnitude is given as a factor to be multiplied with the prediction error standard deviation (PESD).

Table 3.A.12: SIS and LS in the benchmark setup and in alternative detection settings

		Benchmark: 2 blocks, no re-estimation	3 blocks, no re-estimation	4 blocks, no re-estimation	2 blocks, re-estimation[a)]
Potency in %	non-seq.	89.3	99.2	100	19.9
	seq.	90.7	99.9	100	–
Gauge in %	non-seq.	0.04	0.00	0.01	0.77
	seq.	0.01	0.01	0.02	–

[a)] Results are obtained after 1 iteration; sequential selection is not considered in the re-estimation due to high computational expense and high risk of estimation failures.

Table 3.A.13: Probability of first detection of LS using SIS in the benchmark setup and an alternative setup[a)]

Obs. no.		144	145	146	147	148	149	150	151	152	153	154	155
Benchmark: $7 \cdot PESD$	non-seq.	42.5	9.0	2.9	0.8	0.3	0.2	0.1	0.1	0.0	0.1	0.1	0.2
	seq.	85.9	12.6	1.4	0.1	0.0	0.0	0.0	0.0	0.0	0.0	0.0	0.0
$14 \cdot PESD$	non-seq.	96.6	2.7	0.0	0.1	0.1	0.1	0.0	0.0	0.0	0.0	0.0	0.0
	seq.	90.1	9.7	0.2	0.0	0.0	0.0	0.0	0.0	0.0	0.0	0.0	0.0

[a)] Probability is expressed in %.

Table 3.A.14: SIS in presence of temporary LS at different locations[a)]

		1 shift			2 shifts	
		[0.25, 0.35]	[0.45, 0.55]	[0.5, 0.6]	[0.2, 0.3], [0.35, 0.45]	[0.25, 0.35], [0.65, 0.75]
Potency in %	non-seq.	71.95	87.50	81.80	72.05	53.93
	seq.	91.15	94.95	97.05	85.82	94.55
Gauge in %	non-seq.	0.01	0.01	0.02	0.03	0.00
	seq.	0.00	0.00	0.00	0.00	0.00

[a)] Location is given as a share of the sample length T.

Table 3.A.15: Goodness–of–fit and diagnosis tests results for models without IS, with IIS and SIS for five European countries[a)]

			Goodness–of–fit[b)]				Diagnostics[c)]			
			Log-likelihood	R_S^2	AIC	BIC	$Q(24)$	DW	$H(93)$	BS
ES	no IS		−573.568	0.850	2.520	2.743	49.313*	1.996	2.727*	69.524*
	IIS		−550.238	0.869	2.504	2.897	46.382*	1.900	2.289*	27.091*
	SIS	non-seq.	−515.408	0.892	2.395	2.892	34.590	1.953	1.954*	7.765*
		seq.	−564.973	0.858	2.536	2.876	54.074*	1.995	2.497*	89.223*
FR	no IS		−533.839	0.815	2.195	2.417	44.007*	1.968	4.169*	94.560*
	IIS		−471.754	0.873	2.001	2.472	51.892*	1.859	1.697*	1.566
	SIS	non-seq.	−490.836	0.863	1.985	2.352	53.689*	1.879	2.324*	19.513*
		seq.	−490.836	0.863	1.985	2.352	53.689*	1.879	2.324*	19.513*
GER	no IS		−549.799	0.841	2.259	2.481	45.528*	2.191	1.148	41.605*
	IIS		−485.167	0.885	2.124	2.608	51.892*	1.859	1.697*	1.566
	SIS	non-seq.	−494.171	0.886	2.035	2.427	44.016*	2.269	1.585*	11.260*
		seq.	−490.111	0.889	2.010	2.403	44.761*	2.282	1.464	4.700
IT	no IS		−575.599	0.822	2.532	2.755	66.929*	1.998	2.304*	98.834*
	IIS		−537.196	0.854	2.491	2.936	60.213*	1.937	1.321	3.612
	SIS	non-seq.	−545.703	0.854	2.425	2.791	65.207*	1.983	1.566*	0.221
		seq.	−518.960	0.880	2.324	2.795	65.207*	1.956	1.185	10.841*
UK	no IS		−393.953	0.891	1.038	1.260	43.755*	2.002	1.145	40.822*
	IIS		−349.641	0.915	0.903	1.296	24.539	1.995	1.008	28.059*
	SIS	non-seq.	−325.007	0.930	0.740	1.159	29.742	2.061	1.071	2.727
		seq.	−336.676	0.925	0.796	1.189	23.852	2.046	0.909	2.801

[a)] ES: Spain, FR: France, GER: Germany, IT: Italy, UK: United Kingdom

[b)] R_S^2: coefficient of determination suitable for data displaying trend and seasonal movements; AIC and BIC: information criteria based on the prediction error variance

[b)] $Q(p)$: Ljung–Box statistic based on the first p standardised innovations; DW: Durbin–Watson statistic; $H(h)$: heteroscedasticity statistic based on the first h and the last h standardised innovations, with h being the closest integer to $T/3$; BS: Bowman–Shenton normality statistic; * indicates statistical significance at the 5% level.

Table 3.A.16: Outliers detected for five European countries with different software packages[a),b),c)]

	TRAMO		TSW		X13–ARIMA		STAMP[d)]	
ES	2008.M12	(LS)	2008.M12	(LS)	2008.M12	(LS)	1997.M4	(AO)
							2002.M3	(AO)
							2002.M4	(AO)
							2005.M4	(AO)
							2008.M3	(AO)
							2008.M4	(AO)
							2008.M12	(LS)
FR	2000.M5	(AO)	2000.M6	(TC)	2000.M5	(AO)	2008.M12	(LS)
	2008.M11	(LS)	2008.M11	(LS)	2008.M11	(LS)	2011.M5	(AO)
	2009.M1	(LS)	2009.M1	(LS)	2009.M1	(LS)		
	2011.M5	(AO)	2011.M5	(AO)	2011.M5	(AO)		
			2001.M6	(AO)				
GER	2008.M12	(LS)	2000.M5	(AO)	2000.M5	(AO)	2000.M5	(AO)
			2008.M12	(LS)	2008.M12	(LS)	2009.M6	(SC)
			2009.M12	(TC)	2011.M5	(AO)	2011.M5	(AO)
			2011.M5	(AO)				
			2011.M6	(AO)				
IT	2008.M12	(LS)	1991.M4	(AO)	2008.M12	(LS)	2008.M4	(AO)
	2009.M8	(LS)	1998.M12	(TC)	2008.M12	(AO)	2008.M12	(LS)
			2002.M4	(AO)	2009.M1	(LS)		
			2008.M12	(LS)	2009.M8	(LS)		
			2009.M3	(LS)				
			2009.M8	(LS)				
UK	1998.M1	(LS)	1993.M6	(LS)	2002.M6	(AO)	2002.M6	(AO)
	2002.M6	(AO)	1998.M1	(LS)	2008.M11	(LS)	2008.M12	(LS)
	2005.M3	(AO)	2005.M3	(AO)				
	2008.M11	(LS)	2008.M11	(LS)				
	2009.M1	(LS)	2009.M1	(LS)				

[a)] ES: Spain, FR: France, GER: Germany, IT: Italy, UK: United Kingdom

[b)] Acronyms in the parentheses give the type of the outlier; AO: additive outlier, LS: level shift, TC: transitory change, SC: slope change

[c)] TRAMO: see Gómez and Maravall (1996); TSW: TRAMO–SEATS version for Windows, see Caporello and Maravall (2004); X13–ARIMA: see U.S. Census Bureau (2013); STAMP: see Koopman et al. (2009)

[d)] Time points of breaks in particular unobserved components of the BSM are translated to time points of changes in the observed series.

Table 3.A.17: Periods of first detection of the relevant LS for five European countries[a),b)]

			Time point of LS	Time point of first detection
ES	SIS	non-seq.	–	–
		seq.	2008.M10	2009.M6
FR	SIS	non-seq.	–	–
		seq.	2008.M11	2008.M11
GER	SIS	non-seq.	2008.M12	2009.M2
		seq.	2008.M11	2008.M11
IT	SIS	non-seq.	2008.M12	2008.M12
		seq.	2008.M12	2008.M12
UK	SIS	non-seq.	–	–
		seq.	2008.M11	2008.M11

[a)] ES: Spain, FR: France, GER: Germany, IT: Italy, UK: United Kingdom

[b)] Relevant LS refers to the beginning of the economic crisis and and its time point, as detected by SIS, generally differs across countries. Detection is iteratively performed starting with the sample up to 2008.M9 and ending with the sample up to 2009.M8. Cases in which the relevant LS is not detected in the whole time span are indicated by –.

3.B Figures

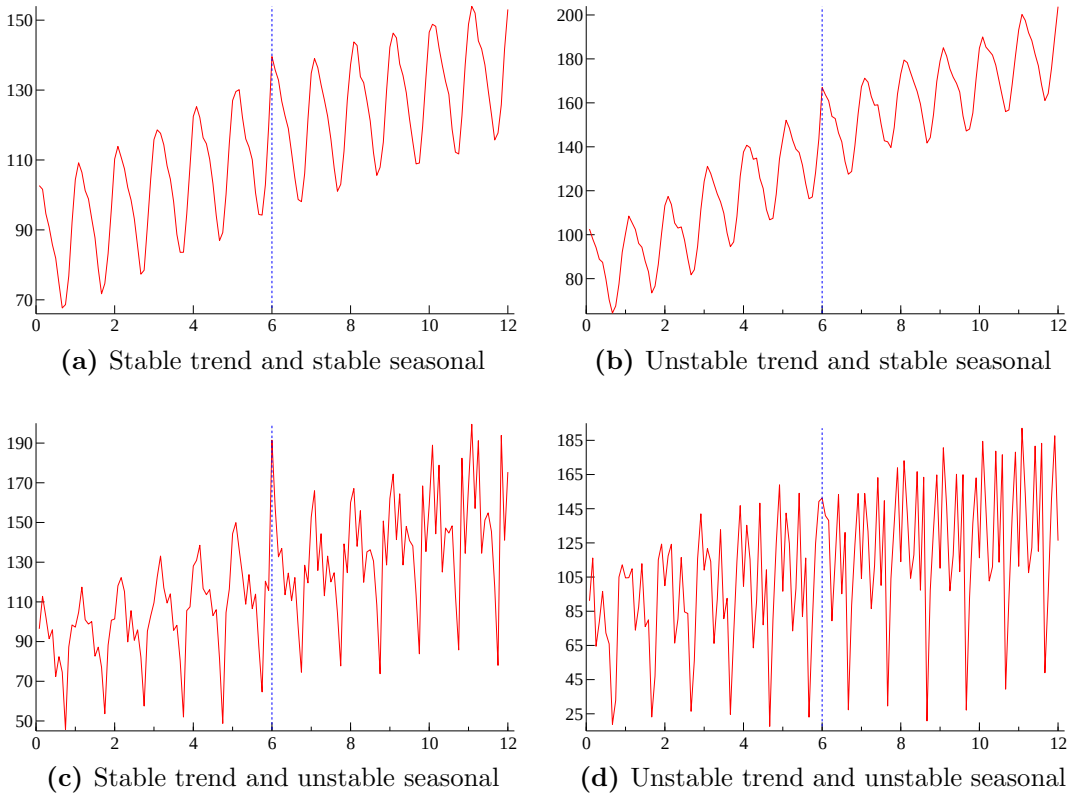

(a) Stable trend and stable seasonal

(b) Unstable trend and stable seasonal

(c) Stable trend and unstable seasonal

(d) Unstable trend and unstable seasonal

Figure 3.B.1: Examples of series simulated with different variance parameters and an additive outlier at 0.5 of the sample

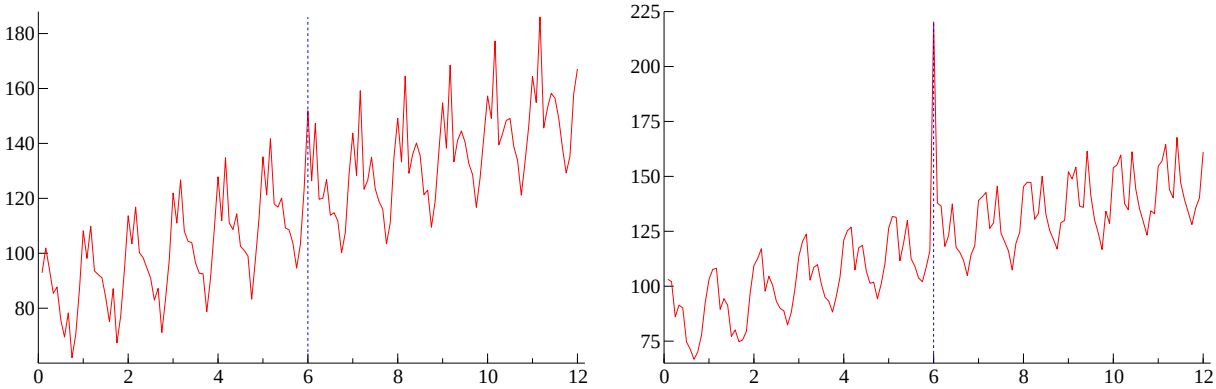

(a) Outlier magnitude given by $2 \cdot PESD$ **(b)** Outlier magnitude given by $14 \cdot PESD$

Figure 3.B.2: Examples of series simulated with an additive outlier of two different magnitudes at 0.5 of the sample

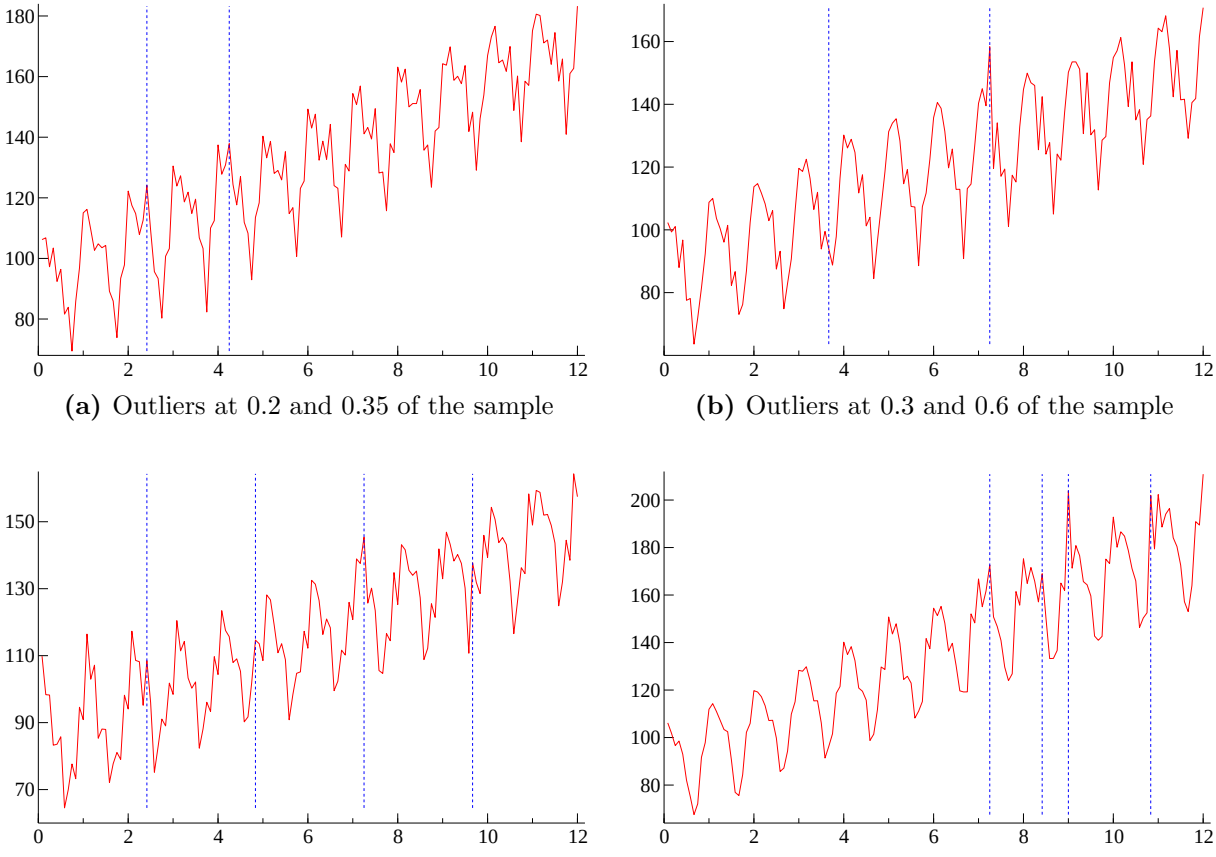

(a) Outliers at 0.2 and 0.35 of the sample

(b) Outliers at 0.3 and 0.6 of the sample

(c) Outliers at 0.2, 0.4, 0.6 and 0.8 of the sample

(d) Outliers at 0.6, 0.7, 0.75 and 0.9 of the sample

Figure 3.B.3: Examples of series simulated with the benchmark specification and multiple outliers at different locations

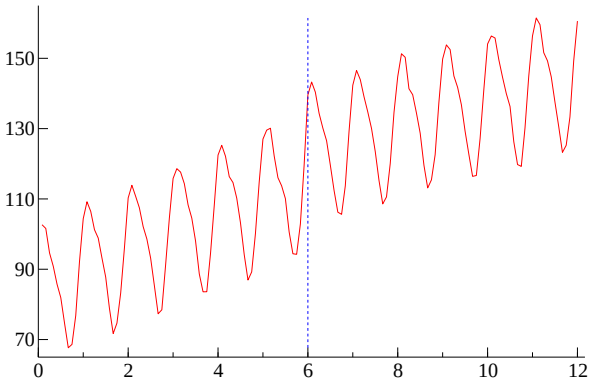

(a) Stable trend and stable seasonal

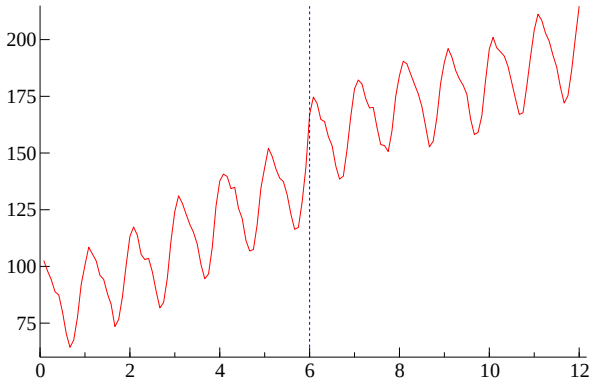

(b) Unstable trend and stable seasonal

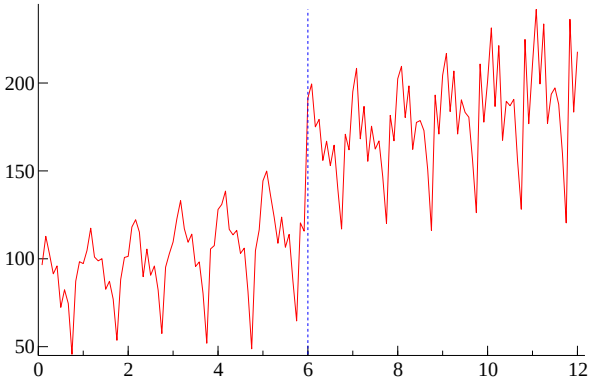

(c) Stable trend and unstable seasonal

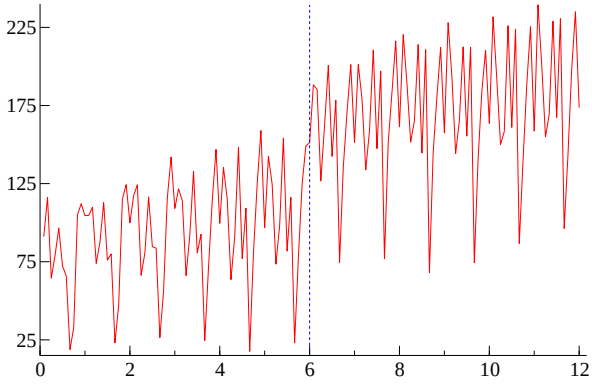

(d) Unstable trend and unstable seasonal

Figure 3.B.4: Examples of series simulated with different variance parameters and a level shift at 0.5 of the sample

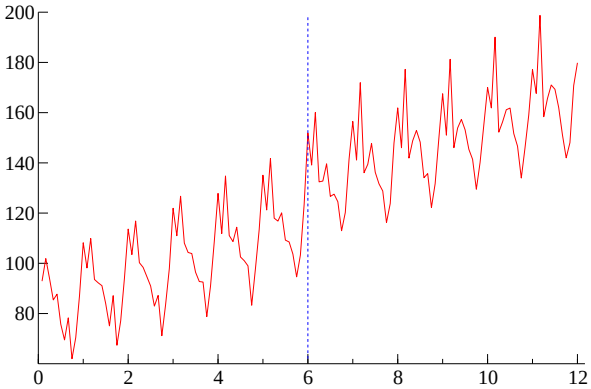

(a) Outlier magnitude given by $2 \cdot PESD$

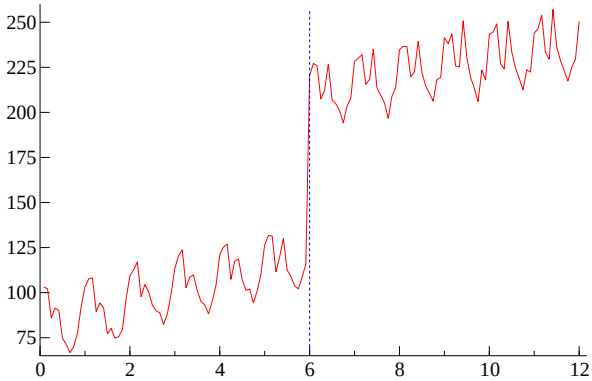

(b) Outlier magnitude given by $14 \cdot PESD$

Figure 3.B.5: Examples of series simulated with a level shift of two different magnitudes at 0.5 of the sample

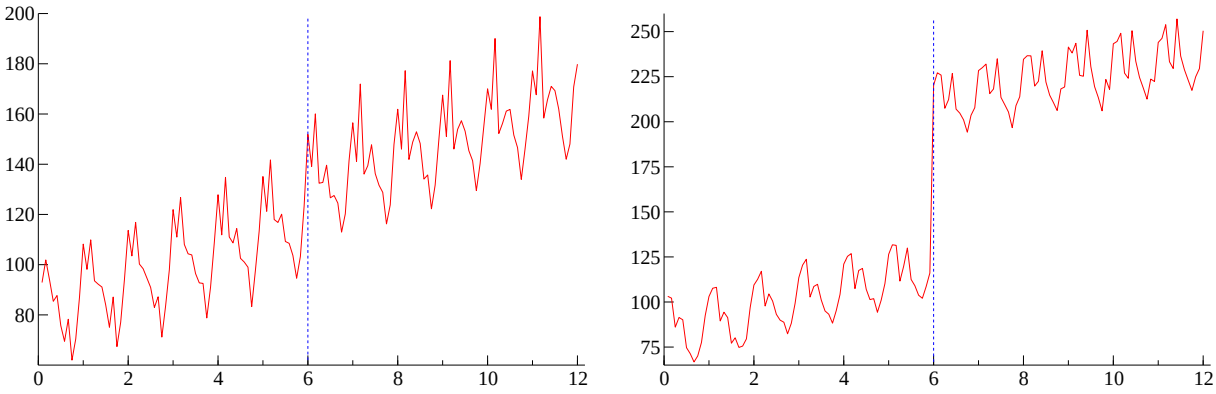

(a) Outlier magnitude given by $2 \cdot PESD$ **(b)** Outlier magnitude given by $14 \cdot PESD$

Figure 3.B.6: Examples of series simulated with a level shift of two different magnitudes at 0.5 of the sample

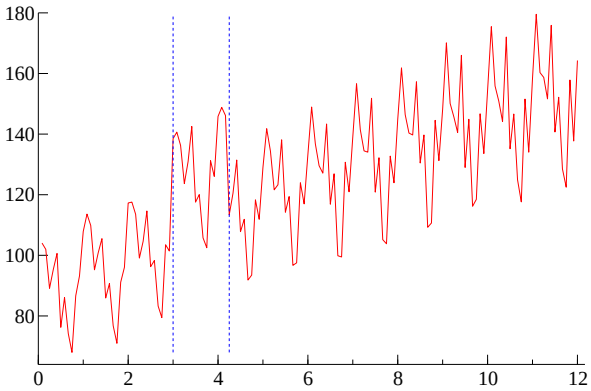

(a) Level shift between 0.2 and 0.35 of the sample

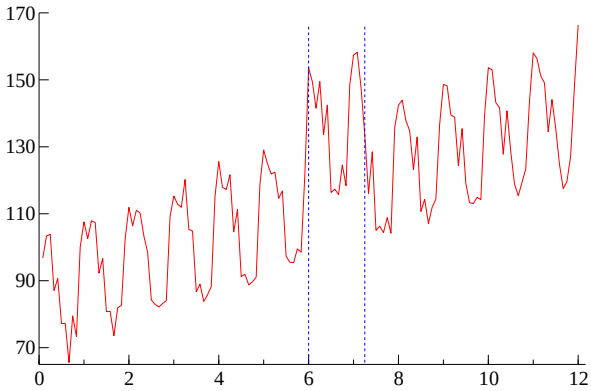

(b) Level shift between 0.5 and 0.6 of the sample

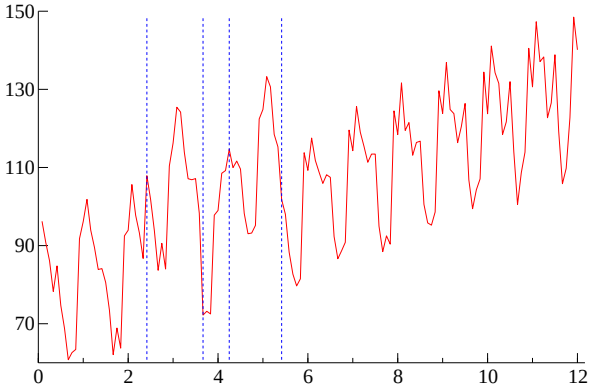

(c) Level shifts between 0.2 and 0.3, and between 0.35 and 0.45 of the sample

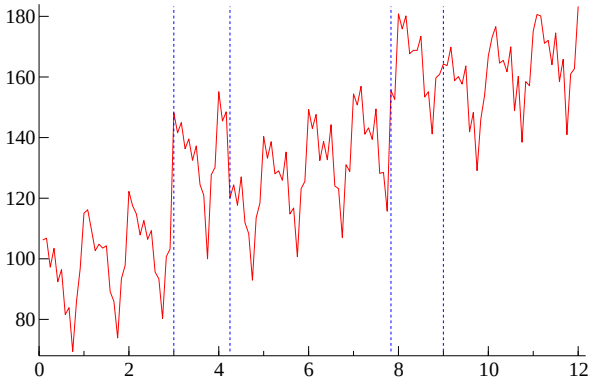

(d) Level shifts between 0.25 and 0.35, and between 0.65 and 0.75 of the sample

Figure 3.B.7: Examples of series simulated with the benchmark specification and multiple interval level shifts at different locations

References

Atkinson, A. C., Koopman, S. J., and Shephard, N. (1997). Detecting Shocks: Outliers and Breaks in Time Series. *Journal of Econometrics*, *80*(2), 387–422.

Caporello, G., and Maravall, A. (2004). *Program TSW: Revised Reference Manual* (Manual). Banco de España.

Castle, J. L., Doornik, J. A., and Hendry, D. F. (2012). Model Selection When There Are Multiple Breaks. *Journal of Econometrics*, *169*(2), 239–246.

Chang, I., Tiao, G. C., and Chen, C. (1988). Estimation of Time Series Parameters in the Presence of Outliers. *Technometrics*, *30*(2), 193–204.

Chen, C., and Liu, L.-M. (1993). Joint Estimation of Model Parameters and Outlier Effects in Time Series. *Journal of the American Statistical Association*, *88*(421), 284–297.

Clements, M. P., and Hendry, D. F. (2011). Forecasting from Mis–specified Models in the Presence of Unanticipated Location Shifts. In M. P. Clements and D. F. Hendry (Eds.), *Oxford Handbook of Economic Forecasting* (chap. 10). Oxford: Oxford University Press.

Doornik, J. A. (2008). *Object-oriented Matrix Programming Ox 6.0*. London: Timberlake Consultants.

Doornik, J. A. (2009a). Autometrics. In J. L. Castle and N. Shephard (Eds.), *The Methodology and Practice of Econometrics: A Festschrift in Honour of David F. Hendry* (pp. 88–121). Oxford: Oxford University Press.

Doornik, J. A. (2009b). *Econometric Model Selection With More Variables Than Observations* (Unpublished paper). Economics Department, University of Oxford.

Doornik, J. A. (2009c). *Object-oriented Matrix Programming using Ox 7*. London: Timberlake Consultants Press.

Doornik, J. A., and Hendry, D. F. (2013). *PcGive 14*. London: Timberlake Consultants. (3 volumes)

Doornik, J. A., Hendry, D. F., and Pretis, F. (2013). *Step–Indicator Saturation* (Discussion Paper No. 658). University of Oxford.

Durbin, J., and Koopman, S. J. (2012). *Time Series Analysis by State Space Methods* (second ed.; O. S. S. Series, Ed.). Oxford: Oxford University Press.

Ericsson, N. R., and Reisman, E. L. (2012). Evaluating a Global Vector Autoregression for Forecasting. *International Advances in Economic Research*, *18*, 247–258.

Gómez, V., and Maravall, A. (1996). *Programs TRAMO and SEATS; Instructions for the User* (Working Paper No. 9628). Servicio de Estudios, Banco de España.

Harvey, A. C. (1989). *Forecasting, Structural Time Series Models and the Kalman Filter*. Cambridge: Cambridge University Press.

Harvey, A. C., and Koopman, J. S. (1992). Diagnostic Checking of Unobserved-Component Time Series Models. *Journal of Business and Economic Statistics*, *10*(4), 377–389.

Harvey, A. C., and Todd, P. H. J. (1983). Forecasting Econometric Time Series with Structural and Box-Jenkins Models (with discussion). *Journal of Business and Economic Statistics*, *1*(4), 299–315.

Hendry, D. F. (1999). An Econometric Analysis of US Food Expenditure, 1931–1989. In J. R. Magnus and M. S. Morgan (Eds.), *Methodology and Tacit Knowledge: Two Experiments in Econometrics* (pp. 341–361). Chichester: John Wiley and Sons.

Hendry, D. F., Johansen, S., and Santos, C. (2008). Automatic Selection of Indicators in a Fully Saturated Regression. *Computational Statistics*, *23*, 317–335.

Hendry, D. F., and Krolzig, H.-M. (2004). *Resolving Three 'Intractable' Problems using a Gets Approach* (Unpublished paper). Economics Department, University of Oxford.

Hendry, D. F., and Mizon, G. E. (2011). Econometric Modelling of Time Series with Outlying Observations. *Journal of Time Series Econometrics*, *3*(1). doi: 10.2202/19411928.1100

Hendry, D. F., and Pretis, F. (2011). *Anthropogenic Influences on Atmospheric CO_2* (Discussion Paper No. 584). University of Oxford.

Hendry, D. F., and Santos, C. (2010). An Automatic Test of Super Exogeneity. In M. W. Watson and T. Bollerslev (Eds.), *Volatility and Time Series Econometrics* (pp. 164–193). Oxford University Press.

Johansen, S., and Nielsen, B. (2009). An Analysis of the Indicator Saturation Estimator as a Robust Regression Estimator. In J. L. Castle and N. Shephard (Eds.), *The Methodology and Practice of Econometrics: A Festschrift in Honour of David F. Hendry* (pp. 1–36). Oxford: Oxford University Press.

Koopman, S. J., Harvey, A. C., Doornik, J. A., and Shephard, N. (2009). *STAMP 8.2: Structural Time Series Analyser, Modeller and Predictor*. London: Timberlake Consultants.

Marczak, M., and Proietti, T. (2014). *Outlier Detection in Structural Time Series Models: The Indicator Saturation Approach* (Discussion Paper No. 90). FZID.

Tsay, R. S. (1986). Time Series Model Specification in the Presence of Outliers. *Journal of the American Statistical Association*, *81*, 132–141.

U.S. Census Bureau. (2013). X–13 ARIMA–SEATS Reference Manual [Computer software manual].

West, M., and Harrison, J. (1997). *Bayesian Forecasting and Dynamic Models* (2nd ed.). New York: Springer–Verlag.

Chapter 4

Real Wages and the Business Cycle in Germany*

4.1 Introduction

At least since Keynes claimed in his General Theory that an increase in employment can only occur with a simultaneous decline in real wages, macroeconomists are debating about whether real wages are anticyclical, procyclical or do not exhibit any systematic relationship with the business cycle. Keynesian economists, for instance, usually justify the hypothesis of anticyclical real wages with rigid nominal wages – at least in the short run. Barro (1990) and Christiano and Eichenbaum (1992) argue that a similar real wage behavior may also arise in models focussing on the intertemporal labor-leisure substitution. The reason is that transitory changes in the real interest rate caused for instance by fiscal policy shocks may shift the labor supply curve and therefore generate anticyclical real wages. In contrast, Kydland and Prescott (1982) or Barro and King (1984) show that real business cycle models that emphasize shifts in labor demand caused by technological shocks lead to procyclical real wages. As argued by Rotemberg and Woodford (1991), a procyclical or an acyclical pattern can result in New Keynesian models under the assumption that the mark–up of monopolistic firms behaves countercyclically. A clearer empirical picture about the adjustment of real wages over the business cycle could shed some light on the main sources of macroeconomic shocks and thereby be of some use in judgements about the empirical relevance of conflicting macroeconomic theories. A clarification of this issue also helps in identifying the sources and features of labor cost dynamics and therefore is of great relevance for monetary policy.

This paper contributes to the literature on the adjustment of aggregate real wages over

*This chapter is the result of the joint work with Thomas Beissinger and has been published in the journal Empirical Economics; see Marczak and Beissinger (2013).

the business cycle in several ways. First, we analyze the comovements between real wages and the cycle not only in the time domain, but also in the frequency domain. So far, most studies have focussed on the time domain approach and described the comovements between variables by traditional cross-correlations measures. However, in the time domain the observed cyclical behavior of the real wage hides a range of economic influences that give rise to cycles of different length and strength, thereby producing a distorted picture of real wage cyclicality, see Hart et al. (2009). The great advantage of an analysis in the frequency domain is that it allows to assess the relative importance of particular frequencies for the behavior of real wages. As has been stressed by Messina et al. (2009), for the analysis of real wage cyclicality it is crucial to differentiate between frequencies or, in other words, between horizons at which comovement is measured. For example, the short-term behavior of real wages may mostly depend on price movements because of short-run nominal wage stickiness, whereas in a later stage of the business cycle real wage changes are more heavily affected by nominal wage adjustments. Considering comovements of real wages and GDP at different frequencies allows to detect such differences in the cyclical behavior of real wages.

An important aspect of the paper lies in the fact that we propose to use the phase angle as a suitable comovement indicator for the business cycle analysis in the frequency domain. In the literature, several frequency-domain concepts have been suggested to measure the comovements between time series processes. These concepts basically differ in the way how they exploit the information contained in the cospectrum and/or the quadrature spectrum. Well-known measures are coherency and squared coherency, also called coherence. Since coherency is based on the cross-spectrum, which is in general a complex-valued function, the interpretation of this measure is somewhat difficult. The problem with squared coherency is that it disregards phase differences between the processes, see Croux et al. (2001) and Tripier (2002). Due to the drawbacks of coherency and squared coherency, Croux et al. (2001) propose another measure, which they term dynamic correlation. Since it is based on the cospectrum, dynamic correlation allows to measure the degree of synchronization between two processes regarding waves with the same frequency. However, as has been pointed out by Mastromarco and Woitek (2007), dynamic correlation does not allow to establish the lead-lag relationship between two processes, since the information contained in the quadrature spectrum is not taken into account. In contrast, with the phase angle we get both, detailed information about the lead-lag behavior of real wages relative to the cyclical behavior of real GDP and information about the correlation be-

tween the particular components of both processes. Following the seminal paper of Burns and Mitchell (1946), the commonly used range for the business cycle length lies between 6 and 32 quarters. We also focus on this periodicity band in our frequency analysis.
A second feature of this paper is the comparison of the comovement results across different detrending methods. More specifically, the methods applied to the time series of aggregate real wages and GDP comprise the Beveridge-Nelson decomposition, the Hodrick-Prescott filter, the Baxter-King filter and the structural time series model of Harvey (1989). Since it is well known from the literature that the results may also be influenced by the price deflator used to compute real wages, we take this into account by considering both producer real wages and consumer real wages.
Third, we analyze the real wage behavior for the economy as a whole whereas many studies only consider real wages in the manufacturing sector, as for example in the recent study of the wage dynamics network of the ECB on real wage behavior in the OECD, see Messina et al. (2009).[1] Because of the much larger shares of the nonmanufacturing sector in total output and employment, empirical results for the economy as a whole are certainly of importance, for instance, for monetary policy.
Forth, whereas the question of the cyclicality of real wages in the US has been analyzed in a host of studies (see the surveys of Abraham and Haltiwanger, 1995, and Brandolini, 1995), surprisingly little systematic empirical evidence exists for Germany. This paper tries to fill this gap and provides a detailed picture of the wage dynamics in an economy in which labor unions (still) affect the majority of employment contracts.
The remainder of the paper is organized as follows. In Section 2 we apply different trend-cycle decompositions to consumer real wages, producer real wages and real GDP. In Section 3 we analyze the comovements between the particular real GDP cycle and the corresponding real wage cycles in the time and frequency domain. Section 4 compares our results to those of the literature. Section 5 summarizes and concludes.

4.2 Identification of the cyclical component

We use seasonally adjusted quarterly data for real GDP, consumer real wages and producer real wages in Germany from 1970.Q1 to 2009.Q1 (157 observations). The data selection is described in more detail in Appendix 4.A. Before we undertake the trend-cycle decompositions we study the stochastic properties of the data. Applying the augmented

[1] In Messina et al. (2009) also time domain and frequency domain methods are used.

Dickey-Fuller (ADF) test and the Phillips-Perron test we find that all series are generated by I(1) processes.

The general framework for the decomposition of each time series into trend and cycle is provided by the following model:

$$y_t = y_t^g + y_t^c + \varepsilon_t, \qquad t = 1, 2, ..., T \tag{4.1}$$

where t is a time index and y_t represents the natural logarithm of the series under consideration, i.e. real GDP, consumer real wages or producer real wages. The series y_t is decomposed into trend y_t^g, cycle y_t^c and (possibly) an irregular component ε_t.

In the structural time series model (STSM), all three components on the RHS of eq. (4.1) are explicitly modeled. The Baxter-King (BK) filter implicitly takes account of these three components. The reason is that the BK filter is an approximate bandpass filter that, with suitably chosen weights, is able to pass through components of the time series with business cycle periodicity while eliminating components at higher and lower frequencies. This can be interpreted as an elimination of the trend and irregular movements from the observed series, thereby extracting the cyclical component. The Hodrick-Prescott (HP) filter and the Beveridge-Nelson decomposition (BN) allow for the removal of the trend and interpret the remaining series as the cyclical component. Hence, these methods attribute any disturbance left in the data after the elimination of the trend to the cyclical component.[2]

As both real GDP and real wages are difference-stationary processes, the approach suggested by Beveridge and Nelson (1981) seems to be a suitable decomposition method for this case. The BN decomposition assumes an I(1) process for the examined series and regards the trend as a prediction of future values of the series. The decomposition leads to a trend component which is a random walk with drift and to a covariance stationary cyclical component which are correlated with each other. However, the BN decomposition also bears some problems. For example, the a priori assumption about the trend being a random walk is somewhat controversial. Another problematic issue concerns the variance of the trend that could even exceed that of the series. Furthermore, the BN decomposition requires an ARMA specification for the examined series. In applied work, however, there often remains some uncertainty about the model specification. Since different model

[2] In the discussion paper version, we also considered the linear trend model with broken trend (LBT). We showed that the LBT cycles do not satisfy the stationarity condition and therefore cannot be used in the comovement analysis.

specifications may lead to different forecasts, they may also imply different trends and cycles. We take the approach of Newbold (1990) which is based on the ARIMA$(p, 1, q)$ representation of the series. According to this method, we have to identify the best ARMA specification for the first differences of real GDP and real wages. Relying on the information criteria (AIC and SIC) we find that the first differences of real GDP and the producer real wage are best described by an AR(4) model, whereas for the consumer real wage in first differences the AR(5) model is the most suitable one.

As the next trend-cycle decompositions we use linear filters, the HP filter and the BK filter, which have proven popular in macroeconomic applications.[3] An advantage of these methods is that they are able to render higher-order integrated processes stationary, up to $I(4)$ and up to $I(2)$ in the case of the HP and BK filter, respectively. However, if these filters are applied to nonstationary processes, they may induce spurious cycles. With respect to the HP filter, Cogley and Nason (1995) and Harvey and Jaeger (1993) show that the frequency components of the resulting series have business cycle periodicity even if there are no important transitory fluctuations in the original data. For the BK filter, Murray (2003) demonstrates that the first difference of an integrated trend enters the filtered series. As a result, the spectral properties of the filtered series depend on the trend in the unfiltered series. Because the analyzed series are nonstationary, the cycles obtained with the HP and the BK filter should be interpreted with some caution.

Finally, we consider structural time series models, which are defined in terms of unobserved components that have a direct economic interpretation, see Harvey (1989, pp. 44–49). The initial specification of the model structure is left to the researcher. Within this framework, the data decide on the characteristics of the particular component. In contrast to the ad hoc filtering approaches, such as the HP and the BK filter, structural time series models rely on the stochastic properties of the data. Moreover, as opposed to ARMA modeling they do not aim at a parsimonious specification. It is quite probable that a parsimonious ARMA model identified by means of standard techniques (e.g. correlograms) does not exhibit properties expected from the examined series. For instance, it could reject cyclical behavior of a series even though such a behavior does really exist. Unfortunately, in applied work finding a "correct" model specification inevitably remains a problem also in

[3]Both filters can be understood as Butterworth filters, see Gomez (2001) and Harvey and Trimbur (2003). For the HP filter we use the value 1600 for the smoothing parameter. For the weights of the BK filter we use the frequencies $\pi/3$ and $\pi/16$ to obtain the business cycle periodicity band between 6 and 32 quarters. We choose 12 for the truncation point, as proposed by Baxter and King (1999) for quarterly data.

the case of structural time series models.

We adopt the model outlined in eq. (4.1) and assume that the irregular component ε_t is normally, independent and identically distributed with variance σ_ε^2. Using the state-space terminology, we refer to eq. (4.1) as the measurement equation. The stochastic trend component y_t^g can be formulated as the so-called local linear trend model (see S. J. Koopman et al., 2008, pp. 22):

$$\begin{aligned} y_{t+1}^g &= y_t^g + \beta_t + \eta_t, & \eta_t &\sim \mathcal{NID}(0, \sigma_\eta^2) \\ \beta_{t+1} &= \beta_t + \zeta_t, & \zeta_t &\sim \mathcal{NID}(0, \sigma_\zeta^2), \end{aligned} \tag{4.2}$$

where β_t is the stochastic slope of the trend. This general model implies an I(2) process for the trend component. Imposing restrictions on this model leads to various trend forms. The assumption $\sigma_\zeta^2 = 0$ implies that the trend is a random walk with drift. If, in addition, β_t is set to zero, the so-called local level model is obtained, i.e. the trend component follows a random walk. The restriction $\sigma_\eta^2 = 0$ results in a relatively smooth I(2) trend, whereas $\sigma_\eta^2 = \sigma_\zeta^2 = 0$ leads to deterministic linear trend. See S. J. Koopman et al. (2009, pp. 55–56) for a model generalization to trends of higher order.

Following S. J. Koopman et al. (2008, p. 23) and Harvey and Streibel (1998), the cycle y_t^c is defined as:

$$\begin{aligned} \begin{bmatrix} y_{t+1}^c \\ y_{t+1}^{c*} \end{bmatrix} &= \rho \begin{bmatrix} \cos(\omega) & \sin(\omega) \\ -\sin(\omega) & \cos(\omega) \end{bmatrix} \begin{bmatrix} y_t^c \\ y_t^{c*} \end{bmatrix} + \begin{bmatrix} \chi_t \\ \chi_t^* \end{bmatrix}, \\ \begin{bmatrix} \chi_t \\ \chi_t^* \end{bmatrix} &\sim \mathcal{NID}(\mathbf{0}, \sigma_\chi^2 \boldsymbol{I}_2), \end{aligned} \tag{4.3}$$

where y_t^{c*} is an auxiliary variable, ω denotes the frequency ($0 \leq \omega \leq \pi$) and ρ is the damping factor ($0 \leq \rho \leq 1$). The period p of the cycle is therefore $p = 2\pi/\omega$. The variance σ_χ^2 is given as $\sigma_\chi^2 = \sigma_c^2(1-\rho^2)$, where σ_c^2 is the variance of the cycle, so that with $\rho = 1$ the cycle is reduced to a deterministic and covariance stationary process. Harvey and Trimbur (2003) generalize the trigonometric version in (4.3) to cycles of higher order.

If the data exhibit specific irregularities, one can take account of them using dummy (or indicator) variables, in this context also called intervention variables, see, e.g., Harvey (1989, pp. 397–408). Their definition and the equation they enter depends on whether the irregularities take the form of outlying observations, a structural break in the level or in the slope of the series. An outlier in the data or a structural break in the level of the series

can be modelled by the corresponding intervention variable in the measurement equation. If a break occurs in the slope of the series, this can be captured by an appropriately defined variable in the slope equation of the trend component.

For all three series we start with the general formulation of the model with a local linear trend as the trend specificaton. The whole model is estimated by maximum likelihood with the Kalman filter. The Kalman smoothing based on the disturbance smoother introduced by J. S. Koopman (1993) provides the estimates of the trend and cycle component. The estimated model parameters, called hyperparameters, that refer to real GDP are reported in Table 4.1. The high value of σ_η^2 relative to σ_χ^2 in model 1 (first row of Table 4.1) indicates

Table 4.1: Estimated hyperparameters of the general and restricted trend-cycle model for real GDP

Model	Hyperparameter[a)]					
	σ_ε^2	σ_η^2	σ_ζ^2	σ_χ^2	ρ	ω
1) no restrictions	0.865	74.98	0.215	11.734	0.976	0.234
2) $\sigma_\eta^2 = 0$	5.032	–	0.449	67.683	0.929	0.194

[a)] The estimated variances have been multiplied by 10^6.

an erratic trend component and a damped cycle component. This result conflicts with the commonly accepted notion of a trend being a slowly evolving component characterized by low frequency movements. Since the restriction $\sigma_\eta^2 = 0$ allows for achieving such a relatively smooth trend, we also estimate the model with this variance restriction.[4] To prove the validity of the variance restriction we apply the likelihood ratio (LR) test. As it is apparent from Table 4.B.1, we find clear evidence (at 5% significance level) that we should not reject the restricted model which performs only slightly worse in terms of goodness-of-fit statistics than the general model. The selected restricted specification implies bigger deviations of the cycle than the general model (see Table 4.1, model 2) and is also able to replicate the German history of booms and recessions.[5]

For the consumer real wage as well as for the producer real wage, the estimation of the

[4] See also Harvey and Jaeger (1993, pp. 236–238) for a similar justification of a smoother trend in the context of Austrian real GDP.

[5] Due to a possible structural break in the data after German reunification, we also considered a model with a slope intervention in 1991.Q1. Yet it generates an almost identical cycle as the selected model and does not provide an improvement in fit over that model. This suggests that our approach of linking the data for West Germany and unified Germany does not influence the stability of the results. The respective results are available on request.

initial model does not lead to a steady state for the Kalman filter.[6] In such case, the results are not reliable and for that reason we do not discuss them. In the next step, we impose the restriction $\sigma_\eta^2 = 0$. The estimated parameters of the restricted model for the consumer and producer real wage are summarized in Table 4.2 (model 1) and in Table 4.3 (model 1), respectively. The high variances of the irregular components with, at the same time, low variances of the cycle components may signalize that, while specifying the model, some information has possibly been omitted. A known event that heavily affected the German labor market was the Hartz reforms starting from January 1, 2003. Regarding the wage setting process, the Hartz reforms may have contributed to a lower

Table 4.2: Estimated hyperparameters of two trend-cycle models for the consumer real wage

Model	Hyperparameter[a)]				
	σ_ε^2	σ_ζ^2	σ_χ^2	ρ	ω
1) $\sigma_\eta^2 = 0$,	33.166	3.298	1.102	0.966	0.468
2) $\sigma_\eta^2 = 0$, slope interv. 2003.Q1	25.399	1.103	18.154	0.934	0.210

[a)] The estimated variances have been multiplied by 10^6

wage growth over the last years. We incorporate this hypothesis into the restricted model for both the consumer and producer real wage using a slope intervention variable from 2003.Q1 on. This model extension induces a fall in the variance of the irregular term and a greater variation of the cycle (see model in Tables 4.2 and 4.3). Moreover, as is readily apparent from Tables 4.B.2 and 4.B.3, model 2 performs at least as well as model 1 in terms of goodness-of-fit. Therefore, for real wages we prefer the specification with a slope intervention in 2003.Q1.[7] Following, e.g. Harvey and Koopman (1992) and Commandeur and Koopman (2007), we then check all selected models with the following diagnostic tests: the Ljung-Box autocorrelation test, the Goldfeld-Quandt heteroscedasticity test and the Doornik-Hansen normality test. The results of the diagnostic tests are summarized in Tables 4.B.1, 4.B.2 and 4.B.3. In all cases, we cannot reject the hypothesis of

[6] Moreover, the reported estimation results would imply a deterministic cycle for both series.

[7] As in the case of real GDP, we considered the possibility of a structural break due to the German reunification. Adding a slope intervention variable in 1991.Q1 in either model 1 or model 2 impairs the fit relative to the preferred specification. The respective results are available upon request. It should also be mentioned that in the discussion paper version we did not take intervention variables into account and as a final specification for both real wages we chose a model with a 3rd order trend. The current model entails better goodness of fit and, in contrast to the previous one, is also capable of generating significant results in the frequency domain.

Table 4.3: Estimated hyperparameters of two trend-cycle models for the producer real wage

Model	Hyperparameter[a)]				
	σ_ε^2	σ_ζ^2	σ_χ^2	ρ	ω
1) $\sigma_\eta^2 = 0$,	30.67	12.293	10.776	0.928	0.505
2) $\sigma_\eta^2 = 0$, slope interv. 2003.Q1	12.987	1.905	64.39	0.94	0.224

[a)] The estimated variances have been multiplied by 10^6

no autocorrelation at the 5% significance level. According to the heteroscedasticity test, the homoscedasticity assumption is only valid for the producer real wage, whereas the Doornik-Hansen test indicates violation of the normality assumption for all series. Nevertheless, since the main concern of time series analysis is the autocorrelation problem we can conclude that these models provide a satisfying approximation to the data generating process.

Apart from being an attractive decomposition method, the framework of structural time series modeling offers the possibility to tie the HP filtering scheme to the model-based approach. This is achieved by rewriting the measurement equation as a trend-irregular model (see, e.g., Harvey and Jaeger, 1993, and Harvey and Trimbur, 2003):

$$y_t = y_t^g + \bar{\varepsilon}_t, \qquad \bar{\varepsilon}_t \sim \mathcal{NID}(0, \sigma_{\bar{\varepsilon}_t}^2) \tag{4.4}$$

where $\bar{\varepsilon}_t$ denotes the irregular component which can be linked to eq.(4.1) through the relationship: $\bar{\varepsilon}_t = y_t^c + \varepsilon_t$. To obtain the HP trend, the term y_t^g is formulated as an $I(2)$ process as in eq. (4.2) with the restrictions $\sigma_\eta^2 = 0$ and $\sigma_\zeta^2 = 1/\lambda$. The parameter λ is the smoothing parameter of the HP filter and is usually set to 1600 for quarterly data. The estimated HP cycle corresponds to the smoothed irregular component. The imposed restrictions can be tested by comparing the fit of the restricted model with the fit of its unrestricted version. We find that, in the case of the examined series, these restrictions lead to inferior goodness-of-fit statistics and that the HP filter is also unfavourable relative to our preferred trend-cycle-irregular specification.[8] Because of the frequent application of the HP filter in the business cycles context, in the following sections we also analyze the HP cycles.

In Figure 5.2, we depict the cyclical component for real GDP and the real wage series

[8]The results can be provided on request.

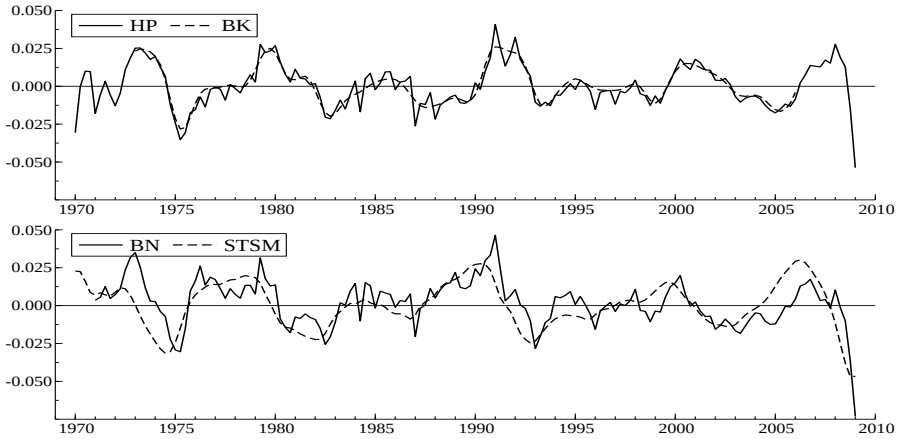

(a) Cycles of real GDP

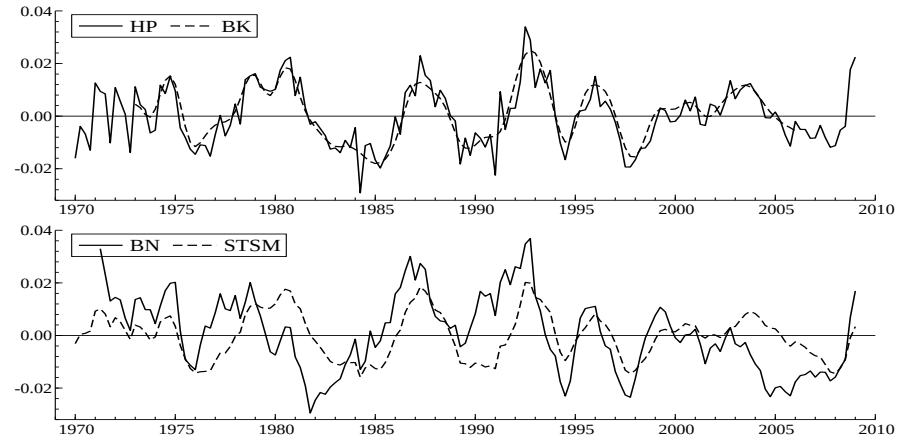

(b) Cycles of the consumer real wage

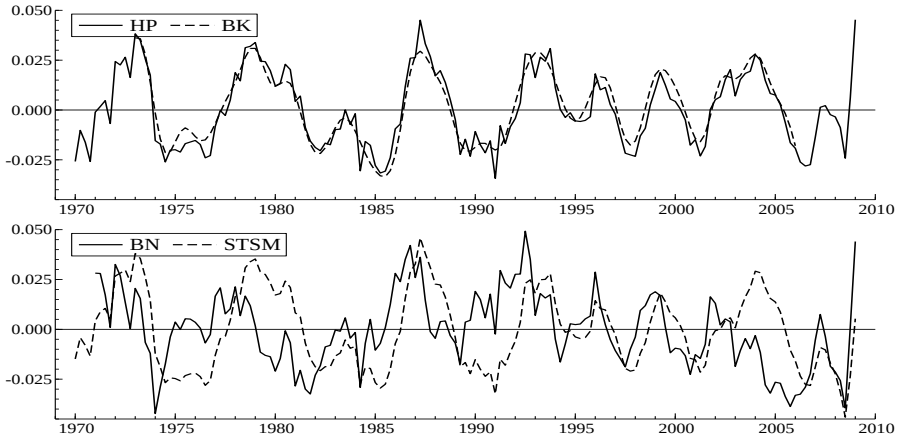

(c) Cycles of the producer real wage

Figure 4.1: Real GDP and real wage cycles

for the different detrending methods outlined above. In the case of real GDP, all cycles behave similarly in that they indicate the periods of booms and recessions that Germany has experienced since 1970.[9] For both the consumer and producer real wage, it is apparent that the BN cycles are shifted relative to the STSM, HP and BK cycles. As regards the smoothness of the cycles, bearing in mind the trend-cycle decomposition of the HP filter and the BN method, it is not surprising that the corresponding cycles display a more irregular course than the other cycles.

4.3 Comovements of real GDP and real wages

4.3.1 Time domain

The analysis of comovements in the time domain between real wage cycles and real GDP cycles as a reference for the business cycle is a natural approach to detect the cyclical behavior of real wages. In the literature several concepts have been suggested for the measurement of comovements in the time domain. One concept is based on the idea of rank reduction and especially common features. In the context of covariance-stationary cyclical components, this amounts to analyzing the so-called common cycles associated with the serial correlation common feature as defined by Engle and Kozicki (1993). Vahid and Engle (1997) extend this method to test for comovements (codependent cycles) if the cycles are not synchronized, i.e. if there is a delay in the response of one cycle to the movements of the other. As stressed by Croux et al. (2001), these measures, however, are not well suited to establish the strength of the correlation between the cycles because they represent only a binary measure. Another route is followed by den Haan (2000) who uses the correlations of VAR forecast errors at different horizons thereby taking the dynamics of the system into account when analyzing the comovements between time series.
Since our focus is on the frequency domain approach which also enables us to unveil the dynamic relationship between real wage cycles and GDP cycles, we restrict our analysis in the time domain to the computation of sample cross-correlations between the cycle of each of the real wage series and the real GDP cycle. We consider not only the contemporaneous relationship but also analyze whether real wages react with delay or run ahead of cyclical movements in real GDP. We classify the considered real wage as procyclical (coun-

[9] The booms and recessions, which could be recognized in Figure 5.2, correspond quite well to the turning points found by Schirwitz (2009).

tercyclical) if the estimated correlation coefficients are positive (negative) taking account of the lead-lag structure of the examined series. If the estimated correlation coefficients are close to zero, the particular real wage is defined to be acyclical. If the largest sample cross-correlation occurs at any lead (lag) relative to the GDP cycle, the particular real wage is lagging (leading) the cycle.

Table 4.4: Contemporaneous and largest sample cross-correlations between the real GDP cycle and the particular real wage cycle by various decomposition methods

Correlation of GDP with	Methods			
	BN	HP	BK	STSM
consumer real wage	0.1169	0.0124	0.1438	-0.2795^*
	$0.4879^*(+6)$	$0.4572^*(+6)$	$0.6346^*(+5)$	$0.3845^*(+11)$
producer real wage	0.0279	-0.0423	0.0314	0.0069
	$0.2718^*(+6)$	$0.2381^*(+7)$	$0.315^*(+7)$	$0.1806^*(+11)$

Notes: * indicates statistical significance at the 5% level

The findings are summarized in Table 4.4. Each cell contains in the first row the contemporaneous sample cross-correlation between the cycle of the real wage series and the corresponding real GDP cycle. The value below is the maximum sample cross-correlation at the kth lead or lag of the real wage cycle relative to the real GDP cycle, where $k \in \{-12, -11, ..., 0, ..., 11, 12\}$. The number in brackets along with the "+" or "−" sign specifies at which lead or lag of the real wage cycle this maximum cross-correlation occurs.[10] We first consider the results for the consumer real wage. Except for the STSM cycle, the estimates of the contemporaneous cross-correlation are positive but statistically insignificant at the 5% level. The low practical significance is most apparent in the case of the HP cycle. Considering the leads of the real wage cycles, we find that for all cycles except for the STSM cycles, the relationship with the corresponding real GDP cycles is still positive but now becomes significant. The sample cross-correlations reach their maximum values at the 6th lead (BN and HP cycles) or 5th lead (BK cycles). In the case of the STSM cycles, there is first a significant negative sample cross-correlation until the 3rd lead. From the 6th lead, it takes high positive values that are statistically significant. We find the greatest cross-correlation at the 11th lead. Examination of the lags of the real wage cycles reveals that almost all sample cross-correlations are statistically insignificant

[10] For clarity reasons, we do not present detailed figures of the lead-lag structure and instead describe some results verbally.

in the case of the HP, BK and BN cycles. The significant ones are small compared to the significant sample cross-correlations at the leads.[11] To sum up, the consumer real wage displays a procyclical pattern and lags the business cycle. The strongest reaction to the actual economic situation can be observed between the 5th and the 11th quarter.
The behavior of the producer real wage differs somewhat from that of the consumer real wage. All estimated contemporaneous cross-correlations are statistically insignificant at the 5% level. Furthermore, although there is a similar cyclical pattern as in the case of the consumer real wage, the sample cross-correlations at the leads of the real wage are not as high. In Table 4.4 this is evident from the differences in the maximum cross-correlations between both wages. The sample cross-correlations at the lags of the producer real wage, with the exception of some lags in the case of the BN cycles, are statistically insignificant. The analysis leads to the conclusion that the producer real wage behaves procyclically and lags the business cycle. The main reaction to the actual economic situation occurs after 6 (BN cycle) to 11 (STSM cycle) quarters.

4.3.2 Frequency domain

A drawback of the above analysis is that the observed behavior of real wages in the time domain possibly results from the countervailing or/and reinforcing influences of cycles of different length and strength. As a consequence, if we want to learn something about the behavior of real wages *over the business cycle*, we could be misled by looking at the time domain results alone. In this section, we resort to some spectral analysis concepts that enable us to assess the relative importance of cycles of different length and therefore provide a comprehensive picture on the cyclical behavior of real wages.
We consider two processes y_{kt} and y_{lt}, where y_{kt} acts as business cycle reference. The frequency by frequency relationship between these processes can be measured by the cross-spectrum $s_{kl}(\omega)$, where ω is the angular frequency. The cross-spectrum, which is a complex-valued function of ω, can be decomposed into the real part $c_{kl}(\omega)$ called cospectrum and the imaginary part $q_{kl}(\omega)$ called quadrature spectrum. The so-called phase angle takes into account information contained in both cospectrum and quadrature spectrum and allows for insights into the lead-lag behavior of real wages relative to the cyclical behavior of real GDP. In addition, this measure enables us to make statements

[11] In the case of the STSM cycles, the significant negative sample cross-correlations emerge at the first 3 lags. In contrast, the BN cycles are characterized by positive cross-correlations which, though, are insignificant.

about the correlation between the particular components of both processes. The phase angle, denoted by $\theta(\omega)$, is defined as:

$$\theta(\omega) = \arctan\left[\frac{q_{kl}(\omega)}{c_{kl}(\omega)}\right] \tag{4.5}$$

Because of the properties of arctangent, the phase angle $\theta(\omega)$ is a multivalued function. For a given ω, the values of arctangent are given by the respective principal value $\pm n\pi$, where $n = 0, 1, 2...$ and the principal value lies in $(-\pi/2, \pi/2)$. It is common to limit values of the phase angle to the interval $[-\pi, \pi]$, see Priestley (1981, p. 661). Note that $\theta(\omega) \equiv \pm\pi/2$ for $c_{kl}(\omega) = 0$ and $q_{kl}(\omega) \gtrless 0$. If $0 < \theta(\omega) < \pi$, the component of y_{lt} with frequency ω lags the corresponding component of y_{kt}, or what amounts to the same thing, the component of y_{kt} leads the corresponding component of y_{lt}. The opposite case is implied by $-\pi < \theta(\omega) < 0$. Both components are in phase if $\theta(\omega)$ equals zero. When one process is lagging (leading) the other process, $\theta(\omega)/\omega$ measures the extent of the time lag (lead). Based on the values of the phase angle we can also make statements about the correlation between the components of y_{kt} and y_{lt}. If the values of the phase angle range between $(-\pi/2, \pi/2)$, the respective components are positively correlated (procyclical behavior), whereas the values of $\theta(\omega)$ in the interval $[-\pi, -\pi/2)$ or $(\pi/2, \pi]$ indicate a negative relationship (countercyclical behavior) between them.

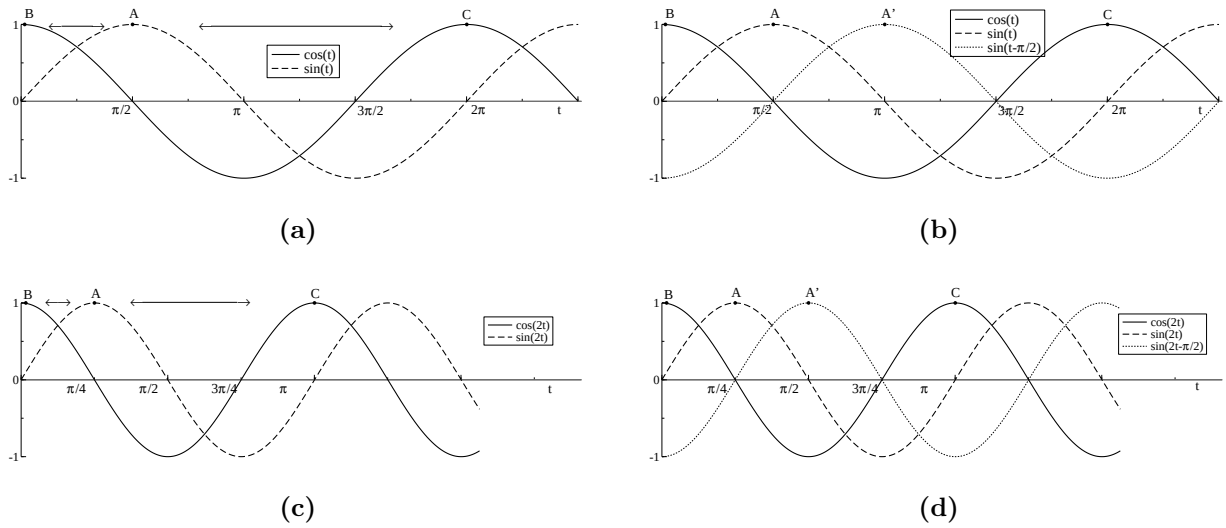

Figure 4.2: Examples of phase shifts between cyclical components

Figure a provides some intuition why the phase angle values are restricted to the interval

$[-\pi, \pi]$. In this simple example, we consider for each process a single cyclical component with the same frequency $\omega = 1$, namely $\cos(t)$ (solid line) for y_{kt} and $\sin(t)$ (dashed line) for y_{lt}. To determine the leading or lagging behavior of y_{lt} relative to y_{kt}, one should consider points that represent similar states in the respective cycle and are "relatively close" to each other. For example, if we focus on the peaks of the two components, it makes more sense to compare peak A of the sine function with peak B and not with peak C of the cosine function, because the time shift between peaks A and B is smaller than between peaks A and C. As a consequence, this frequency component of y_{lt} is lagging the corresponding frequency component of y_{kt} by $\theta(\omega)/\omega = \pi/2$, i.e. $\sin(t+\theta(\omega)/\omega) = \sin(t+\pi/2) = \cos(t)$. From Figure b, it is also evident that shifting the y_{lt} component to the right by $\pi/2$ (dotted line) implies the distance $A'B$ being exactly equal to the distance $A'C$. Hence, the time shift for which the y_{lt} component could as well be characterized as the lagging and as the leading component equals π. Since $\omega = 1$, it follows that in this case $\theta(\omega) = \pi$. The same argumentation can be applied to situations in which the component of y_{lt} leads the corresponding component of y_{kt}, implying negative values for the phase angle. To summarize, for the determination of the lead-lag behavior the phase angle is only considered in the range $(-\pi, \pi)$. If we considered higher values, we would, for example, compare peaks of two time series that are farther away from each other and this way we would compare peaks that belong to different business cycles.

By examining Figure b, we can also make statements about the correlation between the components of y_{kt} and y_{lt}, represented by $\cos(t)$ and $\sin(t)$, respectively. It can be seen that one half of the cosine cycle is negatively correlated with the sine cycle whereas the other half is positively correlated, hence in total no clear-cut conclusion about the correlation between the two components can be drawn. In this case the phase angle equals $\pi/2$. For higher values of the phase angle, a negative correlation would emerge. If, in the extreme case, the component of y_{lt} is supposed to be the wave given by $\sin(t - \pi/2)$ (dotted line) so that the phase angle value equals π, it is immediately obvious that it is perfectly negatively correlated with the y_{kt} component. If, instead of lagging, the y_{lt} component were leading the y_{kt} component by more than $\pi/2$, the correlation between them would also be negative. The above interpretation of the phase angle values restricted to $[-\pi, \pi]$ does not change for frequencies other than $\omega = 1$. Figures c and d illustrate the case when $\omega = 2$. It is apparent that for the appriopriate lead-lag and correlation classification, the time shift between the components has been halved relative to the case of $\omega = 1$. However, the corresponding values of the phase angle still are the same.

Even if we restrict the phase angle values to $[-\pi, \pi]$, $\arctan(\cdot)$ takes on two possible values in this interval. The unique value and therewith the sign of the phase angle can, however, be determined by the signs of the cospectrum and the quadrature spectrum. To understand this, one should bear in mind that the phase angle can be depicted in the Argand diagram in which the cospectrum is represented on the real axis and the quadrature spectrum is represented on the imaginary axis. The phase angle is the angle in the interval $[-\pi, \pi]$ between the positive half of the real axis and the line joining the origin and the point $(c_{kl}(\omega),\, q_{kl}(\omega))$.[12]

We focus on the nonparametric approach to the estimation of spectra and cross-spectra.[13] Figures 4.3 and 4.4 show the estimation results for the phase angle for real GDP cycles and the corresponding consumer and producer real wage cycles, respectively, for all decomposition methods. The 90% confidence bounds for the respective point estimates of the phase angle are constructed as described in Koopmans (1974, pp. 285–287). The frequency range presented here covers all business cycle periodicities, i.e. periods between 1.5 and 8 years, corresponding to frequencies between $2\pi/32$ and $2\pi/6$ for quarterly data. The relationship between frequency ω and period p is given by the formula: $p = 2\pi/\omega$. It should be noticed that the vertical axis representing the values of the phase angle is divided into four regions.[14] If the confidence interval covers one of two upper regions, the real wage cycle significantly lags the real GDP cycle. The opposite holds true if the confidence interval lies in one of the two lower regions. A significant procyclical behavior of the real wage cycle is indicated by the confidence interval in the two regions around 0. If, on the other hand, the confidence interval covers the top or the bottom region we conclude that the real wage behaves countercyclically. If the confidence interval covers at least three regions, we interpret it as being a "no information confidence interval".

In Figure 4.3, it is apparent that for the consumer real wage the point estimates of the phase angle display very similar pattern across all decomposition methods. At all frequencies, the estimated phase angle takes on positive values which suggests a lagging behavior of cycles of the real wage characterized by business cycle frequencies with respect to the corresponding cycles of real GDP. Statistical significance of such a behavior pertains

[12] See Priestley (1981, p. 661). We calculated the unique value of the phase angle in Matlab using the function atan2.

[13] We use the Bartlett window with the lag size of 20, which implies that in total 41 covariances are weighted with positive coefficients of the Bartlett window. For more details on spectrum estimation, see Koopmans (1974) and Priestley (1981).

[14] The results for each frequency are illustrated on a linear scale which can be obtained through "straightening" a circular scale connected by the points representing angles π and $-\pi$.

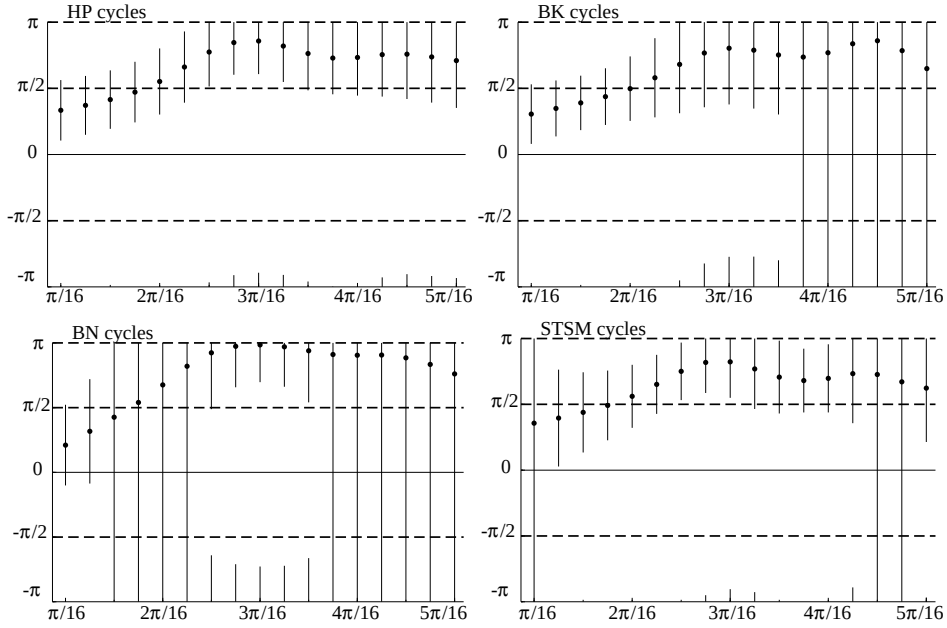

Figure 4.3: Phase angle: real GDP and consumer real wage cycles

Notes: The horizontal axis represents the (angular) frequency ω.

to almost all business cycle frequencies in the case of the HP and STSM cycles. For the BK cycles, a statistically significant lagging pattern is found for components of the consumer real wage with frequencies up to about $5\pi/32 \approx 0.5$. As regards the BN cycles, the lagging behavior cannot be interpreted as statistically significant. We also observe that for all four decomposition approaches, the frequencies up to about $2\pi/16$, corresponding to periods above 16 quarters, are associated with point estimates of the phase angle in the interval $[0, \pi/2)$. The significant ones are confined to the frequencies up to $5\pi/64 \approx 0.25$ in the case of the HP and BK cycles thereby indicating a procyclical pattern of the consumer real wage at these frequencies. In contrast, shorter waves of the real wage are negatively correlated with the respective real GDP component as shown by the estimated phase angle values lying above $\pi/2$. Notice that for the middle range of the considered frequencies between about $5\pi/32$ and $7\pi/32$, the results for the HP, BN and STSM cycles consistently reveal a significant countercyclical pattern of the consumer real wage. Taking all findings into account we can conclude that, in general, longer consumer real wage cycles seem to exhibit a procyclical and lagging behavior, whereas the shorter ones evolve countercyclically and also react with delay to the actual economic situation. For the producer real wage, the point estimates of the phase angle presented in Figure 4.4

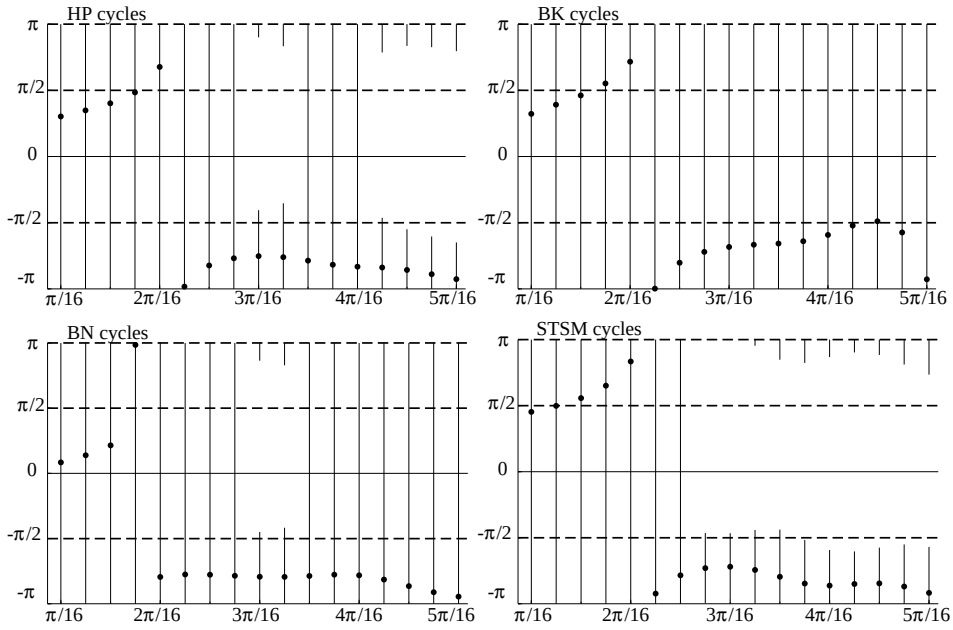

Figure 4.4: Phase angle: real GDP and producer real wage cycles

Notes: The horizontal axis represents the (angular) frequency ω.

look quite similar to the ones for the consumer real wage if we consider the estimated values of the phase angle at lower frequencies. Also the values in the interval $[-\pi, -\pi/2)$ at the frequencies above $9\pi/64 \approx 0.44$ could serve as an indicator for a countercyclical behavior of the producer real wage. Especially the findings for the STSM cycles point to a clear-cut statistically significant negative correlation between the components of the real wage and real GDP beginning at the frequency $11\pi/64 \approx 0.54$. Despite this similarity to the correlation scheme of the shorter cycles of the consumer real wage, it can be noted that for shorter cycles the producer real wage seems to lead the corresponding real GDP cycle. However, the few statistically significant negative values of the phase angle occur only in the case of the STSM cycles. Summing up, the frequency-domain results for producer real wages, with an exception of those related to the correlation pattern at higher frequencies, remain rather inconclusive.

4.4 Comparison with the literature on real wage cyclicality in Germany

As far as we know there exist only a few studies reporting results about the cyclicality of real wages in Germany. Dealing first with studies using aggregate data, the papers of Brandner and Neusser (1992) and Pérez (2001) compute cross-correlations between real wages and GDP in Germany (among others) after detrending the data with the HP filter.[15] Using quarterly data from 1960.Q1 to 1989.Q4 Brandner and Neusser (1992) find a positive contemporaneous cross-correlation between these variables for Germany. Moreover, real wages are leading the GDP cycle and are positively correlated with GDP at these leads. Pérez (2001) considers the period from 1970.Q2 to 1994.Q1. His HP filter results point to acyclical real wages, whereas the robustness checks based on the BK filter find that real wages are procyclical and lagging, which is more in line with the time-domain results of our study. Lucke (1997) applies the methodology of Burns and Mitchell (1946) to the first differences of the logged variables of per-capita GDP and real wages (among others) for the period 1960.Q1–1994.Q4. For the expansionary phase of the business cycle he finds a low negative "conformity" of real wages that can be interpreted as weakly anticyclical real wages, whereas in the contractionary phase no clear-cut pattern emerges. This concept of conformity measures to what extent the cycle of a specific variable coincides with the reference cycle, but the lag-lead structure between these series is not taken into account. Messina et al. (2009) apply the time-domain approach of den Haan (2000) and the dynamic correlation measure of Croux et al. (2001) to the first differences of real wages and the respective business cycle indicator. Using quarterly data from 1960.Q1 to 2004.Q1, they find that real wages in Germany are procyclical at all business cycle horizons considered, irrespective of the deflators used. The difference to our study is that we find a negative correlation at higher business cycle frequencies. This could be due to the fact that, as outlined in the introduction, dynamic correlation does not take the phase shift between the series into account, in contrast to the phase angle used in our study.

The cyclicality of real wages has also been analyzed in some micro-data studies. Anger (2007) and Peng and Siebert (2007) analyze the cyclicality of real wages in Germany for different group of workers and/or for different wage measures using individual based micro-data from the German Socio-Economic Panel Study (SOEP). In these studies a two-step

[15] Pérez (2001) also applies the BK filter and first differences for robustness checks.

estimation technique is applied. In the first step, individual wage changes are explained by individual characteristics and year dummies. In the second step, the coefficients of the year dummies are regressed on the change in aggregate unemployment and a linear time trend. Peng and Siebert (2007) find that real wages of job stayers in the private sector in West Germany — but not East Germany — are procyclical. According to Anger (2007) hourly wages or base salaries seem to be acyclical, whereas overall earnings including overtime pay or bonuses exhibit a procyclical pattern.[16] The advantage of these micro-data studies is that in the first step one can control for changes in sample composition. However, the time series analysis in the second step is quite rudimentary because of relatively few annual observations. For instance, the stochastic properties of the time series are not taken into account and a thorough analysis of the lead-lag structure between real wages and the business cycle variable is missing.

4.5 Summary and conclusions

This paper provides stylized facts about the cyclical behavior of consumer and producer real wages in Germany. To see whether a robust empirical picture on real wage behavior emerges, several detrending methods have been applied to both real wage series and real GDP, including the Beveridge–Nelson decomposition, the Hodrick-Prescott filter, the Baxter–King filter and the structural time series model. The stochastic properties of the original time series and the derived cyclical components were analyzed using a set of unit root tests and other diagnostic tests.

We then analyzed the comovements of the detrended real wage series with real GDP in the time domain and in the frequency domain. For both approaches not only the contemporaneous correlation between real wages and GDP, but also the lag-lead structure has been taken into account. In the time domain the sample cross-correlations between the cycle of each of the real wage series and the GDP cycle have been evaluated. According to our results in the time domain, the contemporaneous correlation between the real wage and GDP is statistically insignificant, with the exception of the cycles from the structural time series model. In the latter case we found a negative contemporaneous correlation. Regarding the lead-lag structure, the consumer real wage displays a procyclical pattern and lags behind the business cycle. The strongest reaction to the actual economic situation

[16] The procyclical pattern of real wages may be related to the anticyclical pattern of real wage rigidity in Germany that is documented in Bauer et al. (2007)

can be observed between the 5th and the 11th quarter. For the producer real wage all estimated contemporaneous cross-correlations are statistically insignificant. Furthermore, although there is a similar cyclical pattern as in the case of the consumer real wage, the sample cross-correlations at the leads of the real wage are not as high.

In the next step, we analyzed the comovements in the frequency domain. The great advantage of an analysis in the frequency domain is that it allows to assess the relative importance of particular frequencies for the behavior of real wages. We followed the nonparametric approach to the estimation of spectra and cross-spectra. The analysis of the phase angle for the consumer real wage shows that the observed cyclicality depends on the frequency range under consideration. All decomposition methods for which we got statistically significant results reveal a similar pattern. The consumer real wage is lagging the real GDP cycle. For shorter time periods up to about four years, the consumer real wage shows an anticyclical behavior, whereas for longer time spans a procyclical behavior can be observed. For the producer real wage, however, the results in the frequency domain remain inconclusive.

Our results for consumer real wages are in line with an economy that is characterized by wage stickiness in the short run. For example, an economic upswing could first lead to a decline in real wages because of rising prices and rigid nominal wages. In the longer run, nominal wages are adjusted upwards eventually leading to a rise in real wages as well.

Appendix

4.A Data selection

In our analysis, we use seasonally adjusted quarterly data. The real GDP series is based on the price adjusted chain index with the base year 2000 (source: Deutsche Bundesbank, series JB5000). The raw data before 1991.Q1 referred to West Germany and after 1991.Q1 to unified Germany. The index series has already been linked over the annual average for 1991. We multiplied the index with the nominal GDP in 2000 and divided it by 100 (source of nominal GDP: Statistisches Bundesamt, GENESIS online database). We obtained the real wage series on the basis of gross wages and salaries (source prior to 1991.Q4 for West Germany: Statistisches Bundesamt, Beiheft zur Fachserie 18, Reihe 3; source from 1991.Q1 on for unified Germany: Statistisches Bundesamt, GENESIS online database). We created a long series of gross wages and salaries by linking the data sets for West and unified Germany over annual average of 1991. Since we were interested in hourly real wages, we divided this series by total working hours of the domestic labor force. The data for working hours from 1970.Q1 to 1991.Q4 referred to West Germany (source: Statistisches Bundesamt, Ergänzung zur Fachserie 13, Reihe S.12) and from 1991.Q1 on to unified Germany (source: Statistisches Bundesamt, GENESIS online database). We linked both series over the annual average for 1991. The nominal hourly wage has been deflated with the consumer price index (CPI) or the producer price index (PPI) in order to generate the respective real wage series. The source of both price indices is Deutsche Bundesbank (CPI: series USFB99, PPI: series USZH99).

4.B Tables

Table 4.B.1: Goodness–of–fit measures and diagnostic tests for two model variants for real GDP

	Models	
	1) no restrictions	2) $\sigma_\eta^2 = 0$
Goodness of fit		
Log–likelihood	711.624	711.205
PEV (prediction error variance)[a)]	99.670	100.464
R_D^2 (relative coefficient of determination)[b)]	0.055	0.047
AIC (based on PEV)	−9.176	−9.168
BIC (based on PEV)	−9.117	−9.109
Diagnostics[c)]		
$Q(16)$ (Ljung-Box statistic)	15.340	14.457
DW (Durbin-Watson statistic)	1.834	1.835
$H(51)$ (heteroskedasticity statistic)	0.592*	0.579*
N_{DH} (Doornik-Hansen normality statistic)	9.817*	9.731*
LR test on restriction $\sigma_\eta^2 = 0$ [d)]	1.230	

[a)] PEV has been multiplied by 10^6.

[b)] R_D^2 measures an improvement in the fit of the considered model relative to the random walk with drift.

[c)] * indicates statistical significance of the test statistics at the 5% level.
$Q(p)$: based on the first p autocorrelations of the residuals
$H(h)$: based on the first h and the last h squared residuals, with h as the closest integer to $T/3$

[d)] Since the considered parameter lies on the boundary of the parameter space under H_0, instead of having the usual χ_1^2 distribution, the LR statistic is distributed asymptotically as a $\frac{1}{2}\chi_0^2 + \frac{1}{2}\chi_1^2$ variable.

Table 4.B.2: Goodness-of-fit measures and diagnostic tests for two model variants for the consumer real wage

	Models	
	1) $\sigma_\eta^2 = 0$	2) $\sigma_\eta^2 = 0$, slope interv. 2003.Q1
Goodness of fit		
Log–likelihood	728.060	722.836
PEV (prediction error variance)[a)]	81.160	80.231
R_D^2 (relative coefficient of determination)[b)]	0.069	0.086
AIC (based on PEV)	−9.381	−9.380
BIC (based on PEV)	−9.322	−9.302
Diagnostics[c)]		
$Q(16)$ (Ljung-Box statistic)	14.461	11.407
DW (Durbin-Watson statistic)	1.934	2.016
$H(51)$ (heteroskedasticity statistic)	0.371*	0.459*
N_{DH} (Doornik-Hansen normality statistic)	10.333*	6.048*

[a)] PEV has been multiplied by 10^6.

[b)] R_D^2 measures an improvement in the fit of the considered model relative to the random walk with drift.

[c)] * indicates statistical significance of the test statistics at the 5% level.
$Q(p)$: based on the first p autocorrelations of the residuals
$H(h)$: based on the first h and the last h squared residuals, with h as the closest integer to $T/3$

Table 4.B.3: Goodness-of-fit measures and diagnostic tests for two model variants for producer real wage

	Models	
	1) $\sigma_\eta^2 = 0$	2) $\sigma_\eta^2 = 0$, slope interv. 2003.Q1
Goodness of fit		
Log–likelihood	691.326	688.195
PEV (prediction error variance)[a)]	131.079	126.183
R_D^2 (relative coefficient of determination)[b)]	0.090	0.130
AIC (based on PEV)	−8.902	−8.927
BIC (based on PEV)	−8.843	−8.849
Diagnostics[c)]		
Q (Ljung-Box statistic)	11.664	9.593
DW (Durbin-Watson statistic)	1.886	1.932
$H(51)$ (heteroskedasticity statistic)	0.855	0.960
N_{DH} (Doornik-Hansen normality statistic)	7.976*	8.022*

[a)] PEV has been multiplied by 10^6.

[b)] R_D^2 measures an improvement in the fit of the considered model relative to the random walk with drift.

[c)] * indicates statistical significance of the test statistics at the 5% level.
$Q(p)$: based on the first p autocorrelations of the residuals
$H(h)$: based on the first h and the last h squared residuals, with h as the closest integer to $T/3$

References

Abraham, K. G., and Haltiwanger, J. C. (1995). Real Wages and the Business Cycle. *Journal of Economic Literature*, *33*(3), 1215–1264.

Anger, S. (2007). *The Cyclicality of Effective Wages within Employer-Employee Matches: Evidence from German Panel Data* (Working Paper No. 783). ECB.

Barro, R. J. (1990). *Macroeconomics* (3rd ed.). New York: John Wiley.

Barro, R. J., and King, R. G. (1984). Time-Separable Preferences and Intertemporal-Substitution Models of Business Cycles. *Quarterly Jounal of Economics*, *99*(4), 817–839.

Bauer, T., Bonin, H., Goette, L., and Sunde, U. (2007). Real and Nominal Wage Rigidities and the Rate of Inflation: Evidence from West German Micro Data. *The Economic Journal*, *117*, 508–529.

Baxter, M., and King, R. G. (1999). Measuring Business Cycles. Approximate Band-pass Filters for Economic Time Series. *Review of Economics and Statistics*, *81*(4), 575–593.

Beveridge, S., and Nelson, C. R. (1981). A New Approach to Decomposition of Economic Time Series into Permanent and Transitory Components with Particular Attention to Measurement of the 'Business Cycle'. *Journal of Monetary Economics*, *7*, 151–74.

Brandner, P., and Neusser, K. (1992). Business Cycles in Open Economies: Stylized Facts for Austria and Germany. *Review of World Economics*, *128*(1), 67–87.

Brandolini, A. (1995). In Search of a Stylized Fact: Do Real Wages Exhibit a Consistent Pattern of Cyclical Variability? *Journal of Economic Surveys*, *9*(2), 103–163.

Burns, A. F., and Mitchell, W. C. (1946). *Measuring Business Cycles*. New York: NBER.

Christiano, L. J., and Eichenbaum, M. (1992). Current Real-Business-Cycle Theories and Aggregate Labor-Market Fluctuations. *American Economic Review*, *82*(3), 430–450.

Cogley, T., and Nason, J. T. (1995). Effects of the Hodrick-Prescott Filter on the Trend and Difference Stationary Time Series: Implications for Business Cycle Research. *Journal of Economic Dynamics and Control*, *19*, 253–278.

Commandeur, J. J. F., and Koopman, S. J. (2007). *An Introduction to State Space Time Series Analysis*. New York: Oxford University Press.

Croux, C., Forni, M., and Reichlin, L. (2001). A Measure of Comovement for Economic

Variables: Theory and Empirics. *Review of Economics and Statistics*, *83*(2), 232–241.

den Haan, W. J. (2000). The Comovement between Output and Prices. *Journal of Monetary Economics*, *46*, 3–30.

Engle, R. F., and Kozicki, S. (1993). Testing for Common Features. *Journal of Business and Economic Statistics*, *11*(4), 369–380.

Gomez, V. (2001). The Use of Butterworth Filters for Trend and Cycle Estimation in Economic Time Series. *Journal of Business and Economic Statistics*, *19*(3), 365–373.

Hart, R. A., Malley, J. R., and Woitek, U. (2009). Real Earnings and Business Cycles: New Evidence. *Empirical Economics*, *37*, 51–71.

Harvey, A. C. (1989). *Forecasting, Structural Time Series Models and the Kalman Filter*. Cambridge: Cambridge University Press.

Harvey, A. C., and Jaeger, A. (1993). Detrending, Stylized Facts and the Business Cycle. *Journal of Applied Econometrics*, *8*, 231–247.

Harvey, A. C., and Koopman, J. S. (1992). Diagnostic Checking of Unobserved-Component Time Series Models. *Journal of Business and Economic Statistics*, *10*(4), 377–389.

Harvey, A. C., and Streibel, M. (1998). Tests for Deterministic versus Indeterministic Cycles. Unpublished Paper: Department of Economics, University of Cambridge.

Harvey, A. C., and Trimbur, T. M. (2003). General Model-Based Filters for Extracting Cycles and Trends in Economic Time Series. *Review of Economics and Statistics*, *85*(2), 244–255.

Koopman, J. S. (1993). Disturbance Smoother for State Space Models. *Biometrika*, *80*(1), 117–126.

Koopman, S. J., Harvey, A. C., Doornik, J. A., and Shephard, N. (2009). *STAMP 8.2: Structural Time Series Analyser, Modeller and Predictor*. London: Timberlake Consultants.

Koopman, S. J., Shephard, N., and Doornik, J. A. (2008). *SsfPack 3.0: Statistical Algorithms for Models in State Space Form*. London: Timberlake Consultants.

Koopmans, L. H. (1974). *The Spectral Analysis of Time Series*. London: Academic Press.

Kydland, F. E., and Prescott, E. C. (1982). Time to Build and Aggregate Fluctuations. *Econometrica*, *50*, 1345–1370.

Lucke, B. (1997). An Adelman-Test for Growth Cycles in West Germany. *Empirical Economics*, *22*, 15–40.

Marczak, M., and Beissinger, T. (2013). Real Wages and the Business Cycle in Germany. *Empirical Economics*, *44*, 469–490.

Mastromarco, C., and Woitek, U. (2007). Regional Business Cycles in Italy. *Computational Statistics and Data Analysis*, *52*, 907–918.

Messina, J., Strozzi, C., and Turunen, J. (2009). Real Wages over the Business Cycle: OECD Evidence from the Time and Frequency Domains. *Journal of Economic Dynamics and Control*, *33*(6), 1183–1200.

Murray, C. J. (2003). Cyclical Properties of Baxter-King Filtered Time Series. *Review of Economics and Statistics*, *85*(2), 472–476.

Newbold, P. (1990). Precise and Efficient Computation of the Beveridge-Nelson Decomposition of Economic Time Series. *Journal of Monetary Economics*, *26*, 453–457.

Peng, F., and Siebert, W. S. (2007). *Real Wage Cyclicality in Germany and the UK: New Results Using Panel Data* (Working Paper No. 2688). IZA.

Pérez, P. J. (2001). *Cyclical Properties in the Main Western Economies* (Working Paper No. 33). The University of Manchester.

Priestley, M. B. (1981). *Spectral Analysis and Time Series* (Z. W. Birnbaum and E. Lukacs, Eds.). London: Academic Press.

Rotemberg, J. J., and Woodford, M. (1991). Markups and the Business Cycle. In O. Blanchard and S. Fisher (Eds.), *NBER Macroeconomics Annual:1991* (pp. 63–129). Cambridge and London: MIT Press.

Schirwitz, B. (2009). A Comprehensive German Business Cycle Chronology. *Empirical Economics*, *37*, 287–301.

Tripier, F. (2002). The Dynamic Correlation Between Growth and Unemployment. *Economics Bulletin*, *5*(4), 1–9.

Vahid, F., and Engle, R. F. (1997). Codependent Cycles. *Journal of Econometrics*, *80*, 199–221.

Chapter 5

Real Wage Cyclicality across Frequencies and over Time: A Comparison of the USA and Germany*

5.1 Introduction

The question of real wage behavior in the course of the business cycle has been analyzed in many studies, particularly in the US case. Most of the studies based on aggregate data concentrate on the analysis in the time domain, see for example, the detailed surveys of Abraham and Haltiwanger (1995) and Brandolini (1995) for the USA and the studies of Brandner and Neusser (1992) and Pérez (2001) for Germany. A disadvantage of common time–domain comovement tools as, for example, sample cross–correlations or regression coefficients of some cycle reference measure is that they are incapable of identifying detailed patterns of cyclicality since they do not differentiate between horizons at which comovement could be detected.

To overcome this shortcoming of the time domain analysis, some studies consider the comovements in the frequency domain where one is able to assess the relative importance of components with different periodicities for the observed behavior. The frequency–domain approach in the investigation of real wage cyclicality is followed in the works of, e.g., Marczak and Beissinger (2013), Hart et al. (2009) and Messina et al. (2009). Standard multivariate spectral techniques, such as cross–spectrum, coherency or phase angle, are, however, time–invariant. In order to additionally take time information into account, wavelet analysis is proposed as an alternative tool to measure comovements between time

*This chapter is my own contribution. It has been used as the groundwork for the later work with Víctor Gómez which has been published in the journal Economic Modelling; see Marczak and Gómez (2015).

series. Applications based on wavelet measures are already widespread in such disciplines as physics, meteorology, geology, medicine, oceanography or engineering. In economics, wavelet analysis was first considered in articles by, e.g., Ramsey et al. (1995), Ramsey and Lampart (1998) and Gençay et al. (2001), but its advantages, in contrast to other sciences, have not been extensively exploited yet. A review of different wavelet concepts with a focus on economic applications is given by Crowley (2007). Wavelet functions which are the building block of the wavelet approach are, unlike the sine and cosine functions used in spectral analysis, local in both the time and frequency domains, which makes wavelets suited to capture changes in behavior patterns. Wavelet analysis can therefore reveal how the relationship between different periodic components of time series evolves over time. This property enables us to obtain a more comprehensive picture of real wage cyclicality. Better understanding of the nature of cyclical behavior of real wages can be of great relevance for monetary policy.

This article is also an attempt to provide a reliable comparison of the real wage cyclicality in the USA and Germany. This particular choice is motivated by the fact that these countries are two large economies with strongly differing labor market institutions. In comparison to the flexible US labor market, the German labor market may be characterized as more rigid because of strong unemployment protection rules, strong unions and a relatively generous unemployment compensation system. This analysis can thus reveal whether the differences in labor market characteristics are reflected in real wage cyclicality in the USA and Germany.

To assess the real wage behavior over the business cycle, wavelet analysis is applied to real wage cycle and a business cycle indicator represented here by the cycle of the industrial production. In this article, two different methods for estimating cycles are applied to check the robustness of the findings: the first one uses the structural time series (STS) model proposed by Harvey (1989) and the second one consists of the ARIMA–model–based (AMB) approach (see, e.g., Box et al., 1978) combined with the canonical decomposition (see Hillmer and Tiao, 1982) and the application of a band–pass filter based on a Butterworth tangent function (see Gómez, 2001). A great advantage of these methods is that they are well suited to remove seasonality from the data. Moreover, they also take into account the stochastic properties of the data as opposed to ad hoc filtering methods like the filters proposed by Hodrick and Prescott (1997) or Baxter and King (1999), which are very popular in macroeconomic applications, mostly because of their convenient implementation. Since the results may also be affected by the price deflator

used to compute real wages, the analysis distinguishes between consumer real wages and producer real wages.
The remainder of the article is organized as follows. In Section 5.2, two decomposition methods are applied to the industrial production index (IPI), consumer real wages and producer real wages in the USA and Germany. In Section 5.3.1, the most important wavelet concepts are set out. More detailed explanations of one of them, the wavelet phase angle, are provided in Section 5.3.2. In Section 5.3.3, it is shown how the previously introduced concepts are implemented in this study. In Section 5.4, the comovements between the particular IPI cycle and the corresponding real wage cycles are examined in the time–frequency domain using wavelet analysis. In Section 5.5, the results of the analysis are interpreted in relation with the existing literature on real wage cyclicality in the US and Germany. Section 5.6 summarizes the results and concludes.

5.2 Cyclical component

In this study, the series of interest are quarterly data on consumer and producer real wages, and the industrial production index (IPI) between 1960.Q1 and 2011.Q3 for the US and between 1970.Q1 and 2011.Q3 for Germany. Data used are not seasonally adjusted to avoid possible influences of different seasonal adjustment methods employed in the computation of official seasonally adjusted figures. Detailed information of the data used in the construction of the final series is provided in Appendix 5.A. In this article, the IPI serves as a reference for the business cycle, whereas other studies on real wage cyclicality often consider business cycle indicators based on real GDP or employment. The motivation for using the IPI instead of real GDP in this article is twofold. Firstly, seasonally unadjusted data on real GDP for the US are not available in the official statistics. Secondly, cyclical behavior of the economy is most strongly pronounced in industrial sectors. Real GDP additionally comprises sectors, like the public sector, less heavily affected by recessions or expansions in the economy. Using real GDP as a reference for the business cycle could therefore mitigate the relationship with real wages and possibly lead to less clear–cut findings. Moreover, in the context of a comparison between the US and Germany the IPI seems to be more suitable as a basis for the business cycle than employment. The reason is that due to differences in labor market institutions, employment volatility in Germany may be different compared to the US, thereby making employment a less suitable business cycle indicator for the purposes of this article.

It is expected that all series under consideration display trend as well as cyclical and seasonal movements. Therefore, it is assumed that the considered time series (in levels or in logs) can be expressed as the sum of several unobserved components. Under this assumption, the series are decomposed as

$$y_t = p_t + s_t + c_t + i_t, \tag{5.1}$$

where p_t is the trend, s_t is the seasonal, c_t is the cyclical and i_t is the irregular component. The different components are assumed to be uncorrelated and they are best defined in the frequency domain. Thus, the trend component is associated with a spectral peak at the zero frequency, the seasonal component has spectral peaks at the seasonal frequencies, defined as $2\pi k/s$, $k = 1, 2, \ldots, [s/2]$, where s is the number of seasons and $[s/2]$ denotes the integer part of $s/2$, and the irregular component is usually assumed to be white noise.[1] Finally, for economic series, the cyclical component is supposed to have some spectral peak in a frequency band corresponding to periods between 1.5 and 8 years. Since the relationship between frequency ω and period p is given by the formula $p = 2\pi/\omega$, the cyclical band for quarterly series is $[\pi/16, \pi/3]$.

To estimate the cyclical component, c_t in (5.1), the usual approach in economics is to apply a fixed filter, like the Hodrick–Prescott or the Baxter–King filter. However, this approach has its limitations because it does not take into account the stochastic characteristics of the series at hand. For example, it is well known that one can generate spurious cycles if one applies a fixed filter to a white noise series. For this reason, in this article two model–based methods are used to estimate the cycle in an economic time series.

The first method is based on the so–called structural models introduced by Harvey (1989). These models assume a decomposition of the form (5.1), where the components follow certain ARIMA models. See Harvey (1989) for details. The model can be put into state space form and the Kalman filter and smoother can be used to estimate the unobserved components. It is to be noted that in this approach the models for the components are specified beforehand.

The second method consists of the AMB approach combined with the canonical decomposition and the application of a band–pass filter. It has two steps. In the first one, an ARIMA model is specified for the series and the canonical decomposition is used to derive models for the trend–cycle, seasonal and irregular components (see Hillmer and Tiao,

[1] For a nonstationary series, the pseudospectrum instead of the spectrum would be considered.

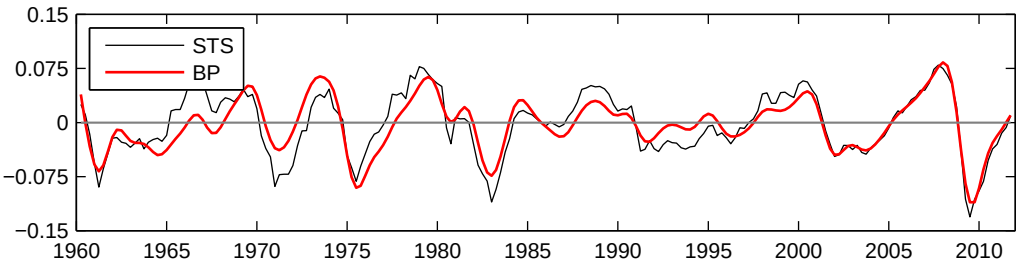

(a) Cycles of the industrial production index (IPI)

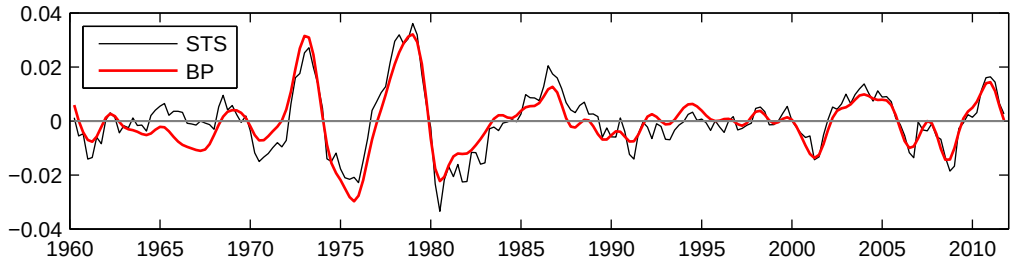

(b) Cycles of the consumer real wage

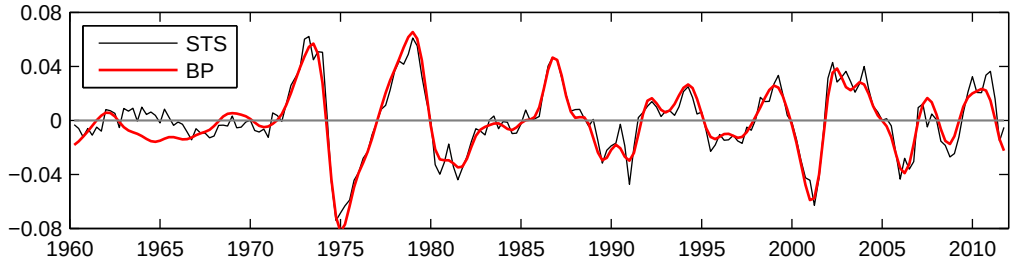

(c) Cycles of the producer real wage

Figure 5.1: US cycles of the IPI and real wages based on the STS approach and a band–pass (BP) filter

1982). In the second step, the cycle is estimated by the application of a band–pass filter, designed to extract the random elements in the cyclical frequency band, to the trend–cycle obtained in the first step. The procedure is fully model–based and is described in Gómez (2001). Once models for the different components, including the cycle, are obtained, the overall model can be put into state space form and the Kalman filter and smoother can be applied to estimate the components as in the first method.

Although both methods are model based, the second one is more likely to extract smoother, more definite, cycles because only those random elements corresponding to the cyclical frequency band are passed by the band–pass filter. The cycle estimated with structural models will usually be less smooth. In order to get smoother cycles with structural models, one should use the generalized cycle models of Harvey and Trimbur (2003). However, the cycles estimated with structural models will be satisfactory enough for the purposes

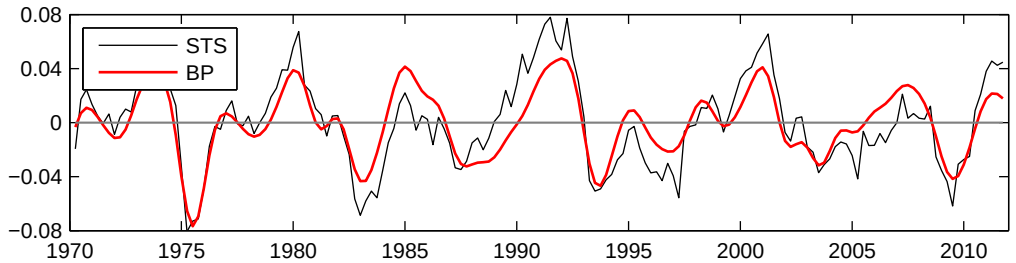

(a) Cycles of the industrial production index (IPI)

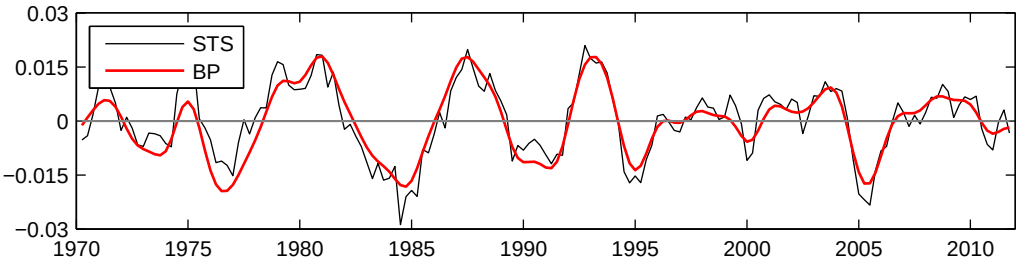

(b) Cycles of the consumer real wage

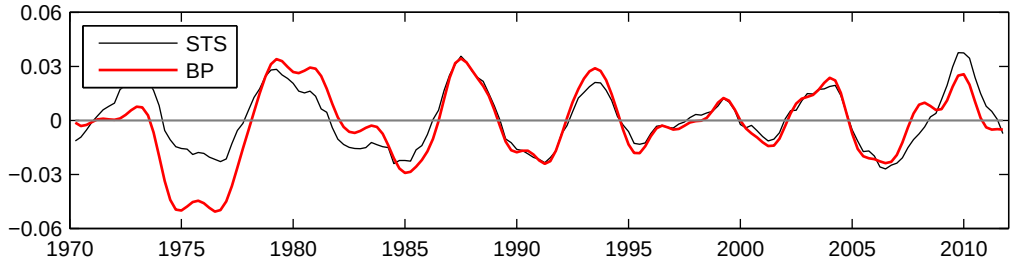

(c) Cycles of the producer real wage

Figure 5.2: German cycles of the IPI and real wages based on the STS approach and a band–pass (BP) filter

of this article.[2]

In Figure 5.1, one can see the cycles estimated with both methods for the US series. As expected, the cycles estimated with the band–pass filter are smoother than the cycles estimated with the structural models.

The cycles estimated with both methods for the German series are displayed in Figure 5.2. Here, one can also see that the cycles estimated with the band–pass filter are smoother.

[2]The SSMMatlab toolbox is used to perform all necessary computations (see Gómez, 2012). Only the identification of an ARIMA model and outlier and regression effects for the series at hand for the AMB approach is made using program TRAMO (see Gómez and Maravall, 1996). The same outlier and regression effects are used with structural models.

5.3 Comovements between time series: wavelet analysis

5.3.1 Wavelet concepts

In the economic literature on wavelet analysis, three directions emerged: the continuous wavelet transform (CWT) (see, e.g., Rua and Nunes, 2009), the discrete wavelet transform (see, e.g., Crowley and Mayes, 2008) and the maximum overlap discrete wavelet transform (see, e.g., Gallegati et al., 2011). They differ in the way how a function of time is mapped onto the time–frequency plane. This analysis relies on the CWT. In this section, some key concepts associated with this type of transform will be discussed.

The building block of wavelet analysis is the so–called mother (or analyzing) wavelet, denoted hereafter as ψ. Suppose that ψ is a real– or complex–valued function in $L^1(\mathbb{R}) \cap L^2(\mathbb{R})$, i.e. :

$$\int_{-\infty}^{\infty} \psi(t)dt < \infty, \qquad \int_{-\infty}^{\infty} |\psi(t)|^2 dt < \infty \tag{5.2}$$

In other words, ψ has finite energy since it holds:

$$\|\psi\|^2 = \langle \psi, \psi^* \rangle = \int_{-\infty}^{\infty} |\psi(t)|^2 dt, \tag{5.3}$$

where $\|\cdot\|$ and $\langle\cdot\rangle$ denote the norm and the inner product, respectively, and ψ^* is the complex conjugate of ψ. Function ψ qualifies for the mother wavelet, if it satisfies the admissibility condition (see, e.g., Farge, 1992, and Daubechies, 1992, p. 24):

$$0 < C_\psi = \int_{-\infty}^{\infty} \frac{|\Psi(\omega)|^2}{|\omega|} d\omega < \infty, \tag{5.4}$$

where ω is the angular frequency, $\Psi(\omega)$ is the Fourier transform of $\psi(t)$ and C_ψ is called the admissibility constant. The admissibility condition implies

$$\Psi(0) = \int_{-\infty}^{\infty} \psi(t)dt = 0$$

Along with the sufficient decay property, this ensures localization in both time and frequency. Moreover, it is usually assumed that $\|\psi\| = 1$, implying unit energy of ψ. On the basis of the mother wavelet, a doubly–indexed family of wavelets is generated by the

so–called translation and dilation (scaling) of ψ:

$$\psi_{\tau,s}(t) = \frac{1}{\sqrt{|s|}}\psi\left(\frac{t-\tau}{s}\right), \qquad \tau, s \in \mathbb{R}, s \neq 0 \tag{5.5}$$

Translation leads to a shift of ψ by the so–called translation parameter τ. Dilation, on the other hand, reduces or increases the support of ψ, if $|s| < 1$ or $|s| > 1$, respectively, where s is the so–called dilation (scaling) parameter. The factor $1/\sqrt{|s|}$ guarantees that $\psi_{\tau,s}$ preserves unit energy.
The CWT of a continuous function x in $L^2(\mathbb{R})$ is given by:

$$\begin{aligned} W_{x,\psi}(\tau, s) &= \langle x(t), \psi^*_{\tau,s}(t)\rangle \\ &= \int_{-\infty}^{\infty} x(t)\frac{1}{\sqrt{|s|}}\psi^*\left(\frac{t-\tau}{s}\right)dt \end{aligned} \tag{5.6}$$

Parseval's relation $\langle x, \psi\rangle = (1/2\pi)\ \langle X, \Psi\rangle$, where X is the Fourier transform of x, allows writing $W_{x,\psi}(\tau, s)$ as:

$$W_{x,\psi}(\tau, s) = \frac{\sqrt{|s|}}{2\pi}\int_{-\infty}^{\infty} \Psi^*(s\omega)\ X(\omega)\ e^{i\omega\tau}d\omega \tag{5.7}$$

Note that in eq. (5.6) and (5.7) τ corresponds to the time dimension, whereas s refers to the scale dimension, implying that $W_{x,\psi}(\tau, s)$ provides a time–scale representation of the analyzed function x. A particular scale represents a frequency band which makes it difficult to interpret the frequency content of x directly (see, e.g., Sinha et al., 2005). However, it is possible to convert scales into Fourier (or angular) frequencies, as there exists a formula that makes use of the so–called center frequency of the wavelet and states an inverse relation between scale and frequency (see, e.g., Abry et al., 1995). For an appropriate choice of the functional form of the wavelet, this relation becomes more straightforward and facilitates the interpretation of the wavelet transform in terms of frequency. In such a case, the terms scale and frequency will be used interchangeably.
The wavelet power spectrum of x is obtained as:

$$P_{x,\psi}(\tau, s) = |W_{x,\psi}(\tau, s)|^2 \tag{5.8}$$

and represents the local variance of x. If the time–frequency relationship between two time series is of interest, it can be measured by the so–called wavelet cross–spectrum

interpreted as the local covariance between these time series. For a pair of functions x and y, both in $L^1(\mathbb{R}) \cap L^2(\mathbb{R})$, the wavelet cross–spectrum is defined as (see Hudgins et al., 1993):

$$W_{xy,\psi}(\tau, s) = W_{x,\psi}(\tau, s)\ W^*_{y,\psi}(\tau, s) \tag{5.9}$$

In general, eq. (5.9) can also be written as:

$$W_{xy,\psi}(\tau, s) = \Re(W_{xy,\psi}(\tau, s)) + \Im(W_{xy,\psi}(\tau, s)) \tag{5.10}$$

$$= |W_{xy,\psi}(\tau, s)|\ e^{\ \phi_{xy,\psi}(\tau,s)}, \tag{5.11}$$

where $\Re(W_{x,y;\psi}(\tau, s))$ denotes the wavelet co–spectrum and $\Im(W_{x,y;\psi}(\tau, s))$ is the wavelet quadrature spectrum, whereas $\phi_{xy,\psi}(\tau, s)$ in the polar form (5.11) corresponds to the wavelet phase angle. If $W_{xy,\psi}(\tau, s)$ is real, the quadrature spectrum and the phase angle are both zero. As the economic data are, in general, real–valued, it is evident that $W_{xy,\psi}$ can be complex–valued only for complex ψ. In the following, only the case of complex wavelet functions will be considered since they allow for a better insight into the comovement between two series by decoupling the amplitude and the phase angle.

In the literature, one can find several concepts that build on the information contained in the wavelet cross–spectrum. The most common ones are wavelet coherency and wavelet squared coherency, also called wavelet coherence (see, e.g., Liu, 1994). Both can be seen as the counterparts of the frequency–domain coherency and coherence, respectively. Wavelet coherency is given by:

$$R_{xy,\psi}(\tau, s) = \frac{W_{xy,\psi}(\tau, s)}{|W_{x,\psi}(\tau, s)|\ |W_{y,\psi}(\tau, s)|} \tag{5.12}$$

Since $W_{xy,\psi}(\tau, s)$ directly enters the formula for $R_{xy,\psi}(\tau, s)$, wavelet coherency is, like wavelet cross–spectrum, complex–valued and therefore difficult to interpret. For that reason, the concept of coherency will not be pursued in this study. Square of the wavelet coherency, wavelet coherence, is defined as:

$$R^2_{xy,\psi}(\tau, s) = \frac{|W_{xy,\psi}(\tau, s)|^2}{|W_{x,\psi}(\tau, s)|^2\ |W_{y,\psi}(\tau, s)|^2} \tag{5.13}$$

$$= \frac{[\Re(W_{xy,\psi}(\tau, s))]^2 + [\Im(W_{xy,\psi}(\tau, s))]^2}{|W_{x,\psi}(\tau, s)|^2\ |W_{y,\psi}(\tau, s)|^2} \tag{5.14}$$

Since the sample analog of $R^2_{xy,\psi}(\tau, s)$ takes on the value one for all τ and s, Liu (1994)

suggests to analyze the real and the imaginary parts separately in order to avoid this problem. I follow the approach of Torrence and Webster (1999) and reformulate $R^2_{xy,\psi}(\tau, s)$ as

$$R^2_{xy,\psi}(\tau, s) = \frac{S(|W_{xy,\psi}(\tau, s)|^2)}{S(|W_{x,\psi}(\tau, s)|^2)\ S(|W_{y,\psi}(\tau, s)|^2)}, \tag{5.15}$$

where S denotes a smoothing operator in both time and scale. Smoothing is achieved by a convolution of the function to be smoothed and a window function. The wavelet coherence is one of the two comovement concepts used in this article. The other one, the wavelet phase angle, is explained in more detail in the next subsection.

5.3.2 Wavelet phase angle and its interpretation

Despite its usefulness in measuring the strength of the time–frequency relationship, $R^2_{xy,\psi}(\tau, s)$ is able neither to determine the direction (positive or negative) of this relationship nor to establish the lead–lag relation between the series at hand. For this purpose, the concept of the phase angle is well suited. The wavelet phase angle that has been already introduced in eq. (5.11) is defined as:

$$\phi_{xy,\psi}(\tau, s) = \arctan\left[\frac{\Im(W_{xy,\psi}(\tau, s))}{\Re(W_{xy,\psi}(\tau, s))}\right] \tag{5.16}$$

From the properties of arctangent it follows that the phase angle $\phi_{xy,\psi}(\tau, s)$ is a multi-valued function. For given τ and s, the values of arctangent are given by the respective principal value $\pm n\pi$, where $n = 0, 1, 2...$, and the principal value lies in $(-\pi/2, \pi/2)$. It is common to limit values of the phase angle to the interval $[-\pi, \pi]$.[3] Note that $\phi_{xy,\psi}(\tau, s) \equiv \pm\pi/2$ for $\Re(W_{xy,\psi}(\tau, s)) = 0$ and $\Im(W_{xy,\psi}(\tau, s)) \gtrless 0$. If, for specific τ and s, the relation $0 < \phi_{xy,\psi}(\tau, s) < \pi$ occurs, y is said to lag x at (τ, s). The opposite case is implied by $-\pi < \phi_{xy,\psi}(\tau, s) < 0$. Both series are in phase for particular (τ, s), if $\phi_{xy,\psi}(\tau, s)$ equals zero. Based on the values of the phase angle statements about the in–phase or anti–phase relation between the components of x and y can also be made. If the values of the phase angle range between $(-\pi/2, \pi/2)$, the respective components are positively related to each other (procyclical behavior/in–phase movement), whereas the values of $\phi_{xy,\psi}(\tau, s)$ in the interval $[-\pi, -\pi/2)$ or $(\pi/2, \pi]$ indicate a negative relationship (countercyclical behavior/anti–phase movement) between them. The interpretation of the

[3] Marczak and Beissinger (2013) provide a rationale for this common practice and an interpretation of the values of the phase angle.

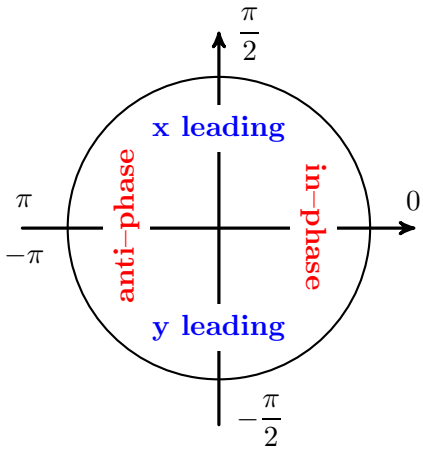

Figure 5.3: Interpretation of the phase angle

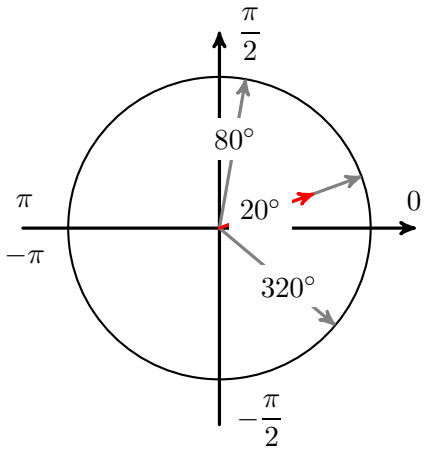

Figure 5.4: Example of a mean of the phase angle samples

phase angle values is summarized in Figure 5.3.

Sometimes, if knowledge about the mean direction of the relationship between time series is desired, it can prove convenient to analyze the mean phase angle. Due to the circular nature of the phase angle, the standard arithmetic mean fails to be an appropriate technique for that purpose. Instead, the concept of a mean specially devoted to the data measured on the angular scale should be employed (see, e.g., Zar, 1999). This concept rests on the fact that for any phase angle ϕ_i it holds that $\tan(\phi_i) = \sin(\phi_i)/\cos(\phi_i)$. Thus, ϕ_i can be represented in the Argand diagram as the angle between the positive half of the real axis and the unit length vector $r_i = (\cos(\phi_i), \sin(\phi_i))$. Averaging over all $r_i, i = 1, ..., n$, where n is the length of the sample of the phase angles, leads to the so–called mean resultant vector $\bar{r}$. The mean phase angle $\bar{\phi}$ is then obtained as $\arctan(\bar{r}_2/\bar{r}_1)$, where $j = 1, 2$ denotes the jth element in $\bar{r}$. In addition, the length of $\bar{r}$ ($\|\bar{r}\|$), ranging from zero to one, quantifies the concentration of the sample around $\bar{r}$ and, therefore, it plays an important role in significance testing. Values $\|\bar{r}\|$ closer to zero (one) indicate higher (smaller) circular spread within the sample. Figure 5.4 illustrates the idea of the mean for circular data with an example of three phase angle values: $20°, 80°$ and $320°$. It is evident that the arithmetic mean being equal to $140°$ would be a misleading measure of the mean since the vectors (gray) corresponding to the sample phase angles point all to the right. The mean resultant vector (red) of length 0.667 points to the same direction and implies the mean value $20°$.

5.3.3 Implementation of wavelet concepts and significance testing

In empirical applications involving wavelets, one of the choices to be made concern the selection of the functional form of the wavelet. As has been pointed out in section 5.3.1, in the case of real–valued series it is more informative to use complex wavelets. I consider the so–called Morlet wavelet which is a complex–valued continuous function:

$$\psi_{\omega_0}(t) = \pi^{-1/4} \left(e^{i\omega_0 t} - e^{-\omega_0^2/2}\right) e^{-t^2/2},$$

where $\pi^{-1/4}$ is a normalization factor. Expression $e^{\omega_0^2/2}$ represents the correction term to enforce the term in brackets to have zero mean, thereby ensuring that the admissibility condition is satisfied. One of the advantages of the Morlet wavelet is that the aforementioned inverse relation between scale s and Fourier frequency f (or angular frequency ω) becomes very simple for the common choice $\omega_0 = 6$, i.e. $f \approx 1/s$ ($\omega \approx 2\pi/s$).
Moreover, the Morlet wavelet allows for the optimal time–frequency localization. According to the Heisenberg uncertainty principle, there is always a trade–off between the precisions obtained in the time and frequency spaces. It can be shown that for the Morlet wavelet with $\omega_0 = 6$, total uncertainty is minimized, and, in addition, the uncertainty associated with time localization is equal to that associated with frequency localization so that the best time–frequency balance can be attained (see Aguiar-Conraria and Soares, 2014).
As outlined before, the analysis will be restricted to the usage of the wavelet coherence and the wavelet phase angle. Since the analysis is dealing with discrete data, the wavelet measures described in section 5.3.1 have to be discretized. Derivation of the discrete version of the CWT in eq. (5.7) which can serve as a basis for the discrete version of the other wavelet tools is presented by Aguiar-Conraria and Soares (2014). Due to the finite length of the series, it is common to pad the series with zeros prior to the application of the transform. This procedure helps to avoid wrap–around effects that arise because the used discrete Fourier transform assumes that the data are periodic. However, zero–padding also leads to underestimation of the CWT values near the ends of the sample. This problem becomes more severe with increasing scales as the wavelet support increases and hence more zeros are involved in the computation of the CWT at the beginning and at the end of the series. Regions affected from these border distortions are called cone of influence (COI). Values of the wavelet measures that fall into the COI should be

interpreted with caution.[4]

The calculated measures are estimates of their theoretical counterparts and therefore it is important to assess the significance of the results. One of the first works where the significance issue is addressed in the context of wavelet analysis is the article by Torrence and Compo (1998) who obtain the empirical distribution for the wavelet power spectrum as well as for the wavelet cross–spectrum. Even though computationally very efficient, this approach has some drawbacks, for example it is applicable only to these two measures and it requires specific assumptions for the derivation of the distribution. An alternative to this kind of significance test are tests that rely on bootstrapped data. Some authors apply nonparametric bootstrap methods, as, e.g., Cazelles et al. (2007). In contrast, in their examples with economic data Aguiar-Conraria and Soares (2014) consider a parametric approach and generate new samples by bootstrapping ARMA models for the analyzed data, for instance the cycles. The approach used in this article builds on Stoffer and Wall (1991) whereby the state space representation is exploited with which the original cycle estimates were obtained. This approach avoids imposing models for the estimated cycles or making additional choices needed for nonparametric methods, as for example selection of the block size when resampling blocks of data (see Berkowitz and Kilian, 2000). More specifically, the procedure involves in two steps. In the first one, bootstrap samples of the observations are obtained. For that purpose, bootstrapping on the standardized innovations is performed. The standardized innovations result from the estimation of the models described in Section 5.2. With the estimated matrices of the state space models and each bootstrap sample of standardized innovations a set of observations is constructed. In the second step, using each of the bootstrap samples of observations a set of smoothed cyclical components using the Kalman smoother is obtained. In wavelet analysis, the bootstrapped cycles are resorted to when computing the bootstrapped values of the wavelet coherence. For the identification of the significant regions of coherence, p–values based on the replicated coherence values are employed.[5]

[4] Computation of $R^2_{xy,\psi}(\tau, s)$ and $\phi_{xy,\psi}(\tau, s)$ is carried out using programs based on the ASToolbox by Aguiar-Conraria and Soares (2011a). Mean values of $\phi_{xy,\psi}(\tau, s)$ are obtained with the CircStat Toolbox by Berens (2009). For graphical illustration of these measures, modified programs from the toolbox by Grinsted et al. (2008) are utilized.

[5] For the generation of the bootstrapped cycles, the procedures bootsam and bootcomp from the SSM-Matlab toolbox are used. Confidence intervals for the mean values of $\phi_{xy,\psi}(\tau, s)$ are calculated with the CircStat Toolbox.

5.4 Results of wavelet analysis

The results for the US case are presented in Figures 5.5 and 5.6. Figure 5.5 shows the estimated wavelet coherence and phase angle for the IPI cycles acting as business cycle indicators and the consumer real wage cycles, whereas Figure 5.6 contains the corresponding estimation results for the IPI cycles and the producer real wage cycles. The left panel of the figures refers to the cycles obtained with the STS approach and the right panel corresponds to the band–pass cycles. For ease of reference, scales at which the wavelet measures have been computed are converted to periods according to the formula $p = 2\pi/\omega$, where p denotes the period and ω is the frequency which is in this case, as mentioned in the previous subsection, derived as $\omega = 2\pi/s$. It should be noticed that the considered periods cover all business cycle periodicities, i.e. periods between 1.5 and 8 years. Figures in the upper row depict the estimated time–frequency wavelet coherence and phase angle. Low values of the coherence are represented by blue, warmer colors designate higher values with red corresponding to the strongest coherence. Areas delimited by the black lines cover coherence values that are significant at the 5% level. Values of the time–frequency phase angle are illustrated by arrows. Direction of an arrowhead can be related to the phase angle in the unit circle and can be thus interpreted as shown in Figure 5.3. Arrows pointing to the right/left indicate an in–phase/anti–phase relationship between the real wage cycle and the business cycle. Arrows pointing up/down suggest lagging/leading of the real wage cycle over the business cycle. Shaded regions show the COI. The figures in the middle and in the lowest part illustrate the phase angle averaged over scales corresponding to the business cycle periodicities, and the phase angle averaged over time, respectively. Black lines give the 95% confidence bounds for the mean values depicted by red dots.

In Figures 5.5a and 5.5d, it is apparent that, irrespective of the decomposition method, the strongest and statistically significant coherence between the consumer real wage cycle and the IPI cycle can be observed between 1965 and 1985 and from about 2000 on. Arrows pointing to the right between 1965 and 1985 reveal a procyclical pattern of the consumer real wage in this time interval. The greatest contribution to this behavior comes from the components with periodicities between approximately 3 and 8 years. In addition, the relevance of shorter period components decreases over time. After 2000, the consumer real wage becomes countercyclical at rather higher periods. The strongest coherence occurs at periodicities between 6 and 8 years. In contrast, lower periods are associated with a

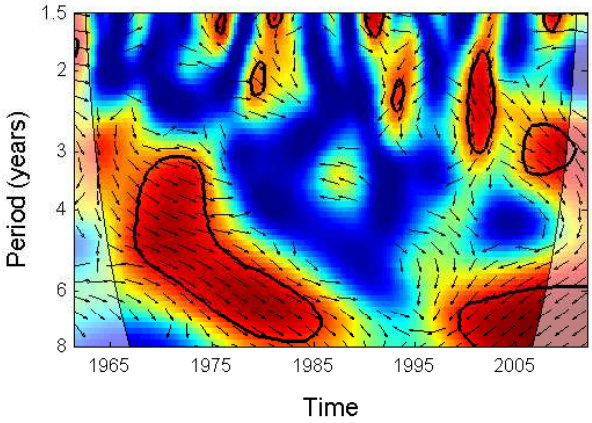

(a) Wavelet coherence and phase angle: STS

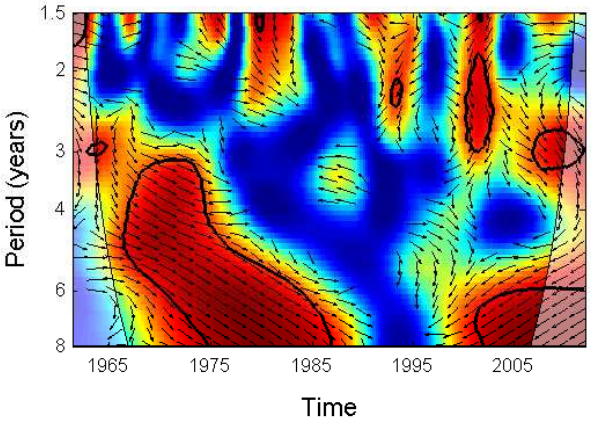

(d) Wavelet coherence and phase angle: BP

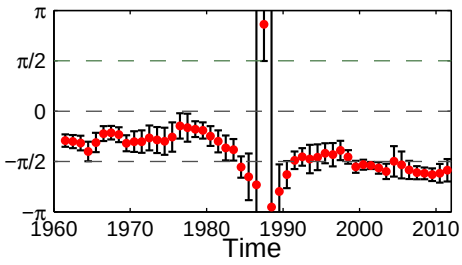

(b) Mean phase angle over scales: STS

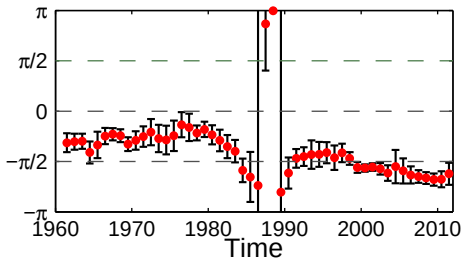

(e) Mean phase angle over scales: BP

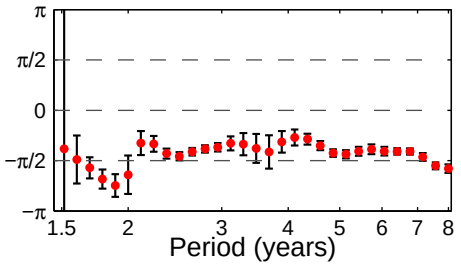

(c) Mean phase angle over time: STS

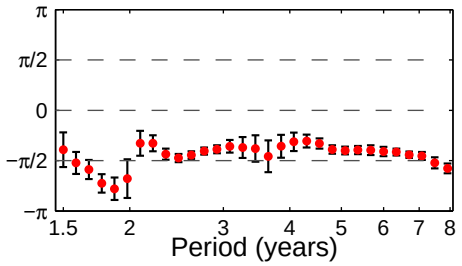

(f) Mean phase angle over time: BP

Figure 5.5: Wavelet coherence and phase angle: US IPI and US consumer real wage cycles based on the STS approach and a band–pass (BP) filter

Notes: a), d) Coherence ranges from low values (blue) to high values (red). Shaded regions represent the COI. Black contours show significance at the 5% level based on p–values calculated with 1000 bootstrapped cycles. Arrows designate the phase angle (pointing right/left: in–phase/anti–phase, pointing up/down: lag/lead of the producer real wage cycle). b), c), e), f) Red points depict the mean values. Black lines correspond to their 95% confidence intervals.

rather procyclical pattern. In the entire time interval, at least for significant coherence values, the consumer real wage is leading the business cycle. These observations can be confirmed by the mean phase averaged over scales (see Figures 5.5b and 5.5e). It takes negative values in the entire time span with an exception of single outlying positive values. However, these outliers as well as other mean values falling into the interval

from 1985 to 1995 will not be interpreted as they are not informative due to the very low and insignificant coherence in this time span. From 1965 to 1985 the mean phase angle values lie between 0 and $-\pi/2$, thereby indicating a clear–cut procyclical pattern. Towards the end of the sample, the mean values fall slightly below $-\pi/2$ which is the consequence of an important contribution of countercyclical low–frequency components of the IPI cycle and the consumer real wage cycle. It is also worth noting that, as is evident from Figures 5.5c and 5.5f, the components with periodicities above 2 years are on average in–phase, whereas the shorter components of the IPI cycle and the real wage cycle exhibit on average an anti–phase relation.

As regards the producer real wage, I find a similar time–frequency behavior to the case of the consumer real wage (see Figures 5.6a and 5.6d). The only difference is that for the producer real wage more pronounced significant coherence between 1985 and 2000 can be detected. It can be observed at lower periodicities, between about 3.5 to 4.5 years starting from 1985 and between 1.5 and 3 years until 2000. Change in the direction of arrows in the mid–1980's at almost all periods suggests a change from an in–phase into an anti–phase relation. Figures 5.6b and 5.6e show this trend explicitly. Taking all periods into account, the producer real wage becomes countercyclical in the early 1980's. In Figures 5.6c and 5.6f, it is evident that the components with periodicities up to approximately 4 years are responsible for the anti–phase behavior whereas the components between 4 and 7 years induce on average a procyclical behavior of the producer real wage. Across all periods and times, the producer real wage leads the business cycle.

Summing up, both US real wages seem to have a similar scheme of comovements with the business cycle. They are leading the business cycle in the entire time interval and at all periodicities. Until the mid–1980's, a procyclical pattern predominates. The significant coherence comes from the components in the range of middle and higher business cycle periodicities. Thereafter, the real wages become less procyclical and towards the end of the series even anticyclical.

The findings for Germany are summarized in Figures 5.7 and 5.8. As for the consumer real wage, Figures 5.7a and 5.7d show that the strongest coherence occurs until 1980 at periods up to about 4 years. From the mid–1980's to the mid–1990's, components with higher periodicities up to about 7 years are associated with strong and statistically significant coherence. Afterwards, the importance of lower components with lower and middle periodicities decreases. In contrast, the ones from the upper range of the business cycle periodicities make the major contribution to the overall coherence in this time

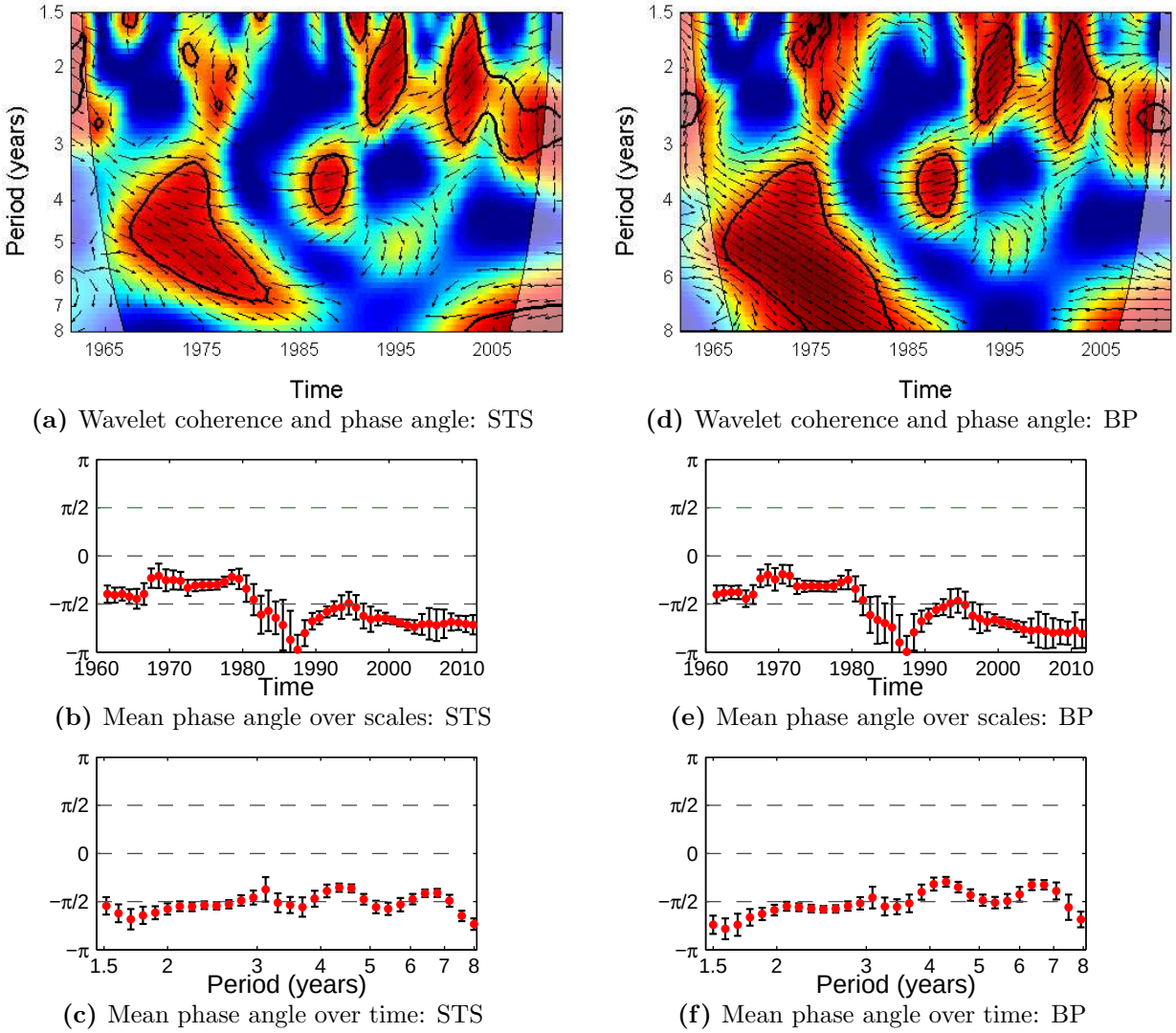

(a) Wavelet coherence and phase angle: STS

(d) Wavelet coherence and phase angle: BP

(b) Mean phase angle over scales: STS

(e) Mean phase angle over scales: BP

(c) Mean phase angle over time: STS

(f) Mean phase angle over time: BP

Figure 5.6: Wavelet coherence and phase angle: US IPI and US producer real wage cycles based on the STS approach and a band–pass (BP) filter

Notes: a), d) Coherence ranges from low values (blue) to high values (red). Shaded regions represent the COI. Black contours show significance at the 5% level based on p–values calculated with 1000 bootstrapped cycles. Arrows designate the phase angle (pointing right/left: in–phase/anti–phase, pointing up/down: lag/lead of the producer real wage cycle). b), c), e), f) Red points depict the mean values. Black lines correspond to their 95% confidence intervals.

interval. Arrows pointing up at all times and almost all periodicities indicate a lagging behavior of the consumer real wage in Germany. Significant values of the mean phase above $\pi/2$ illustrated in Figures 5.7b and 5.7e can be an evidence for a countercyclical consumer real wage in the considered time span. This anti–phase behavior is especially attributed to the components with periodicities below 6 years. At higher periodicities,

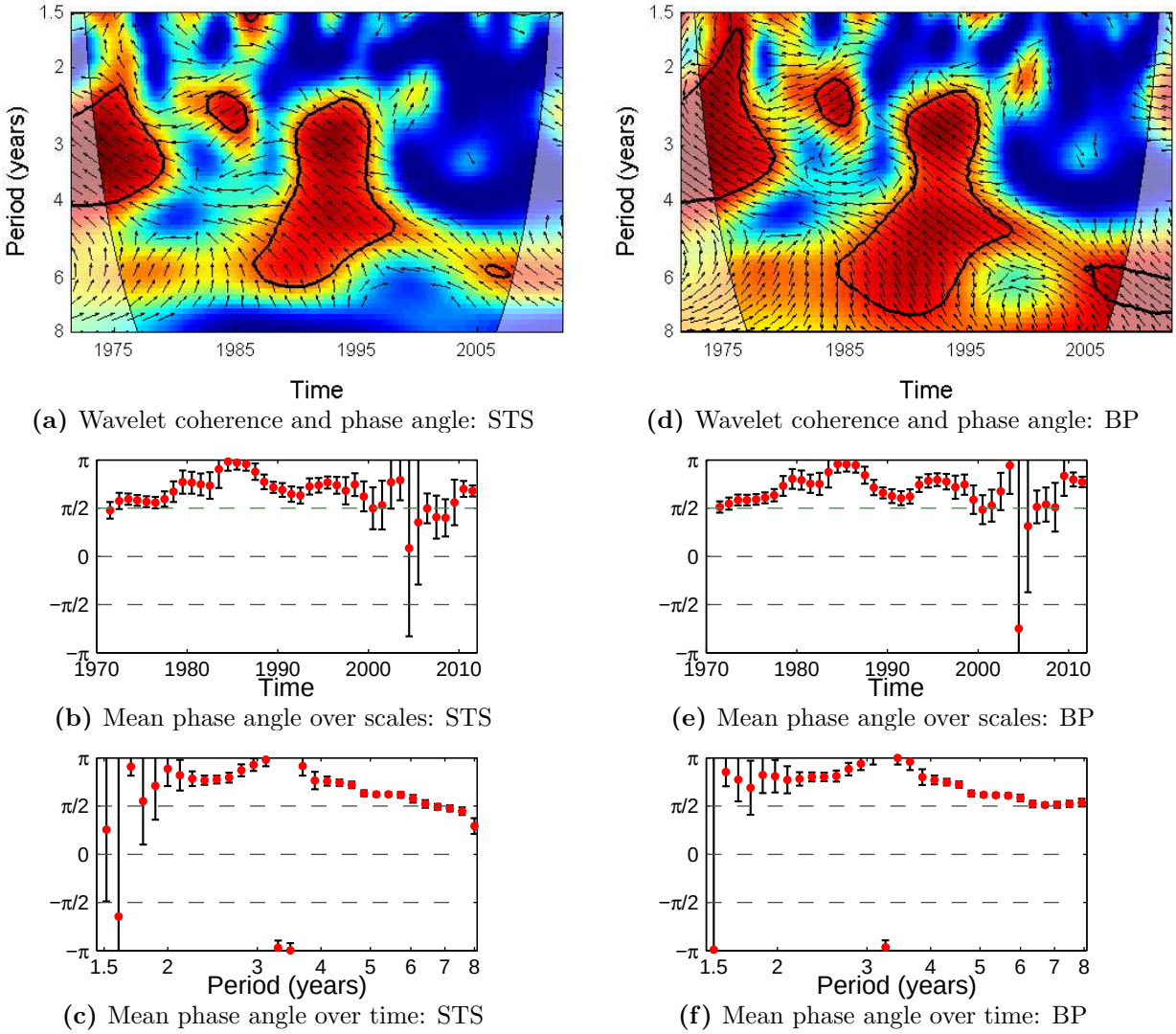

(a) Wavelet coherence and phase angle: STS

(d) Wavelet coherence and phase angle: BP

(b) Mean phase angle over scales: STS

(e) Mean phase angle over scales: BP

(c) Mean phase angle over time: STS

(f) Mean phase angle over time: BP

Figure 5.7: Wavelet coherence and phase angle: German IPI and German consumer real wage cycles based on the STS approach and a band–pass (BP) filter

Notes: a), d) Coherence ranges from low values (blue) to high values (red). Shaded regions represent the COI. Black contours show significance at the 5% level based on p–values calculated with 1000 bootstrapped cycles. Arrows designate the phase angle (pointing right/left: in–phase/anti–phase, pointing up/down: lag/lead of the producer real wage cycle). b), c), e), f) Red points depict the mean values. Black lines correspond to their 95% confidence intervals.

less anticyclical and even a slightly procyclical pattern can be identified.

After an inspection of Figures 5.8a and 5.8d, it becomes clear that despite the similar significance regions for the wavelet coherence as in the case of the consumer real wage, the results for the producer real wage with respect to the lead–lag classification are not as homogeneous. Until the mid–1980' and from 2000 on, the producer real wage leads the

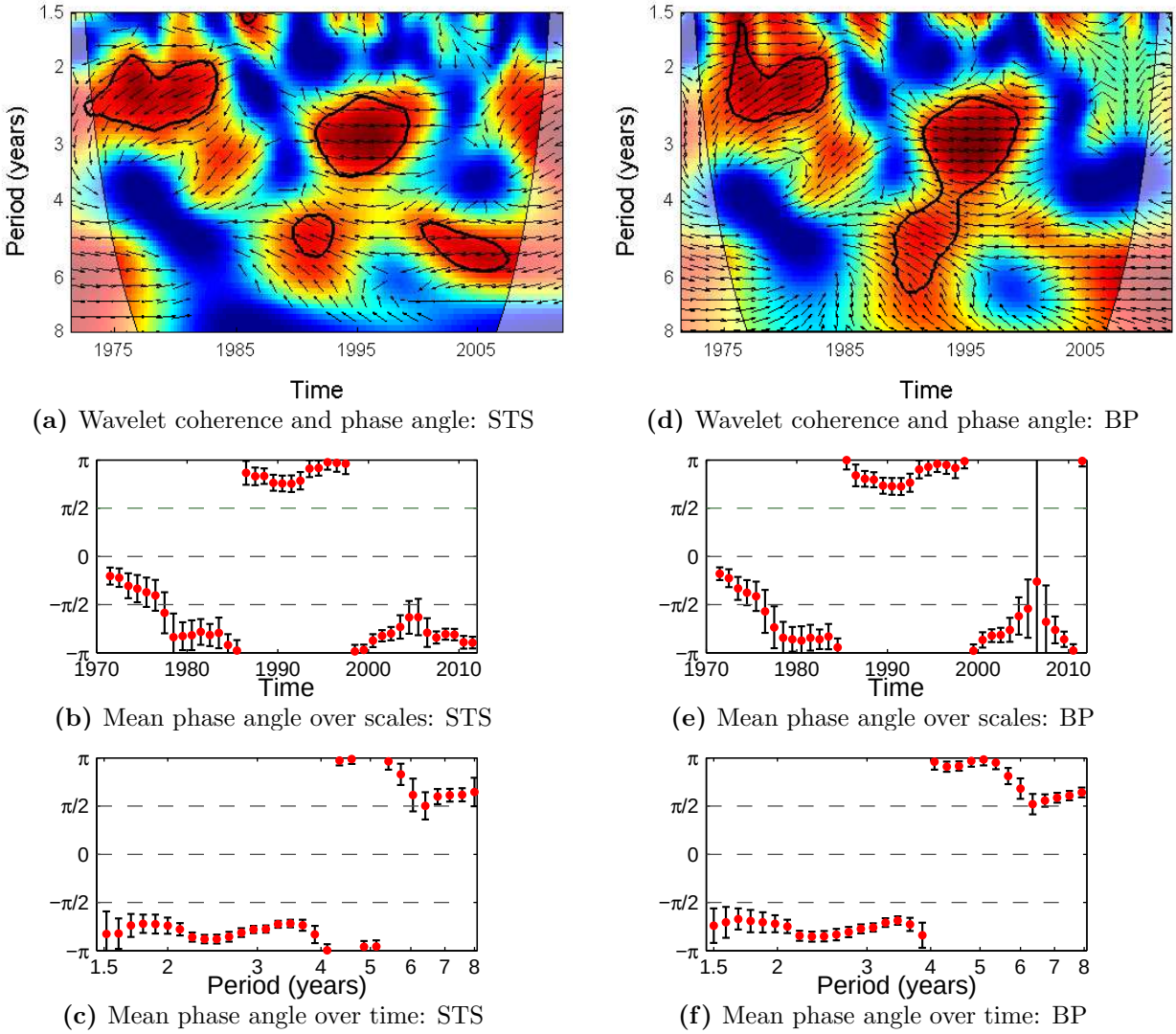

(a) Wavelet coherence and phase angle: STS

(d) Wavelet coherence and phase angle: BP

(b) Mean phase angle over scales: STS

(e) Mean phase angle over scales: BP

(c) Mean phase angle over time: STS

(f) Mean phase angle over time: BP

Figure 5.8: Wavelet coherence and phase angle: German IPI and German producer real wage cycles based on the STS approach and a band–pass (BP) filter

Notes: a), d) Coherence ranges from low values (blue) to high values (red). Shaded regions represent the COI. Black contours show significance at the 5% level based on p–values calculated with 1000 bootstrapped cycles. Arrows designate the phase angle (pointing right/left: in–phase/anti–phase, pointing up/down: lag/lead of the producer real wage cycle). b), c), e), f) Red points depict the mean values. Black lines correspond to their 95% confidence intervals.

business cycle whereas in the interval between 1985 and 2000, a lagging behavior of the producer real wage emerges (see Figures 5.8b and 5.8e). On average, the leading scheme can be assigned to the components up to approximately 4 years. In contrast, components with higher periodicities are responsible for the lagging scheme (see Figures 5.8c and 5.8f). In addition, an anti–phase relationship between the producer real wage and the business

cycle across almost all times and periodicities can be detected, except for time periods prior to 1975. Analogous to the case of the consumer real wage, the negative relationship between the producer real wage cycle and the business cycle vanishes for periods above 6 years.

To sum up, German real wages turn out to be countercyclical in almost the entire time span. As regards their behavior across different periodicities, the anti–phase relation is not present any more for higher periodicities. German consumer real wage is lagging the business cycle at all times, as opposed to the producer real wage which is leading the business cycle until the mid–1980's and from 2000 on. Similarly to the US case, the results remain robust independent of the decomposition method.

A comparison of the results for the USA and Germany unveils the differences in the lead–lag behavior of real wages in both countries. Real wages in the USA are both leading the business cycle whereas in Germany the lead–lag relation with the business cycle differs between these real wage series. The consumer real wage in Germany reacts with delay to the actual economic situation. In contrast, the producer real wage is, at least for the most part of the considered time interval, leading the business cycle. Both countries also differ with respect to the regions with the strongest and statistically significant coherence. In the USA, they are observed from the mid–1960's to the mid–1980's and after 2000, whereas in the German case the most pronounced comovements are associated with time periods until the late 1970's and between about 1990 and 2000. Moreover, the classification of real wages as being in–phase or in anti–phase with the business cycle is differently distributed across periods in both countries. Apart from this discrepancy, a similar overall tendency present in both countries is detected – from a procyclical or an acyclical behavior prior to 1980 to an unambiguously countercyclical behavior thereafter.

5.5 Interpretation of the results in comparison with the literature

5.5.1 Studies based on US aggregate data

Empirical research on real wage cyclicality in the US using aggregate data has a long history which was initiated by the works by Dunlop (1938) and Tarshis (1939) proclaiming procyclical real wages. Since then, outcomes of the US studies have been ambiguous. The simplest approach employed in early studies to investigate the real wage reaction

to changes in the business cycle are static regressions. In his analysis with quarterly data covering different time intervals, Bodkin (1969) finds that the results are sensitive to the deflator used. Real constructed with the consumer price index (CPI) are procyclical, whereas those constructed with the producer price index (PPI) are countercyclical. Chirinko (1980) computes real wages using industry weights thus controlling for changes in industry composition. Using annual data from the mid–1950's to the mid–1970's, he concludes that real wages are countercyclical. Some authors emphasize the necessity of dynamic approaches due to possible interactions between real wages and employment. Using PPI for construction of real wages, Neftci (1878) finds countercyclical behavior of real wages, whereas with data from a different time span and CPI instead of PPI as a deflator Geary and Kennan (1982) do not find any consistent relationship between real wages and employment. Studies by Sumner and Silver (1989) and Mocan and Topyan (1993) are examples of works paying particular attention to the different behavior of real wages in presence of demand and supply shocks. In periods dominated by demand shocks, prices move procyclically and real wages show countercyclical tendencies. In contrast, in times of supply side shocks prices evolve against the economic situation and real wages move procyclically.

These results for the US do not reveal any large differences in the cyclical pattern with respect to either the method used for cycles estimation or the price deflator. However, the analysis explicitly shows that the pattern changes over time which confirms the finding of previous studies that the examined period plays a critical role. Until the early 1980's, a procyclical pattern predominates which may suggest that the evolution of real wages in the first part of the considered sample is driven by supply shocks. In fact, oil crises in 1973 and 1979 were the major factors responsible for the recessions in this time span. The procyclical reaction of real wages until the mid–1980's is associated with lower periodicities indicating a rather slow adjustment of real wages in the presence of supply shocks. After that, both real wages become strongly countercyclical. This switch in the cyclical pattern seems to be accompanying the recession in the late 1980's evoked by a restrictive policy of the Federal Reserve. The subsequent change into more procyclical pattern may reflect the consequences of the oil price hike in 1990. Thereafter, the consumer real wage becomes acyclical or slightly countercyclical and for the producer real wage the countercyclical behavior seems to be more pronounced. This change can result from demand shocks outweighing supply shocks after the mid–1990's. The difference between both real wages with respect to the magnitude of the countercyclical response can be explained by a higher

sensitivity of the producer price index. One of the explanations for the overall reversal of the cyclical scheme of real wages is the fact that in the main recessions after 1990 demand–side factors played a major role – collapse of a speculative Internet bubble in 2000 and burst of the housing bubble in 2007. Moreover, it has been shown in the literature that the inflationary impact of oil price shocks notably decreased after the mid–1980's (see, e.g., Mork, 1989, and Hooker, 1996, and Hamilton, 2003, and Aguiar-Conraria and Soares, 2011b). It is also worth noting that the strong counteryclical reaction observed at higher periodicities can serve as evidence that the real wage adjustment occurs faster when demand shocks prevail.

5.5.2 Studies based on German aggregate data

In the following, I consider studies containing results on real wage cyclicality in Germany based on aggregate data. One of the approaches pursued in this literature is to compute cross–correlations between real wages and GDP after detrending the data with the HP filter, see the papers of Brandner and Neusser (1992) and Pérez (2001). Using quarterly data from 1960.Q1 to 1989.Q4, Brandner and Neusser (1992) find a positive contemporaneous cross–correlation between these variables for Germany. Moreover, real wages are leading the GDP cycle and are positively correlated with GDP at these leads. Pérez (2001) considers the period from 1970.Q2 to 1994.Q1. His HP–filter results point to acyclical real wages, whereas the robustness checks based on the BK filter find that real wages are procyclical and lagging. Lucke (1997) applies the methodology of Burns and Mitchell (1946) to the first differences of the lagged variables of per–capita GDP and real wages (among others) for the period 1960.Q1–1994.Q4. For the expansionary phase of the business cycle he finds a low negative "conformity" of real wages that can be interpreted as weakly anticyclical real wages, whereas in the contractionary phase no clear–cut pattern emerges. This concept of conformity measures to what extent the cycle of a specific variable coincides with the reference cycle, but the lag–lead structure between these series is not taken into account. Messina et al. (2009) apply the time-domain approach of den Haan (2000) and the dynamic correlation measure of Croux et al. (2001) to the first differences of real wages and the respective business cycle indicator. Using quarterly data from 1960.Q1 to 2004.Q1, they find that real wages in Germany are procyclical at all business cycle horizons considered, irrespective of the deflators used. In their analysis for the time span 1970.Q1–2009.Q1, Marczak and Beissinger (2013) distinguish between

consumer and producer real wages and apply the concept of the phase angle in the frequency domain. For shorter time periods up to about four years, the consumer real wage shows an anticyclical behavior, whereas for longer time spans a procyclical behavior can be observed. For the producer real wage, however, the results in the frequency domain remain inconclusive.

Most of the existing studies for Germany, except for, e.g., Marczak and Beissinger (2013), find that real wages are procyclical or acyclical which, generally speaking, contradicts the evidence from this analysis. However, it should be noted that in these works the examined time intervals are usually shifted to the past by several years relative to the time interval considered in this article. Since, as shown before, the real wages seemed to exhibit a rather acyclical or procyclical behavior in the more distant past, this fact could explain the contrasting outcomes of this article and most of the studies dealing with German data. The explanation for the acyclical behavior in the case of the consumer real wage and the procyclical behavior in the case of the producer real wage during the 1970's may be based on two observations. Firstly, similarly as in the US, oil crises representing supply shocks led to recessions in this period. Secondly, German economy additionally experienced demand shocks as in 1973 the Deutsche Bundesbank exploited the leeway after the Bretton Woods system collapse and started to conduct restrictive policy to fight inflation. These shocks had counteracting effects on the real wage cyclicality which is mirrored in the acyclical behavior of the consumer real wage. The producer real wage remains procyclical, possibly due to a stronger response of PPI to the adverse oil price shocks. After 1980 both real wages become countercyclical pointing to a dominating role of demand shocks for the real wage behavior. Indeed, the early 1980's were marked by monetary tightening combined with expansionary fiscal policy before fiscal contraction took place until 1990. German reunification in 1990 induced a strong boom in aggregate demand, followed by the restrictive policy of the Bundesbank.

Although the observed cyclical scheme in Germany complies, in essence, with the pattern in the US, it is worth noting that no definite pro– or counteryclical behavior can be identified in the US case if different periodicities are considered. This may be seen as a symptom of parallel movements of nominal wages and price deflators in the US in the short run as well as in the medium run. In contrast, both German real wages are clearly countercyclical at most business cycle periodicities, only in in the medium run this scheme turns to a rather acyclical one. During the 1970's, strong German labor unions could enforce massive wage hikes. Together with supply–induced price rises, this contributed to

the acyclical pattern identified in the medium run which can be expressed by the highest business cycle periodicities. Even though after 1980's German labor unions in general pursued a policy of wage moderation, slight nominal wage increases in conjunction with pronounced demand–driven price developments translated into countercyclical real wages associated with the short–run.[6]

5.5.3 Micro–data based studies

In the 1980's, some researchers have started using micro data to reexamine real wage cyclicality. The main drawback they have seen in the use of aggregate data is the so–called composition bias. According to the literature employing micro data, this means that acyclical or weakly procyclical pattern of real wages found in many studies results from the decrease (increase) in working hours of low–skilled workers during recessions (expansions) imparting countercyclical bias to aggregate measures of real wages. This distortion can be avoided when using micro data. What is more, micro data also enable researchers to take individual characteristics, i.e. worker, firm and job heterogeneity, into account.

As regards the US, some early studies have employed panel data from the National Longitudinal Survey (NLS), like works by Bils (1985) or Keane et al. (1988). Another data source for the early and more recent studies has been the Panel Study of Income Dynamics (PSID), see Solon et al. (1994), Devereux (2001), Shin and Solon (2007). One of the latest studies has been provided by Elsby et al. (2013) who include in their analysis data from the Current Population Survey (CPS) covering the last recession. The approach adopted in most of these studies rests on a regression of a growth rate of real wages on a business cycle measure, like the first difference of the unemployment rate or real GDP. All studies find that real wages behave procyclically. Their outcomes primarily differ in the extent of the countercyclical bias only, being rather small according to studies using NLS and rather large according to studies based on PSID.

[6] These arguments are supported by an additional analysis of the single components of the real wage series. More specifically, I examined the cyclical behavior of nominal wages, the CPI and the PPI using the wavelet phase angle. The findings show that the price deflators have similar cyclical properties in both countries. The most striking difference pertains to the evolution of nominal wages for different periodicities. In the US, the qualitative results for nominal wages are in line with those for both price indexes across all business cycle periods. In Germany, nominal wages are countercyclical at all business cycle periodicities. Price deflators, on the other hand, display more distinct procyclicality in the short run, possibly due to more offensive strategy of the Bundesbank compared to the Federal Reserve. All additional results are available upon request.

As for Germany, Anger (2007) and Peng and Siebert (2007) analyze the cyclicality of real wages for different groups of workers and/or for different wage measures using individual based micro–data from the German Socio–Economic Panel Study (SOEP). These studies apply a two–step estimation technique. In the first step, individual wage changes are explained by individual characteristics and year dummies. In the second step, the coefficients of the year dummies are regressed on the change in aggregate unemployment and a linear time trend.Peng and Siebert (2007) find that real wages of job stayers in the private sector in West Germany — but not East Germany — are procyclical. According to Anger (2007) hourly wages or base salaries seem to be acyclical, whereas overall earnings including overtime pay or bonuses exhibit a procyclical pattern. The procyclical pattern of real wages may be related to the anticyclical pattern of real wage rigidity in Germany that is documented in Bauer et al. (2007).

Despite its substantial merits mentioned above, use of panel data has also some limitations. One of them is the fact that the time series analysis is quite rudimentary because of relatively few annual observations. For instance, the stochastic properties of the time series are not taken into account and a thorough analysis of the lead–lag structure between real wages and the business cycle variable is missing. Another disadvantage of methods employed in the existing panel–data based studies is that they do not use a proper business cycle measure. Moreover, these methods are neither capable of detecting time–varying behavior nor can they distinguish between short–term and medium–term effects of economic fluctuations on real wages. The procyclical pattern consequently detected in the panel–data based studies may be inconsistent with the argument that different types of shocks hitting the economy lead to different price and wage responses.

5.6 Summary and conclusions

This article sheds new light on the cyclical behavior of the consumer and producer real wages in the USA and Germany. As a tool to investigate comovements, wavelet analysis is proposed as a tool allowing for insights that cannot be provided by standard time–domain or spectral techniques. Wavelet methods can reveal whether the comovement pattern between components with particular periodicities is subject to any changes or whether it remains stable in the course of time. More specifically, the concepts of wavelet coherence and wavelet phase angle are applied. In order to establish the general tendency of the in–phase or anti–phase relation and the lead–lag relation between real wages and the business

cycle across time periods and across different time horizons, interpretation of the mean phase angle over time and over business cycle periodicities, respectively, is additionally provided. To obtain a robust and reliable picture on cyclicality of real wages, two model–based methods are applied for extraction of the cyclical components of the underlying time series: the structural time series (STS) approach and the ARIMA–model–based (AMB) approach combined with the canonical decomposition and a band–pass filter.

The analysis of the wavelet coherence and phase angle shows that the cyclicality in both countries is of a somewhat different nature. In the USA, the strongest and statistically significant coherence falls within the time interval from the mid–1960's to the mid–1980's and after 2000. On the contrary, the strongest and statistically significant coherence in Germany mainly pertains to the years until the late 1970's and the time period between 1990 and 2000. Furthermore, both US real wages are leading the business cycle in the entire time span and at most business cycle periodicities. In Germany, on the other hand, the outcomes depend on whether the consumer or the producer real wage is examined. For the consumer real wage, a lagging behavior at all times as well as at all business cycle periodicities is found. The producer real wage lags the business cycle only between 1985 and 2000 and only at the periodicities up to 4 years. Similarities between both countries emerge if the focus is put on the identification of the in–phase or anti–phase movements of real wages with the business cycle. Until 1980, real wages behave acyclically or pro-cyclically and they change their behavior to an anticyclical one afterwards. The detected cyclicality patterns for both real wages and both countries remain robust regardless of the methods used for the extraction of the cycles.

Appendix

5.A Data selection

The US production index refers to the manufacturing sector after the SIC classification (source: Board of Governors of the Federal Reserve System, series: G.17). I obtained the US real wage series by deflating nominal hourly wages of production and nonsupervisory employees in manufacturing sector (source: FRED Economic Data, series ID: AHEMAN) with the consumer price index (source: FRED Economic Data, series ID: CPIAUCNS) or the producer price index (source: FRED Economic Data, series ID: PPIIDC). As for Germany, I use the production index in industry without construction that has already been linked over the annual average in 1991 (source: Deutsche Bundesbank, series ID: BBDE1.M.DE.N.BAA1.A2P200000.G.C.I05.L). Since, in contrast to the US case, nominal hourly wage series is not directly available, I create it by dividing the data on gross wages and salaries by the data on working hours, both corresponding to industry without construction. Prior to this, I link in both cases data sets up to 1991.Q4 referring to West Germany and from 1991.Q1 on referring to unified Germany over the annual averages in 1991. The source for the West German series is Statistisches Bundesamt, Fachserie 18, Reihe S.27 (revised quarterly results), whereas the source for the German series is Statistisches Bundesamt, GENESIS-Onlinedatenbank. The nominal hourly wages are in the next step deflated with the consumer price index (source: Deutsche Bundesbank, series ID: UUFB99) or the producer price index (source: Deutsche Bundesbank, series ID: UUZH99).

References

Abraham, K. G., and Haltiwanger, J. C. (1995). Real Wages and the Business Cycle. *Journal of Economic Literature*, *33*(3), 1215–1264.

Abry, P., Gonçalvès, P., and Flandrin, P. (1995). Wavelets, Spetrum Analysis and $1/f$ Processes. In A. Antoniadis and G. Oppenheim (Eds.), *Lecture Notes in Statistics* (Vol. 103, pp. 15–30). Springer.

Aguiar-Conraria, L., and Soares, M. J. (2011a). *ASToolbox.* Downloadable at `http://sites.google.com/site/aguiarconraria/joanasoares-wavelets/the-astoolbox`

Aguiar-Conraria, L., and Soares, M. J. (2011b). Oil and the Macroeconomy: Using Wavelets to Analyze Old Issues. *Empirical Economics*, *40*, 645–655.

Aguiar-Conraria, L., and Soares, M. J. (2014). The Continuous Wavelet Transform: Moving Beyond Uni– and Bivariate Analysis. *Journal of Economic Surveys*, *28*(2), 344–375.

Anger, S. (2007). *The Cyclicality of Effective Wages within Employer-Employee Matches: Evidence from German Panel Data* (Working Paper No. 783). ECB.

Bauer, T., Bonin, H., Goette, L., and Sunde, U. (2007). Real and Nominal Wage Rigidities and the Rate of Inflation: Evidence from West German Micro Data. *The Economic Journal*, *117*, 508–529.

Baxter, M., and King, R. G. (1999). Measuring Business Cycles. Approximate Band-pass Filters for Economic Time Series. *Review of Economics and Statistics*, *81*, 575–593.

Berens, P. (2009). CircStat: A MATLAB Toolbox for Circular Statistics. *Journal of Statistical Software*, *31*(10), 1–21.

Berkowitz, J., and Kilian, L. (2000). Recent Developments in Bootstrapping Time Series. *Econometric Reviews*, *19*(1), 1–48.

Bils, M. J. (1985). Real Wages over the Business Cycle: Evidence from Panel Data. *Journal of Political Economy*, *93*(4), 666–689.

Bodkin, R. G. (1969). Real Wages and Cyclical Variations in Employment: A Re-examination of the Evidence. *The Canadian Journal of Economics*, *3*(2), 353–374.

Box, G. E. P., Hillmer, S. C., and Tiao, G. C. (1978). Analysis and Modeling of Seasonal Time Series. In A. Zellner (Ed.), *Seasonal Analysis of Economic Time Series* (pp. 309–334). Washington, DC: U.S. Dept. Commerce, Bureau of the Census.

Brandner, P., and Neusser, K. (1992). Business Cycles in Open Economies: Stylized Facts

for Austria and Germany. *Review of World Economics*, *128*(1), 67–87.

Brandolini, A. (1995). In Search of a Stylized Fact: Do Real Wages Exhibit a Consistent Pattern of Cyclical Variability? *Journal of Economic Surveys*, *9*(2), 103–163.

Burns, A. F., and Mitchell, W. C. (1946). *Measuring Business Cycles*. New York: NBER.

Cazelles, B., Chavez, M., de Magny, G. C., Guégan, J.-F., and Hales, S. (2007). Time–Dependent Spectral Analysis of Epidemiological Time–Series with Wavelets. *Journal of the Royal Society Interface*, *4*, 625–636.

Chirinko, R. S. (1980). The Real Wage Rate over the Business Cycle. *The Review of Economic and Statistics*, *62*(3), 459–461.

Croux, C., Forni, M., and Reichlin, L. (2001). A Measure of Comovement for Economic Variables: Theory and Empirics. *Review of Economics and Statistics*, *83*(2), 232–241.

Crowley, P. M. (2007). A Guide to Wavelets for Economists. *Journal of Economic Surveys*, *21*(2), 207–267.

Crowley, P. M., and Mayes, D. G. (2008). An Evaluation of Growth Cycle Co-movement and Synchronization Using Wavelet Analysis. *Journal of Business Cycle Measurement and Analysis*, *4*(1), 63–95.

Daubechies, I. (1992). Ten Lectures on Wavelets. In *CBMS–NSF Conference Series in Applied Mathematics* (Vol. 61). Philadelphia: SIAM.

den Haan, W. J. (2000). The Comovement between Output and Prices. *Journal of Monetary Economics*, *46*, 3–30.

Devereux, P. J. (2001). The Cyclicality of Real Wages Within Employer–Employee Matches. *Industrial and Labor Relations Review*, *54*(4), 835–850.

Dunlop, J. T. (1938). The Movement of Real and Money Wage Rates. *Economic Journal*, *48*(191), 413–434.

Elsby, M. W., Shin, D., and Solon, G. (2013). *Wage Adjustment in the Great Recession* (Working Paper No. 19478). NBER.

Farge, M. (1992). Wavelet Transforms and their Applications to Turbulence. *Annual Review of Fluid Mechanics*, *24*, 395–457.

Gallegati, M., Gallegati, M., Ramsey, J. B., and Semmler, W. (2011). The US Wage Phillips Curve across Frequencies and over Time. *Oxford Bulletin of Economics and Statistics*, *73*(4), 489–508.

Geary, P. T., and Kennan, J. (1982). The Employment–Real Wage Relationship: An International Study. *Journal of Political Economy*, *90*(4), 854–871.

Gençay, R., Selçuk, F., and Whithcher, B. (2001). Scaling Properties of Foreign Exchange Volatility. *Physica A: Statistical Mechanics and its Applications*, *289*, 249–266.

Gómez, V. (2001). The Use of Butterworth Filters for Trend and Cycle Estimation in Economic Time Series. *Journal of Business and Economic Statistics*, *19*(3), 365–373.

Gómez, V. (2012). *SSMMATLAB, a Set of MATLAB Programs for the Statistical Analysis of State–Space Models.* Downloadable at `http://www.sepg.pap.minhap.gob.es/sitios/sepg/en-GB/Presupuestos/Documentacion/Paginas/SSMMATLAB.aspx`

Gómez, V., and Maravall, A. (1996). *Programs TRAMO and SEATS; Instructions for the User* (Working Paper No. 9628). Servicio de Estudios, Banco de España.

Grinsted, A., Moore, J. C., and Jevrejeva, S. (2008). *Cross Wavelet and Wavelet Coherence Package WTC-R16.* Downloadable at `http://www.pol.ac.uk/home/research/waveletcoherence/download.html`

Hamilton, J. D. (2003). What Is an Oil Shock? *Journal of Econometrics*, *113*, 363–398.

Hart, R. A., Malley, J. R., and Woitek, U. (2009). Real Earnings and Business Cycles: New Evidence. *Empirical Economics*, *37*, 51–71.

Harvey, A. C. (1989). *Forecasting, Structural Time Series Models and the Kalman Filter.* Cambridge: Cambridge University Press.

Harvey, A. C., and Trimbur, T. M. (2003). General Model-Based Filters for Extracting Cycles and Trends in Economic Time Series. *Review of Economics and Statistics*, *85*, 244–255.

Hillmer, S. C., and Tiao, G. C. (1982). An ARIMA–Model–Based Approach to Seasonal Adjustment. *Journal of the American Statistical Association*, *77*(377), 63–70.

Hodrick, R. J., and Prescott, E. C. (1997). Postwar U.S. Business Cycles: An Empirical Investigation. *Journal of Money, Credit and Banking*, *29*, 1–16.

Hooker, M. A. (1996). What Happened to the Oil Price–Macroeconomy Relationship? *Journal of Monetary Economics*, *38*, 195–213.

Hudgins, L., Friehe, C. A., and Mayer, M. E. (1993). Wavelet Transforms and Atmospheric Turbulence. *Physical Review Letters*, *71*(20), 3279–3282.

Keane, M., Moffitt, R., and Runkle, D. (1988). Real Wages over the Business Cycle: Estimating the Impact of Heterogeneity with Micro Data. *Journal of Political Economy*, *96*(6), 1232–1266.

Liu, P. C. (1994). Wavelet Spectrum Analysis and Ocean Wind Waves. In E. Foufoula-Georgiou and P. Kumar (Eds.), *Wavelets in Geophysics* (pp. 151–166). London:

Academic Press.

Lucke, B. (1997). An Adelman-Test for Growth Cycles in West Germany. *Empirical Economics*, *22*, 15–40.

Marczak, M., and Beissinger, T. (2013). Real Wages and the Business Cycle in Germany. *Empirical Economics*, *44*, 469–490.

Marczak, M., and Gómez, V. (2015). Cyclicality of Real Wages in the USA and Germany: New Insights from Wavelet Analysis. *Economic Modelling*, *47*, 40–52.

Messina, J., Strozzi, C., and Turunen, J. (2009). Real Wages over the Business Cycle: OECD Evidence from the Time and Frequency Domains. *Journal of Economic Dynamics and Control*, *33*(6), 1183–1200.

Mocan, N., and Topyan, K. (1993). Real Wages Over the Business Cycle: Evidence from a Structural Time Series Model. *Oxford Bulletin of Economics and Statistics*, *55*(4), 363–389.

Mork, K. A. (1989). Oil and the Macroeconomy When Prices Go Up and Down: An Extension of Hamilton's Results. *Journal of Political Economy*, *97*(3), 740–744.

Neftci, S. N. (1878). A Time–Series Analysis of the Real Wage–Employment Relationship. *The Journal of Political Economy*, *86*(2), 281–291.

Peng, F., and Siebert, W. S. (2007). *Real Wage Cyclicality in Germany and the UK: New Results Using Panel Data* (Working Paper No. 2688). IZA.

Pérez, P. J. (2001). *Cyclical Properties in the Main Western Economies* (Working Paper No. 33). The University of Manchester.

Ramsey, J. B., and Lampart, C. (1998). Decomposition of Economic Relationships by Time Scale Using Wavelets: Money and Income. *Macroeconomic Dynamics*, *2*, 49–71.

Ramsey, J. B., Usikov, D., and Zaslavsky, G. M. (1995). An Analysis of US Stock Price Behavior Using Wavelets. *Fractals*, *3*(2), 377–389.

Rua, A., and Nunes, L. (2009). International Comovement of Stock Market Returns: A Wavelet Analysis. *Journal of Empirical Finance*, *16*, 632–639.

Shin, D., and Solon, G. (2007). New Evidence on Real Wage Cyclicality Within Employer–Employee Matches. *Scottish Journal of Political Economy*, *54*(5), 648–660.

Sinha, S., Routh, P. S., Anno, P. D., and Castagna, J. P. (2005). Spectral Decomposition of Seismic Data with Continuous–Wavelet Transform. *Geophysics*, *70*(6), 19–25.

Solon, G., Barsky, R., and Parker, J. A. (1994). Measuring the Cyclicality of Real Wages: How Important is Composition Bias. *The Quarterly Jounal of Economics*, *109*(1),

1–25.

Stoffer, D. S., and Wall, K. D. (1991). Bootstrapping State–Space Models: Gaussian Maximum Likelihood Estimation and the Kalman Filter. *Journal of the American Statistical Association*, *86*(416), 1024–1033.

Sumner, S., and Silver, S. (1989). Real Wages, Employment, and the Phillips Curve. *Journal of Political Economy*, *97*(3), 706–720.

Tarshis, L. (1939). Changes in Real and Money Wages. *Economic Journal*, *49*(193), 150–154.

Torrence, C., and Compo, G. P. (1998). A Practical Guide to Wavelet Analysis. *Bulletin of the American Meteorological Society*, *79*, 61–78.

Torrence, C., and Webster, P. J. (1999). Interdecadal Changes in the ENSO–Monsoon System. *Journal of Climate*, *12*, 2679–2690.

Zar, J. H. (1999). *Biostatistical Analysis* (4th ed.). New Jersey: Prentice Hall.

Chapter 6

Conclusions

The analysis of business cycles has been continuously attracting a lot of attention in empirical macroeconomics since a long time. Its usefulness for economic policy is beyond dispute. For example, forecasts of recessions or expansions allow for forecasts of tax revenues or help central banks to conduct their monetary policy. Empirical business cycle research can also be a great support for macroeconomic theory which still leaves many unresolved questions concerning the sources of business cycles or the mechanisms that govern relationships between macroeconomic variables. In this sense, this thesis reflects the very essence of empirical business cycle research – providing a proper indicator about economic activity and shedding some light on the relevance of, often conflicting, theories through the analysis of the cyclical behavior of macroeconomic variables. The construction of a business cycle indicator can be challenging in light of the fact that aggregate economic activity can experience structural breaks or be contaminated with seasonal and higher frequency movements. This thesis offers some methodological advances and addresses problems surrounding the analysis of recessions and expansions. It also contributes to the empirical literature on real wage cyclicality which still has not found a clear answer to the conflict of different macroeconomics theories explaining the behavior of real wages over the business cycle. To reveal patterns of this behavior which have not been found before, the studies in this thesis resort to new promising methods successfully used in other subject areas, as well as to old methods by rediscovering their value in the context of the examined research question.

After an introductory chapter, in the second chapter of the thesis a new approach has been proposed to construct monthly business cycle indicators for the US. This approach is based on a multivariate structural model and a univariate band–pass filter. Two business cycle indicators have been presented, both simultaneously obtained after the application of the methodology to the US dataset with mixed (monthly and quarterly) frequencies.

These indicators correspond to the estimated cycles of the industrial production index and real GDP, respectively. Both of them are given on a monthly basis despite the fact that real GDP itself is a quarterly series.

It has been shown that this method is able to replicate historical recessions. Furthermore, a pseudo out–of–sample forecasting exercise has demonstrated good forecasting performance of the approach. These very promising results indicate that the approach is flexible enough to accommodate the dynamics of the US economy without explicit modeling of, e.g., the significant decline in the output volatility after the mid–1980's, also known as Great Moderation.

The proposed method has proved convincing by being relatively simple on the one hand, on the other hand elaborate enough to produce timely and precise information of the state of the economy. These attractive properties make the presented approach an interesting and recommendable framework for monitoring economic activity.

In Chapter 3, a new view is given to the detection of structural breaks and outliers if the series at hand is nonstationary and not seasonally adjusted. Indicator saturation has been considered for this purpose as an outlier detection method. Being a general–to–specific approach, indicator saturation differs from the specific–to–general approaches implemented in the official seasonal adjustment procedures. Two versions of indicator saturation, impulse–indicator and step–indicator saturation (IIS and SIS), have been applied in combination with the basic structural time series model that serves as a seasonal adjustment method for the purpose of this study.

Up to now, this combination of methods has not been applied in the literature. The properties of the suggested approach have been explored both in a Monte Carlo simulation exercise and in an empirical application. The simulation study has shown that the IIS and SIS are successful in the baseline setting. In settings other than the benchmark case, the performance of the IIS and SIS depends on the factor considered in the particular setting. For example, if the examined factor is the time location of an additive outlier, the IIS works worse the closer to either end of the sample the outlier occurs. Similar observations have been made for the SIS applied to the detection of level shifts. In this case, however, the performance does not vary symmetrically with respect to the level shift.

In the empirical part of the study, both indicator saturation versions have been applied to the industrial production series in five European countries. The focus of this analysis has been on the question whether the recessionary episode starting towards the end of 2008 can be described by the inherent model dynamics, or whether it represents a major

structural change. In fact, SIS detected level shifts in November or December of 2008 for almost all considered countries. Accounting for this structural break has, in general, given a better fit. In addition, results of a pseudo real–time recursive forecasting exercise have shown that detection of this level shift can also substantially improve the forecast accuracy. The sooner the shift is found, the bigger are the gains in terms of the forecast precision.

Chapter 4 has been dealing with real wage cyclicality from the empirical perspective. The aim has been to provide stylized facts for Germany and to investigate whether the results are sensitive to such factors as the detrending method and the choice of the price index used for the construction of real wages. The detrending methods have included the Hodrick–Prescott filter, the Baxter–King filter, the Beveridge–Nelson decomposition and the structural time series model. The consumption and the production price index have been used as price deflators.

To uncover the cyclical behavior of real wages, comovements between the obtained cycles of real wages and the business cycle indicator have been studied both in the time and in the frequency domain. As regards the time domain, the analysis has shown that the consumer real wage is procyclical and lags behind the business cycle. Albeit less pronounced, a similar pattern also holds for the producer real wage.

In the frequency domain, the phase angle has been adopted as a comovement concept. Even though being an old and established concept, its usefulness for this particular research question has been too seldom appreciated in the literature. Regardless of the detrending method, the analysis based on the phase angle has revealed a lagging behavior of the consumer real wage. Moreover, in the short run, the consumer real wage seems to be rather countercyclical, whereas in the long run the pattern switches to a procyclical one. The findings for the producer real wage, in contrast, have not been clear–cut. The results for the consumer real wage seem to accord with the predictions of the New Keynesian theory proclaiming rigid nominal wages in the short run.

In Chapter 5, the topic of the preceding chapter has been taken up again. The novelty of this study primarily relies on its new approach for investigating comovements. More specifically, wavelet analysis has been proposed as a method that allows for identifying changes in the comovement patterns at particular periodicities over time. This study has tried to exploit the appealing properties of wavelet analysis in a comparison of the USA and Germany – two large economies with strongly differing labor market institutions.

The results have shown that both consumer and producer real wages in the US are leading

the business cycle in the entire time span and at most business cycle periodicities. In contrast, the German consumer real wage is lagging the business cycle. For the producer real wage, the results are rather ambiguous. The periods of the strongest relationship between real wages and the business cycle are different in both countries as well. Some similarities have been uncovered for both countries, though. Until 1980, US and German real wages behave procyclically or acyclically and they change their behavior to an anticyclical one afterwards.

The overall different findings for both countries have been traced back to the differences not only in their institutional setup but also in their history of different political interventions and other sources of dynamics. Conjectures about the role of demand and supply shocks in the course of time have become possible by disentangling the frequency– and time–dependent patterns of cyclicality. It is also to be noted that the dynamics might have been additionally affected by the changing importance of factors responsible for recessions, like oil price shocks. These observations highlight the multidimensional nature of real wage cyclicality and may explain the lack of clear empirical evidence in the literature so far. They also demonstrate that pinpointing one correct theoretical explanation may not be possible as theories, in general, assume particular types of shocks driving the business cycle whereas the reality reflects the interaction of different shocks and transmission channels.

Appendix A

Matlab toolbox SPECTRAN*

A.1 Covariances and correlations

Even though SPECTRAN is a toolbox developed for spectral analysis, before different spectral concepts are introduced and their implementation is described, a little attention should be given to the estimation of covariances and correlations. As will become clear later in this document, these quantities play an important role in deriving spectral measures. Both auto– and cross–covariances are estimated in SPECTRAN by the function **crosscov**. For the computation of the autocovariances of a series x_t $(t = 1, ..., N)$ **crosscov** applies the formula

$$\hat{\gamma}_x(j) = \frac{1}{N} \sum_{t=j+1}^{N} (x_t - \bar{x})(x_{t-j} - \bar{x}), \tag{A.1}$$

where $\hat{\gamma}_x(j)$ is the sample autocovariance of x_t at the lag j and $\bar{x}$ is the estimated mean value of x_t given by

$$\bar{x} = \frac{1}{N} \sum_{t=1}^{N} x_t$$

In the case of the cross–covariances between two series x_t and y_t $(t = 1, ..., N)$, the following formula is used:

$$\hat{\gamma}_{xy}(j) = \frac{1}{N} \sum_{t=j+1}^{N} (x_t - \bar{x})(y_{t-j} - \bar{y}) \tag{A.2}$$

*This chapter is the result of the joint work with Víctor Gómez and has appeared as Marczak and Gómez (2012).

The function **crosscor** calculates the sample auto– and cross–correlations based on eq. (A.1) and eq. (A.2), respectively.
The user may want to study the sample covariances or correlations prior to the spectral analysis. To this end, he can use the function **corwrite** which writes the sample covariances or correlations up to a specified lag to a text file.

```
function corwrite(fid,ns,cr,corlag,vnames)
%*********************************************************************
%
%      This function writes the autocorrelations or
%      cross correlations in a text file
%
%    INPUTS:
%------------
%        fid : id of the text file where the output is to be written
%         ns : number of series (1 or 2)
%         cr : autocorrelations or cross correlations
%     corlag : number of leads and lags at which the
%              auto/cross correlations are computed;
%     vnames : name/s of the series
```

A.2 Univariate spectral analysis

Spectrum estimation

The spectrum of a time series constitutes the central concept of spectral analysis. It enables the identification of frequency components that make the greatest contribution to the overall variance of the series at hand. The spectrum is given as the Fourier transform of the autocovariance function (Priestley, 1981, p. 213):

$$f_x(\omega) = \frac{1}{2\pi} \int_{-\infty}^{\infty} \gamma_x(\tau) e^{-i\omega\tau} d\tau, \tag{A.3}$$

where ω denotes the angular frequency, $f_x(\omega)$ denotes the spectrum of x_t and $\gamma_x(\tau)$ is the autocovariance function of x_t. In the case of discrete data, eq. (A.3) becomes:

$$\begin{aligned} f_x(\omega) &= \frac{1}{2\pi} \sum_{j=-\infty}^{\infty} \gamma_x(j) e^{-i\omega j} \\ &= \frac{1}{2\pi} \sum_{j=-\infty}^{\infty} \gamma_x(j) \cos(\omega j) \end{aligned} \tag{A.4}$$

Since the data usually are finite and discrete in practice, the sample counterpart of the theoretical spectrum, called periodogram, can be seen as a truncated version of the theoretical spectrum with theoretical covariances replaced by their estimates. The periodogram is an unbiased but inconsistent spectrum estimate. In order to reduce its variance, the so–called smoothing is applied. In the time domain, it reduces to the application of a window function to the sample autocovariance function (Priestley, 1981, p. 502):

$$\hat{f}_x(\omega) = \frac{1}{2\pi} \sum_{j=-(N-1)}^{N-1} w_m(j) \hat{\gamma}_x(j) \cos(\omega j), \tag{A.5}$$

where $\hat{f}_x(\omega)$ denotes the estimate of $f_x(\omega)$, $\hat{\gamma}_x(j)$ is given by eq. (A.1) and $w_m(j)$ represents a window function. Function $w_m(j)$ satisfies the following properties (Koopmans, 1974, p. 266):

i) $0 \leq w_m(j) \leq w_m(0) = 1$,

ii) $w_m(j) = w_m(-j)$ for all k,

iii) $w_m(j) = 0$ for all $|j| > m$

where $m < N - 1$ is an integer called truncation point or lag number. In SPECTRAN, three window function types are available: the Blackman–Tukey window (or simply Tukey window), the Parzen window and the Tukey–Hanning window. In addition, confidence intervals for the smoothed spectrum estimates can be computed as described in Koopmans (1974, p. 274). The function **periodg** is used in SPECTRAN for spectrum estimation.

```
function sp = periodg(x,win,winlag,alpha)
%************************************************************************
%       This function computes the (smoothed) periodogram
```

```
%
%    INPUTS:
%------------
%  REQUIRED
%         x :  series
%
%  OPTIONAL
%       win :  window used for smoothing the periodogram;
%              = 0 :  no smoothing is performed
%              = 1 :  Blackman-Tukey window
%              = 2 :  Parzen window
%              = 3 :  Tukey-Hanning window
%              Parzen window is used,  if  win  is  not  input  to  periodg  or
%              if  win  is  empty,
%    winlag :  window lag size ;  if  it  is  empty, winlag  is  computed by the program
%    alpha  :  significance  level  needed  for  calculaction  of  the  confidence
%              intervals ;  if  alpha  is  not  input  to  periodg  or  if  alpha  is
%              empty, confidence  intervals  are  not  computed
%
%
%    OUTPUTS:
%------------
%        sp :  structure  with  the  following  fields :
%              .f       :  (smoothed) periodogram
%              .n       :  length  of  x
%              .win     :  window used for smoothing the periodogram
%              .winlag  :  window lag size ;  empty  if  no smoothing was
%                          performed
%              .a       :  parameter of the Blackman-Tukey window; a is field
%                          of  sp  if  win = 1
%              Additional  field ,  if  alpha  is  input  to  periodg and is  not
%              empty
%              .fconf   :  confidence  intervals  for  f
```

If the computation of confidence intervals for the estimated spectrum is desired, the user can either pass the value for the significance level (*alpha*) to **periodg** or he can leave this

argument unspecified and, instead, use the function **spconf** after calling **periodg**.

```
function fconf = spconf(sp,alpha)
%*********************************************************************
%
%   This function computes the confidence intervals for the smoothed
%   periodogram
%   See Koopmans, L.H.(1974), "The Spectral Analysis of Time Series",
%   p.274, 279
%
%     INPUTS:
%-------------
%    REQUIRED
%         sp : structure , output of function periodg
%
%    OPTIONAL
%     alpha : significance level needed for calculation of
%             the confidence intervals ;
%             alpha = 0.05, if alpha is not input to spconf or
%              if alpha is empty
%
%     OUTPUT:
%-------------
%     fconf : confidence intervals for the smoothed periodogram
```

Output files and plots

It may be convenient to save the estimation output in a text file. In this way, the user can have access to the results at any time. In SPECTRAN, the function **specwrite** is designed to write the output of the spectral analysis to a text file. Function **specwrite** let the user decide for which frequency band the results are to be displayed.

```
function specst = specwrite( fid , per , sp , fband , mph , mphconf , phfband , vnames , ppi)
%*********************************************************************
% This function writes results of the spectral analysis to a text file
```

```
%
%     INPUTS:
%-------------
%        fid  : id of the text file where the output is to be written
%        per  : frequency of the data (number of periods per year)
%         sp  : structure being output of the function periodg, crosspan or
%               mulparspan
%     fband  : frequency interval for which results are displayed;
%               default is [0, pi]
%        mph : mean phase angle;
%               it should be empty if sp is output of periodg
%   mphconf : confidence interval for mph
%               it should be empty if sp is output of periodg
%   phfband : frequency interval for which results for the mean phase angle
%               are displayed; default is [0, pi]
%               it should be empty if sp is output of periodg
%    vnames : name/s of the series; it can be empty
%        ppi  : 0, do not express angular measures in terms of pi (default)
%               1, express all angular measures in terms of pi
%
%     OUTPUT: (optional)
%-------------
%     specst: structure depending on sp; all fields refer to the
%               interval given by fband
%
%               All possible fields, if sp is output of periodg:
%               .frq      : frequencies
%               .f        : spectrum of the series
%               .fconf    : confidence interval
%
%               All possible fields, if sp is output of crosspan:
%               .frq      : frequencies
%               .fx       : (smoothed) periodogram of the reference series
%               .fy       : (smoothed) periodograms of all other series
%               .co       : matrix with columns containing coherency
%                           between the ref. series and a particular series
```

```
%           .sco      : matrix with columns containing coherence
%                       (squared coherency) between the ref. series
%                       and a particular series
%           .ga       : matrix with columns containing gain
%                       between the ref. series and other series
%           .ph       : matrix with columns containing phase angle
%                       between the ref. series and other series
%           .pht      : matrix with columns containing phase delay
%                       of a particular series relative to the ref. series
%           .phd      : matrix with columns containing group delay
%                       of a particular series relative to the ref. series
%           .mph      : vector with mean phase angle values
%                       between the ref. series and other series
%           .fxconf   : confidence intervals for fx
%           .fyconf   : confidence intervals for fy
%           .cconf    : confidence intervals for co
%           .gconf    : confidence intervals for ga
%           .pconf    : confidence intervals for ph
%           .mphconf  : confidence intervals for mph
%
%           All possible fields, if sp is output of mulparspan:
%           .frq      : frequencies
%           .fx       : (smoothed) periodogram of the reference series
%           .fy       : (smoothed) periodograms of all other series
%           .mco      : matrix with columns containing multiple coherency
%                       between the ref. series and other series
%           .msco     : matrix with columns containing multiple coherence
%                       (multiple squared coherency) between the ref. series
%                       and a particular series
%           .pco      : matrix with columns containing partial coherency
%                       between the ref. series and other series
%           .psco     : matrix with columns containing partial coherence
%                       (partial squared coherency) between the ref. series
%                       and a particular series
%           .pga      : matrix with columns containing partial gain
%                       between the ref. series and a particular series
```

```
%              .pph     : matrix with columns containing partial phase angle
%                         between the ref. series and a particular series
%              .ppht    : matrix with columns containing partial phase delay
%                         of a particular series relative to the ref. series
%              .pphd    : matrix with columns containing partial group delay
%                         of a particular series relative to the ref. series
%              .mpph    : vector with mean phase angle values
%                         between the ref. series and a particular series
%              .fxconf  : confidence intervals for fx
%              .fyconf  : confidence intervals for fy
%              .mpphconf: confidence intervals for mpph
```

In addition to the written output, the user may want to study the graphical representation of the estimated spectra. In SPECTRAN, the function **specplot** is designed for plotting, e.g., the estimated spectra along with their confidence bands. Moreover, function **specplot** also provides a feature, particulary interesting for business cycle analysts. If the user does not restrict the frequency band to the band exactly covering the frequencies corresponding to the business cycle periodicities, **specplot** highlights the results in the business cycle frequency band by separating them with lines from the results in the remaining region.

```
function specplot(frq,per,mul,spec,fband,specconf,alpha,specname,vnames)
%*********************************************************************
%       This function plots (non-angular) spectral measures and their
%       confidence intervals
%
%    INPUTS:
%------------
%       frq : frequencies
%       per : frequency of the data (number of periods per year)
%       mul : 0, if univariate spectral measures are to be plotted
%             1, if multivariate spectral measures are to be plotted
%      spec : matrix with uni- or multivariate spectral measures with
%             columns corresponding to a particular series or
%             a pair of series
%     fband : frequency interval for which results are displayed;
```

```
%                default is [0, pi]
% specconf : confidence intervals for spec; it can be empty
%    alpha : significance level ; it can be empty
% specname : name of the spectral measure; it can be empty
%   vnames : name/s of the series ; it can be empty
```

A.3 Multivariate spectral analysis

Bivariate spectral measures

Analogously to the spectrum in the univariate case, the cross–spectrum is the central concept in the analysis of multivariate time series. The cross–spectrum $f_{xy}(\omega)$ between two time series x_t and y_t is given by the Fourier transform of the covariance function $\gamma_{xy}(\tau)$. As it is complex–valued, it can be decomposed into the real part $c_{xy}(\omega)$ (cospectrum) and the imaginary part $q_{xy}(\omega)$ (quadrature spectrum) which in the case of discrete data are given by the following formulas (Priestley, 1981, p. 659):

$$c_{xy}(\omega) = \frac{1}{2\pi} \sum_{j=-\infty}^{\infty} \gamma_{xy}(j) \cos(\omega j)$$

$$q_{xy}(\omega) = -\frac{1}{2\pi} \sum_{j=-\infty}^{\infty} \gamma_{xy}(j) \sin(\omega j)$$

In SPECTRAN, the estimates of the cospectrum and the quadrature spectrum are computed by the function **cospqu** in the following way:

$$\hat{c}_{xy}(\omega) = \frac{1}{2\pi} \sum_{j=-(N-1)}^{N-1} w_m(j) \hat{\gamma}_{xy}(j) \cos(\omega j) \tag{A.6}$$

$$\hat{q}_{xy}(\omega) = -\frac{1}{2\pi} \sum_{j=-(N-1)}^{N-1} w_m(j) \hat{\gamma}_{xy}(j) \sin(\omega j), \tag{A.7}$$

where in the case of smoothed quantities $w_m(j)$ represents a window function. If raw quantities should be obtained, $w_m(j)$ can be set to one for $|j| < m = N - 1$ and to zero otherwise.

```
function cqsp = cospqu(x,y,win,winlag)
%*********************************************************************
%    This function computes the (smoothed) cross-periodogram
%
%    INPUTS:
%------------
%  REQUIRED
%       x,y : series
%
%  OPTIONAL
%      win : window used for smoothing the periodogram;
%            = 0 : no smoothing is performed
%            = 1 : Blackman-Tukey window
%            = 2 : Parzen window
%            = 3 : Tukey-Hanning window
%            Parzen window is used, if win is not input to cospqu or
%            if win is empty,
%   winlag : window lag size; if it is not input to cospqu or if it
%            is empty, winlag is computed by the program
%
%
%   OUTPUTS:
%------------
%     cqsp : structure with the following fields :
%            .c      : cospectrum
%            .q      : quadrature spectrum
%            .n      : length of x and y
%            .win    : window used for smoothing the periodogram
%            .winlag : window lag size; empty if no smoothing was
%                      performed
%            .a      : parameter of the Blackman-Tukey window;
%                      a is field of sp if win = 1
```

To measure comovements between time series, several concepts based on the cospectrum and the quadrature spectrum have been proposed in the literature. The most commonly used are coherency, squared coherency, phase angle and gain; see, e.g., Koopmans (1974,

pp. 135). Coherency is defined as:

$$R_{xy}(\omega) = \sqrt{\frac{c_{xy}^2(\omega) + q_{xy}^2(\omega)}{f_x(\omega) f_y(\omega)}} \tag{A.8}$$

whereas coherence $R_{xy}^2(\omega)$ is the squared value of $R_{xy}(\omega)$. Their values can vary between zero and one and measure the strength of the relationship between the considered series at each frequency. Another very useful cross–spectral measure, the phase angle, is defined as follows:

$$\phi_{xy}(\omega) = \arctan\left[\frac{q_{xy}(\omega)}{c_{xy}(\omega)}\right] \tag{A.9}$$

The phase provides information on the lead–lag relation between two series at each frequency. This aspect will be addressed in more detail in the next subsection. Moreover, by the examination of the phase angle values one can also identify a positive or negative relationship between two series at each frequency. A comprehensive discussion of the phase angle can be found in, e.g., Marczak and Beissinger (2013). Gain is referred to as the gain function of the filter which transforms x_t into the best approximation to y_t in the mean square sense. In other words, it represents a function which changes the amplitude of each frequency component of x_t to obtain the best approximation to y_t. The formal definition of the gain is given by:

$$B_{xy}(\omega) = \frac{\sqrt{c_{xy}^2(\omega) + q_{xy}^2(\omega)}}{f_x(\omega)} \tag{A.10}$$

Estimates of the comovement indicators above are obtained by substituting $c_{xy}(\omega)$, $q_{xy}(\omega)$, $f_x(\omega)$ and $f_y(\omega)$ in eq. (A.8), (A.9) and (A.10) with the quantities computed according to eq. (A.5), (A.6) and (A.7). This procedure has been implemented in SPECTRAN in the function **cohepha**.

```
function cgpsp = cohepha(cqsp,fxx,fyy)
%************************************************************************
%     This function computes coherency, coherence (squared coherency),
%     gain and phase angle
%
%     INPUTS:
%------------
```

```
%      cqsp : structure , output of function cospqu
%       fxx : (smoothed) periodogram of x
%       fyy : (smoothed) periodogram of x
%
%
%    OUTPUTS:
%-------------
%     cgpsp : structure with the following fields :
%             .co      : coherency
%             .sco     : coherence (squared coherency)
%             .ga      : gain
%             .ph      : phase angle
%             .n       : length of x and y
%             .win     : window function
%             .winlag  : window lag size
```

Confidence intervals for the coherency, gain and the phase angle can be computed as described in Koopmans (1974, pp. 282–287) by the function **cgpcof**.

```
function [cconf,gconf,pconf] = cgpconf(cgpsp,fx,fy,alpha)
%*********************************************************************
%  This function computes the confidence interval for the coherency,
%  gain and phase angle
%  See Koopmans, L.H.(1974), "The Spectral Analysis of Time Series",
%  pp. 282-287, Table 8.1 (p.279)
%
%      INPUTS:
%-------------
%     REQUIRED
%      cgpsp : structure , output of function cohepha
%         fx : smoothed periodogram of x
%         fy : smoothed periodogram of y
%
%     OPTIONAL
%      alpha : significance level needed for calculation of
%              the confidence intervals ;
```

```
%              alpha = 0.05, if alpha is not input to cgpsp or
%               if alpha is empty
%
%    OUTPUTS:
%-------------
%      cconf : confidence intervals for the coherency
%      gconf : confidence intervals for the gain
%      pconf : confidence intervals for the phase angle
```

The user may want to directly compute spectra, coherency, gain and phase angle, possibly also with the respective confidence intervals, all at once. This can be accomplished by using the function **crosspan**. Function **crosspan** additionally calculates the so–called phase delay and the group delay. The phase delay, $\phi_{t,xy}(\omega) = \phi_{xy}(\omega)/\omega$, expresses the shift of each frequency component of one series relative to the corresponding component of the other series in terms of time units depending on the data periodicity. The group delay, $\phi_{g,xy}(\omega) = d\phi_{xy}(\omega)/d\omega$, measures the change of the shift of both frequency components relative to each other. Calculation of both measures is based on the estimated phase angle, $\hat{\phi}_{xy}(\omega)$.

```
function crossp = crosspan(y,win,winlag,alpha)
%*********************************************************************
%   This function performs the cross-spectral analysis and optionally
%    calculates the confidence intervals for the estimated spectra of
%   two time series , coherency, gain and phase angle
%
%
%    INPUTS:
%------------
%  REQUIRED
%        y : (ly x ny) matrix with the series ;
%            the program assumes that the first column contains
%            the reference series
%
%  OPTIONAL
%      win : window used for smoothing the periodogram;
%            = 0 : no smoothing is performed
```

```
%              = 1 : Blackman-Tukey window
%              = 2 : Parzen window
%              = 3 : Tukey-Hanning window
%              Parzen window is used, if win is not input to crosspan or
%              if win is empty,
%    winlag : window lag size; if it is not input to crosspan or if it
%              empty, winlag is computed by the program
%     alpha : significance level needed for calculaction of the confidence
%              intervals; if alpha is not input to crosspan or if alpha is
%              empty, confidence intervals are not computed
%
%
%     OUTPUT:
%-------------
%    crossp : structure with the following fields :
%              .frq     : frequencies
%              .fx      : (smoothed) periodogram of the reference series
%              .fy      : (smoothed) periodograms of all other series
%              .co      : matrix with columns containing coherency
%                         between the ref. series and a particular series
%              .sco     : matrix with columns containing coherence
%                         (squared coherency) between the ref. series
%                         and a particular series
%              .ga      : matrix with columns containing gain
%                         between the ref. series and a particular series
%              .ph      : matrix with columns containing phase angle
%                         between the ref. series and a particular series
%              .pht     : matrix with columns containing phase delay
%                         of a particular series relative to the ref. series
%              .phd     : matrix with columns containing group delay
%                         of a particular series relative to the ref. series
%              .n       : length of the series
%              Additional fields, if alpha is input to crosspan and is not
%              empty:
%              .fxconf : confidence intervals for fx
%              .fyconf : confidence intervals for fy
```

```
%          .cconf  : confidence intervals for co
%          .gconf  : confidence intervals for ga
%          .pconf  : confidence intervals for ph
```

Multiple coherence and partial spectral measures

So far, the multivariate concepts and their implementation were restricted to the bivariate case. If more than two series are involved, the overall relationship between a reference series and the other series, in following referred to as inputs, can be assessed. Moreover, to determine the relationship between a reference series and an input series, one should take account of the interactions between this input series and the remaining ones. These considerations imply that in a multivariate situation with more than two variables, concepts are needed that imitate the ideas well known from the multivariate linear regression theory. The formal representation of the concepts reviewed in this subsection primarily follows Jenkins and Watts (1968, pp. 487–490).

The measure that can be considered as a frequency domain counterpart of the coefficient of determination is called multiple coherence and measures the proportion of the reference series spectrum that can be explained by the input series. The multiple coherence between the series x_{1t} and the inputs $x_{2t,3t,...,pt}$ is defined as:

$$R^2_{1\cdot 2,3,...,p}(\omega) = 1 - \frac{\det F(\omega)}{F_{11}(\omega)M_{11}(\omega)}, \tag{A.11}$$

where $F(\omega)$ is the cross–spectral matrix. Its diagonal elements $f_{ii}(\omega)$ $(i = 1, ..., p)$ represent spectra of the corresponding series whereas the off–diagonal elements $f_{ij}(\omega)$ $(i, j = 1, ..., p$ and $i \neq j)$ represent cross–spectra between series x_i and x_j and have the property $f_{ij}(\omega) = f^*_{ji}(\omega)$, where "*" denotes the complex conjugate. $F_{ij}(\omega)$ denotes the (ij)-th element of $F(\omega)$ $(i, j = 1, ..., p)$, $\det F(\omega)$ is the determinant of $F(\omega)$ and $M_{ij}(\omega)$ is the (ij)-th minor of $F(\omega)(i, j = 1, ..., p)$. The multiple coherency $R_{1\cdot 2,...,p}(\omega)$ is given as the positive square root of $R^2_{1\cdot 2,...,p}(\omega)$.

In analogy to the partial correlation coefficient, the partial coherence or its square root, partial coherency, measures the cet. par. relationship between the reference series and an input series at each frequency. The partial coherence between x_{1t} and x_{jt} $(1 < j \leq p)$ is

given by:

$$r^2_{1j|q(j)}(\omega) = \frac{|M_{j1}(\omega)|^2}{M_{11}(\omega)M_{jj}(\omega)}, \tag{A.12}$$

where $q(j)$ is a set of indices such that $q(j) = \{2, ..., p\} \setminus j$.
It is also possible to quantify the so–called partial phase angle between x_{1t} and x_{jt}, i.e the phase difference between x_{1t} and x_{jt} after allowing for the phase differences between all inputs and between x_{1t} and x_{kt} ($k \in q(j)$). Formally, it can be described as follows:

$$\phi_{1j|q(j)}(\omega) = \arctan\left[\frac{\Im(M_{j1}(\omega))}{\Re(M_{j1}(\omega))}\right], \tag{A.13}$$

where $\Re(\cdot)$ and $\Im(\cdot)$ denote the real part and the imaginary part of a complex number, respectively. Strongly related to the partial phase angle are the concepts of the partial phase delay, $\phi_{t,1j|q(j)}(\omega) = \phi_{1j|q(j)}(\omega)/\omega$, and the partial group delay, $\phi_{g,1j|q(j)}(\omega) = d\phi_{1j|q(j)}(\omega)/d\omega$.
Similarly to the concept of the gain function introduced in the bivariate case, the partial gain between x_{1t} and x_{jt} is defined as:

$$B_{1j|q(j)}(\omega) = \frac{|M_{j1}(\omega)|}{F_{11}(\omega)} \tag{A.14}$$

The estimates of the multiple coherence (coherency), partial coherence (coherency), partial phase angle and partial gain can be obtained in the following way. First, elements of the cross–spectral matrix $F(\omega)$ are replaced by their sample counterparts, thereby yielding the estimate of $F(\omega)$, $\hat{F}(\omega)$. Then, eq. (A.11), (A.12), (A.13) and (A.14) are applied by substituting values derived from $F(\omega)$ with those derived from $\hat{F}(\omega)$. In SPECTRAN, this procedure is implemented in the function **mulparspan**.

```
function mulsp = mulparspan(y,win,winlag,alpha)
%*********************************************************************
%      This function computes multiple (squared), partial (squared)
%      coherency, partial phase angle and partial gain between
%      the reference series and other series
%
%    INPUTS:
%------------
%  REQUIRED
```

```
%         y : (ly x ny) matrix with the series ;
%             the program assumes that the first column contains
%             the reference series
%
%  OPTIONAL
%       win : window used for smoothing the periodogram;
%             = 0 : no smoothing is performed
%             = 1 : Blackman-Tukey window
%             = 2 : Parzen window
%             = 3 : Tukey-Hanning window
%             Parzen window is used, if win is not input to crosspan or
%             if win is empty,
%    winlag : window lag size ; if it is not input to crosspan or if it
%             empty, winlag is computed by the program
%     alpha : significance level needed for calculaction of the confidence
%             intervals ; if alpha is not input to crosspan or if alpha is
%             empty, confidence intervals are not computed
%
%    OUTPUT:
%------------
%     mulsp : structure with following fields :
%             .frq     : frequencies
%             .fx      : (smoothed) periodogram of the reference series
%             .fy      : (smoothed) periodograms of all other series
%             .mco     : matrix with columns containing multiple coherency
%                        between the ref. series and a particular series
%             .msco    : matrix with columns containing multiple
%                        coherence (squared multiple coherency) between
%                        the ref. series and a particular series
%             .pco     : matrix with columns containing partial coherency
%                        between the ref. series and a particular series
%             .psco    : matrix with columns containing partial
%                        coherence (squared partial coherency) between
%                        the ref. series and a particular series
%             .pga     : matrix with columns containing partial gain
%                        between the ref. series and a particular series
```

```
%               .pph    : matrix with columns containing partial phase angle
%                         between the ref. series and a particular series
%               .ppht   : matrix with columns containing partial phase delay
%                         of a particular series relative to the ref. series
%               .pphd   : matrix with columns containing partial group delay
%                         of a particular series relative to the ref. series
%               .n      : length of the series
%               Additional fields, if alpha is input to mulparspan and is not
%               empty:
%               .fxconf : confidence intervals for fx
%               .fyconf : confidence intervals for fy
```

Mean (partial) phase angle

Sometimes, if mean direction of the relationship between time series in a certain frequency band is of interest, it seems natural to compute mean values of some comovement measure in this frequency band. However, in the case of the phase angle, building the standard arithmetic mean fails to be the appropriate procedure. Due to circular nature of the phase angle, one should compute the mean according to the concept specially devoted to the data measured on the angular scale; see, e.g., Zar (1999). In SPECTRAN, this can be achieved by using the function **meanphconf** which additionally returns confidence intervals for the mean values. The user can supply either the values of the ordinary phase angle obtained with **crosspan** (or **cohepha**) or the values of the partial phase angle computed with **mulparspan**. Calculations made by **meanphconf** are based on functions provided by Berens (2009).

```
function [mph,mphconf] = meanphconf(ph,frq,pband)
%*****************************************************************
% This function computes the mean (partial) phase angle values and
% their confidence intervals.
% Computation is based on the circular statistics.
% This function uses functions circ_mean and cir_confmean from the toolbox
% CircStats2011f by Philipp Berens.
%
%    INPUTS:
```

```
%-------------
%  REQUIRED
%        ph : matrix with columns containing ( partial ) phase angle
%             corresponding to the ref. series and a particular series
%       frq : frequencies, frq and ph must be of the same size;
%             the program assumes that the rows of frq and ph correspond to
%             each other
%
%  OPTIONAL, if the (partial) phase angle values are to be averaged
%             over a specified interval
%    pband : time interval expressed in time units;
%             ( partial ) phase angle values are averaged over pband
%
%
%   OUTPUTS:
%-------------
%       mph : mean (partial) phase angle values
%  mphconf : confidence intervals for mph
```

Output files and plots

The output of the multivariate spectral analysis described in Section A.3 or A.3 can be written to a text file by the function **specwrite** (see the description in Section A.2. To this end, the user has to supply the structure being output of **crosspan** or **mulparspan**, respectively. Optionally, the mean (partial) phase angle values and their confidence intervals, both computed with **meanphconf** can also be written if *mph* and *mphconf* are passed to the function. Similarly to the univariate case, the function **specplot** is as well capable of plotting most of the multivariate spectral measures (see Section A.2). As for the (partial) phase angle, the function **phplot** is more suitable since it depicts phase angle values in form of dots and, if desired, the confidence intervals for the estimates as lines. This allows to illustrate the results for each frequency on a linear scale as if it were a "straightened" circular scale.

```
function phplot(frq,per,ph,fband,phconf,alpha,vnames,mulvar)
%*****************************************************************
```

```
%    This function plots the ( partial ) phase angle values with
%    their confidence intervals .
%
%     INPUTS:
%------------
%        frq  :  frequencies
%        per  :  frequency of the data (number of periods per year)
%         ph  :  matrix with phase angle values with columns
%                corresponding to the reference series and
%                a particular series
%     fband  :  frequency interval for which results are displayed ;
%                default is [0, pi]
%    phconf  :  confidence intervals for ph; it can be empty
%     alpha  :  significance level ; it can be empty
%    vnames  : name/s of the series ; it can be empty
%    mulvar  :  0, ordinary phase angle ( default )
%               1, partial phase angle
```

Lead–lag analysis

One of the tasks of the SPECTRAN user, e.g.a business cycle analyst, may be to establish the lead–lag relation between two time series. As already mentioned in Section A.3, the concept of the phase angle plays a major role in this context. One can draw on either the ordinary phase angle given by eq. (A.9) or the partial phase angle given by eq. (A.13). The interpretation of each (partial) phase angle value may, however, be somewhat cumbersome. To simplify the identification of the lead–lag pattern, SPECTRAN proposes two strategies. The first one relies on finding that frequency which corresponds to the strongest relationship between the series, here represented by the highest (partial) coherence. The (partial) phase angle value at this frequency serves then as an indicator for the leading or lagging behavior. The second possibility is to consider the (partial) phase angle values averaged over certain frequencies. The function **leadlagan** designed in SPECTRAN for the lead–lag analysis takes account of these two possibilities. To take advantage of them by calling **leadlagan**, the user has to provide the structure being the output of **crosspan** or **mulparspan** depending on whether he wants to pin down the analysis to the ordinary or the partial phase angle, respectively. Optionally, the user can

also pass the mean (partial) phase angle values along with their confidence intervals and the frequency band over which the (partial) phase angle values have been averaged. The output of **leadlagan** is written to a text file.

```
function llst = leadlagan(fid,per,sp,fband,mph,mphconf,phfband,vnames,ppi)
%%%%%%%%%%%%%%%%%%%%%%%%%%%%%%%%%%%%%%%%%%%%%%%%%%%%%%%%%%%%%%%%%%%%%%%%
%                        LEAD-LAG ANALYSIS
%
%   Phase shifts between the reference series and an other series
%   at the most important frequency are computed.
%   The most important frequency is defined as the one at which the
%   highest (partial) coherence occurs; (partial) coherence is used as
%   a measure of the relationship between two cycles.
%
%
%    INPUTS:
%------------
%       fid : id of the text file where the output is to be written
%       per : frequency of the data (number of periods per year)
%        sp : structure being output of crosspan or mulparspan
%     fband : frequency interval for which results are displayed;
%             default is [0, pi]
%       mph : mean (partial) phase angle; it can be empty
%   mphconf : confidence interval for mph; it should be empty if mph is
%             empty
%   phfband : frequency interval for which results for the mean (partial)
%             phase angle are displayed; default is [0, pi]
%    vnames : name/s of the series
%       ppi : 0, do not express angular measures in terms of pi (default)
%             1, express all angular measures in terms of pi
%
%    OUTPUT: (optional)
%------------
%      llst : structure with following fields:
%             .masco    : maximum (partial) coherences
%             .maxfrq   : frequencies corresponding to maxsco
```

```
%              .maxph     : ( partial ) phase angle values corresponding
%                           to maxsco
%              .mapht     : ( partial ) phase delay values corresponding
%                           to maxsco
%              .maxphconf : confidence intervals for maxph;
%                           field if pconf is field of sp
```

A.4 Function *spectran*

SPECTRAN is a toolbox which tries to bring in line two important properties. One of them is its flexibility which allows the user to customize his analysis by picking functions yielding the most desired output only. The other one is the user–friendliness manifested by the possibility of obtaining quite a large output in a few steps. In light of the idea of the user–friendliness, the function **spectran** has been designed. This function combines all building blocks described in the previous sections concerning computational aspects and output representation. The function **spectran** offers the user a choice of numerous options. As regards the methodology, he can decide whether in case of more than two series standard bivariate measures or partial measures are to be computed, whether the lead–lag analysis should be performed etc. As for the output files, it is left up to the user whether the text file should be written, whether the results should be plotted, whether the confidence intervals should be plotted, for which periodicity band the results should be displayed etc. With an appropriate configuration, the user can thus arrive at the desired function output in one step instead of calling several functions.

```
function spectr = spectran(y,per, varargin )
%*****************************************************************
%                          SPECTRAL ANALYSIS
%
% This program computes spectrum, (multiple/ partial ) coherence,
% ( partial ) phase angle, ( partial ) phase delay, ( partial ) gain and
% auto- or cross-correlations between a reference series and other series.
%
%                        The syntax :
% spectr = spectran(y,per,'option1', optionvalue1,'option2', optionvalue2 ,...)
```

```
%
%
%       INPUTS :
%-------------------
%      REQUIRED
%            y : (ly x ny) matrix with the series ;
%                if ny = 1, univariate spectral analysis and computation
%                of autocorrelations of y are performed,
%                if ny > 1, bivariate or multivariate spectral analysis
%                and computation of cross-correlations are performed;
%                the program assumes that the first column contains
%                the reference series
%          per : frequency of the data (number of periods per year)
%-------------------
%       OPTIONS
%     'vnames' : string array with names for the series ; the program
%                assumes that their order coincides with the order in y;
%                default : refseries , series1 , series2 ,...
%     'corlag' : number of leads and lags at which the
%                auto-/cross-correlations are computed; default: ly-1
%        'win' : window function used for (cross-)periodogram smoothing
%                0, no window is applied (nonsmoothed periodogram).
%                1, the Blackman-Tukey window
%                2, the Parzen window (default)
%                3, the Tukey-Hanning window
%     'winlag' : window lag size ;
%                default : depending on the window function
%     'mulvar' : 0, if bivariate analysis in case of ny > 2
%                   is to be performed ( default );
%                   (always 0 for ny <= 2)
%                1, if multivariate analysis in case of ny > 2
%                   is to be performed
%       'conf' : 0, do not compute confidence intervals for the spectral
%                   measures ( default )
%                1, compute confidence intervals
%      'alpha' : significance level ; default ( if conf = 1): 0.05
```

```
%      'pband' : time interval expressed in time units corresponding to
%                per, results are displayed and saved for the chosen
%                pband; default:
%                [2, inf] corresponding to frequency interval [0, pi]
%     'phmean' : 0, do not compute the mean phase angle values and their
%                   confidence intervals (default)
%                1, compute the mean phase angle values and their
%                   confidence intervals
%    'phpband' : time interval expressed in time units corresponding to
%                per, phase angle is averaged over phpband;
%                default (if phmean = 1): [2,inf]
%      'graph' : 0, do not produce graphs
%                1, produce graphs (default)
% 'graphconf' : 0, do not plot confidence intervals (default)
%                1, plot confidence intervals (phmean or alpha must then
%                   be specified)
%        'out' : 0, do not write the output to a text file
%                1, write output to a text file (default)
%       'path' : string specifying the path to the directory where the
%                output file/s should be written;
%                default: folder 'results' in the current directory
%       'save' : 0, do not save the graphs (default)
%                1, save the graphs;
%                   the graphs will be saved in the subfolder 'plots'
%                   in the directory given by path, with default
%                   extension .fig (if ext or format are not specified)
%        'ext' : extension for saving the graphs (see function saveas)
%     'format' : format for saving the graphs (see function saveas)
%    'leadlag' : 0, do not produce separate file with the lead-lag
%                   analysis (default)
%                1, produce separate file 'leadlag.txt' with the lead-lag
%                   analysis
%         'pi' : 0, (default)
%                1, express all angular measures in terms of pi
%
%
```

```
%       OUTPUT :
%-----------------------
%       spectr : structure containing all results depending on the
%                dimension of y and options chosen; all fields refer to the
%                interval given by fband
%
%                All possible fields for ny = 1:
%                .frq     : frequencies
%                .f       : spectrum of the series
%                .fconf   : confidence interval
%
%                All possible fields for ny = 2 and ny > 2, if value for
%                'mulvar' is 0:
%                .frq     : frequencies
%                .fx      : (smoothed) periodogram of the reference series
%                .fy      : (smoothed) periodograms of all other series
%                .co      : matrix with columns containing coherency
%                           between the ref. series and a particular series
%                .sco     : matrix with columns containing coherence
%                           (squared coherency) between the ref. series
%                           and a particular series
%                .ga      : matrix with columns containing gain
%                           between the ref. series and a particular series
%                .ph      : matrix with columns containing phase angle
%                           between the ref. series and a particular series
%                .pht     : matrix with columns containing phase delay
%                           of a particular series relative to the
%                           ref. series
%                .phd     : matrix with columns containing group delay
%                           of a particular series relative to the
%                           ref. series
%                .mph     : vector with mean phase angle values
%                           between the ref. series and a particular series
%                .fxconf  : confidence intervals for fx
%                .fyconf  : confidence intervals for fy
%                .cconf   : confidence intervals for co
```

```
%                .gconf  : confidence intervals for ga
%                .pconf  : confidence intervals for ph
%                .mphconf: confidence intervals for mph
%
%                All possible fields for ny > 2, if value for 'mulvar' is 1:
%                .frq    : frequencies
%                .fx     : (smoothed) periodogram of the reference series
%                .fy     : (smoothed) periodograms of all other series
%                .mco    : matrix with columns containing multiple coherency
%                          between the ref. series and a particular series
%                .msco   : matrix with columns containing multiple
%                          coherence (squared multiple coherency) between
%                          the ref. series and a particular series
%                .pco    : matrix with columns containing partial coherency
%                          between the ref. series and a particular series
%                .psco   : matrix with columns containing partial
%                          coherence (squared partial coherency) between
%                          the ref. series and a particular series
%                .pga    : matrix with columns containing partial gain
%                          between the ref. series and a particular series
%                .pph    : matrix with columns containing partial phase angle
%                          between the ref. series and a particular series
%                .ppht   : matrix with columns containing partial phase delay
%                          of a particular series relative to the
%                          ref. series
%                .pphd   : matrix with columns containing partial group delay
%                          of a particular series relative to the
%                          ref. series
%                .mpph   : vector with mean partial phase angle values
%                          between the ref. series and a particular series
%                .fxconf : confidence intervals for fx
%                .fyconf : confidence intervals for fy
%                .mpphconf: confidence intervals for mpph
%
%    Examples:
%
```

```
%     s = spectran(y,per,'vnames',{'GDP','IPI'},'conf',1,'graphconf',1)
%     s = spectran(y,per,'pband',[8,32],'save',1)
%     s = spectran(y,per,'alpha',0.01,'phmean',1,'graph',0)
```

It is to be noted that the function **spectran** internally determines the name of the output files. If **spectran** has been called in a script file, the name of the output file (with either spectral analysis or lead–lag analysis results) contains the name of this script. The name of the output file is also denoted by a number that allows for distinction between files associated with different **spectran** calls. If at the beginning of each script run all existing variables are removed from the base workspace (but this does not happen between several possible **spectran** calls within the same script run), then the output files will be identified with the number of the corresponding **spectran** call. In case **spectran** is called from the command line or while evaluating a cell in the script file, the output files corresponding to spectral analysis become the name *spectran* and those referring to the lead–lag analysis – the name *leadlag*. For both types of files, also in this case a number is additionally appended to the file name. The number depends on how many structures from **spectran** calls already exist in the base workspace.

A.5 Examples

Example 1

The first example deals with quarterly cycles of the German industrial production index (IPI) and the consumer real wage in the time span 1970.Q1 – 2011.Q3. The data is stored in the files *PRGer.dat* and *CWGer.dat* in the subdirectory *data*. The demo file corresponding to this example is *exGER.m*. In the following, the discussion of the script files will be constrained to the selected code lines. The code below illustrates the estimation of spectra of the IPI cycle and the consumer real wage cycle.

```
% Settings for the spectral analysis:
alpha = 0.05;  % compute conf. intervals with the significance level alpha
win = 1;       % Blackman-Tukey window
winlag = [];   % default window lag size

% Spectral analysis of the IPI
```

```
spx = periodg(x,win,winlag,alpha);

% Spectral analysis of the real wage
spy = periodg(y,win,winlag,alpha);
```

The following lines show how the estimated IPI spectrum can be written to a text file.

```
per = 4;        % frequency of the data
% frequency band for which the results are displayed;
% it corresponds to business cycle periodicities (periods between 6 and 32
% quarters)
fband = 2*pi./[32 6];
% IPI
fid = fopen('results\specPRGer.txt','w');
specwrite(fid,per,spx,fband,[],[],[],'PRGer')
fclose(fid);
```

Finally, with the code below the estimated IPI spectrum is plotted.

```
frq = spx.frq;
mul = 0;
fx = spx.f;
fxconf = spx.fconf;
specplot(frq,per,mul,fx,fband,fxconf,alpha,'Spectrum','PRGer')
```

Example 2

In the second example, three monthly US series between 1953.M4 and 2007.M9 are considered: the cycles of the industrial production index (IPI), consumption and working hours. The IPI cycle is here considered as the reference series and acts as the business cycle indicator. The code for this example can be found in the script file *exUS1.m* and the corresponding data in the file *DataUS.xls*. The following lines show how to compute the bivariate cross–spectral measures and how to allow for computing confidence intervals.

```
[ser,headers] = xlsread('data\DataUS.xls');
fband = 2*pi./[96 18];
vnames = headers;
% Compute confidence intervals with the significance level alpha
alpha = 0.05;
% default window function (Parzen window) and window lag size
cross = crosspan(ser ,[],[], alpha);
```

In the next step, the mean phase angle values with their confidence intervals are calculated. The phase angle values are thereby averaged over the frequency band corresponding to the business cycle periodicities.

```
ph = cross.ph;
frq = cross.frq;
pband = [18,96];
[mph,mphconf] = meanphconf(ph,frq,pband);
```

The code below shows how to establish the lead–lag relation between the IPI cycle and the other series.

```
fid = fopen('results\leadlagUS.txt','w');
leadlagan(fid,per,cross,fband,mph,mphconf,fband,vnames,ppi)
fclose(fid);
```

Plots of the estimated phase angle values with their confidence bounds can be created in the following way:

```
phconf = cross.pconf;
phplot(frq,per,ph,fband,phconf,alpha,vnames)
```

The following code lines demonstrate how to calculate the multiple and the partial coherence (coherency), the partial phase angle and the partial gain between the IPI cycle and the other series. In addition, it is also shown how to write the results to a text file.

```
mulsp = mulparspan(ser ,[],[], alpha);
fid  = fopen('results\mulparUS.txt','w');
specwrite(fid ,per,mulsp,fband  ,[],[],[],  headers)
fclose(fid);
```

Using the output of the partial analysis, the partial phase angle can be plotted as follows:

```
parph = mulsp.pph;
phplot(frq ,per,parph,fband  ,[],[], vnames)
```

Example 3

The third example refers to the demo file *exUS2.m* and to the same data set as used in the previous subsection. The purpose of this example is to present an alternative way to produce output similar to the one obtained with the script *exUS1.m*.

```
[ser,headers] = xlsread('data\DataUS.xls');
% Settings for spectran:
per = 12;           % frequency of the data
pband = [18,96];   % Business cycle  periodicities  (expressed in months)
path = 'results';
% Other parameters are set to their default values
specb = spectran(ser,per,'vnames',headers,'corlag',12,'conf' ,1,...
        'pband',pband,'phmean',1,'phpband',pband,'graph',1,'graphconf' ,1,...
        'path',path,'leadlag',1,'pi',1);
```

To conduct the partial analysis instead, the value of the option "mulvar" must only be set to one, as is shown below:

```
specp = spectran(ser,per,'vnames',headers,'corlag',12,'conf' ,1,...
        'pband',pband,'phmean',1,'phpband',pband,'graph',1,'graphconf' ,1,...
        'path',path,'leadlag',1,'pi',1,'mulvar',1);
```

References

Berens, P. (2009). CircStat: A MATLAB Toolbox for Circular Statistics. *Journal of Statistical Software*, *31*(10), 1–21.

Jenkins, G. M., and Watts, D. G. (1968). *Spectral Analysis and its Applications*. San Francisco: Holden-Day.

Koopmans, L. H. (1974). *The Spectral Analysis of Time Series*. London: Academic Press.

Marczak, M., and Beissinger, T. (2013). Real Wages and the Business Cycle in Germany. *Empirical Economics*, *44*, 469–490.

Marczak, M., and Gómez, V. (2012). *SPECTRAN, A Set of Matlab Programs for Spectral Analysis* (Discussion Paper No. 60). FZID. Downloadable at `https://labour.uni-hohenheim.de/81521`

Priestley, M. B. (1981). *Spectral Analysis and Time Series* (Z. W. Birnbaum and E. Lukacs, Eds.). London: Academic Press.

Zar, J. H. (1999). *Biostatistical Analysis* (4th ed.). New Jersey: Prentice Hall.